

**GEOMETRIC AND MOBILITY ANALYSIS OF
THE MIURA-ORI PATTERN AND ITS
DERIVATIONS**

**A Thesis Submitted to
the Graduate School of Engineering and Sciences of
Izmir Institute of Technology
in Partial Fulfillment of the Requirements for the Degree of**

MASTER OF SCIENCE

in Architecture

**by
Aytan HUSEYNLI**

**December 2016
IZMIR**

We approve the thesis of **Aytan HUSEYNLI**

Examining Committee Members:

Assoc.Prof.Dr. Koray KORKMAZ

Name of the Department, Institution/University

Assoc.Prof.Dr. Emre İLAL

Name of the Department, Institution/University

Assoc.Prof.Dr. Ahmet Vefa ORHON

Name of the Department, Institution/University

26 December 2016

Assoc.Prof.Dr. Koray KORKMAZ

Supervisor, Name of the Department
Institution/University

Assoc. Prof. Dr. Şeniz ÇIKIŞ

Head of the Department of Architecture

Prof. Dr. Bilge KARAÇALI

Dean of the Graduate School of
Engineering and Sciences

ACKNOWLEDGEMENTS

All praises to Allah for the strengths and blessings in completing this thesis.

I would like to express my deepest gratitude to my supervisor Assoc. Prof. Dr. Koray Korkmaz for his guidance, insight, support and patience. I am aware of how much he had taken initiative and helped me in all my challenges. Thanks to him giving me the opportunity to fulfill my master thesis under his supervision.

I am grateful to Prof. Dr. Serdar Kale, Assoc. Prof. Dr. Tuğçe Kazanasmaz, Instructor Dr. Ülkü İnceköse, Assist. Prof. Dr. Gökhan Kiper and Instructor Dr. Can Gündüz for their unique contributions during my master education in Izmir Institute of Technology.

Thanks to research assistance Talha Eraz for his constructive comments on my draft.

Special thanks to my faithful friends Subaha Mahmuda.

Finally, I would like to express my gratitude to my parents Elxan Hüseynov and Mahizer Aliyeva and my sisters Aygün Hüseynli and Nurana Hüseynli. Throughout this period and my whole life, they have always loved, encouraged and supported me. Thanks to all, for their prayers.

And finally, I acknowledge my husband Tehran Abdurrahimov, who is my life coach and best friend. Thanks to him for his love and kindness.

ABSTRACT

GEOMETRIC AND MOBILITY ANALYSIS OF THE MIURA-ORI PATTERN AND ITS DERIVATIONS

Origami is a Japanese art of folding paper. Recently it has started to be used in aerospace applications such as deployable masts, satellite antennas, and in architectural applications such as emergency shelters, temporary shelters, portable exhibition stands.

Deployable plate structures based origami art are attractive to both architects and engineers because of their structural and spatial qualities. They have special geometries according to the rigid origami patterns. The Miura-Ori is a rigid origami pattern that is formed from a tessellated arrangement of a single repeated unit consists of four quadrangle plates. It has fully folded and fully deployed configurations.

This research investigates geometric and mobility aspects of Miura-Ori pattern with its derivations and explore the possibilities of constructing a deployable plate structure using the same pattern. The first part of the research investigates geometry of the Miura patterns. The aim is to generate derivations by changing the input parameters. Small scale physical models are built to verify the geometric design guidelines.

Miura unit consisted of four plates and four joints is a single degree of freedom spherical mechanism. The second part of the research is concentrated on mobility analysis. The aim is to develop a method for removing excessive plates and joints without changing the mobility. The established equations assist us to determine n^{th} term of the excessive plates and joints. A Method of Double Arrangement (MoDA) is developed in order to determine the placement of excessive plates.

Finally, a deployable plate structure based on Miura-Ori pattern is proposed for an architectural application. However, the plates cause obstruction of the sky, thereby affecting sunlight and daylight availability inside the building. Thus, some excessive plates are reduced according to the proposed method. The final form of the structure lets to get more energy from the sun to provide heating and lighting.

Keyword: rigid origami, Miura-Ori, spherical mechanisms, mobility.

ÖZET

MİURA-ORİ VE TÜREVLERİNİN GEOMETRİK VE SERBESTLİK DERECESİ ANALİZİ

Origami bir Japon kağıt katlama sanatıdır. Son yıllarda açılıp-kapanan direkler, uydu antenleri gibi uzaya dair uygulamalarda, acil ve geçici sığınaklar, taşınabilir sergi stantları gibi mimari alanlarda uygulanmaya başlamıştır.

Origamiden esinlenen açılıp kapanabilen plak strüktürler yapısal ve mekansal özellikleri nedeniyle mimar ve mühendisler tarafından ilgi çekmektedir. Bu strüktürlerin rijit origami desenlerinden kaynaklanan özel geometrileri vardır. Miura-Ori rijit origami dört plakadan oluşan bir birimin tekrarlanmasından oluşur. Tam kapanıp açılabilme özelliğine sahiptir.

Bu tez Miura-Ori ve türevlerini geometrisi ve serbestlik derecesi açısından inceleyerek bir hareketli plak strüktür oluşturma olasılıklarını incelemektedir. Tezin ilk kısmı Miura-Ori rijit origaminin geometrisini önceden belirlenmiş parametreleri ile hesaplamalı incelemektedir. Amaç, istenilen formlara ulaşmak için geometrik kısıtlamaları türetmektir. Küçük ölçekli fiziksel modeller, geometrik tasarım yönergelerini doğrulamak için oluşturulmuştur.

Miura birimi dört adet sert plakadan ve dört adet döner mafsaldan oluşan tek serbestlik dereceli bir küresel mekanizmadır. Tezin ikinci kısmı serbestlik derecesi analizi üzerine yoğunlaşmıştır. Amaç tek serbestlik dereceli olma durumunu değiştirmeden elimine edilebilecek plaka ve mafsalları belirlemek için bir yöntem geliştirmektir.

Son olarak, mimari bir uygulama için Miura-Ori modeline dayanan hareketli bir plak strüktür önerilmiştir. Ancak mimari uygulama düşünüldüğünde plakalar gökyüzünü kapatarak binanın içinde güneş ışığı ve gün ışığının kullanılabilirliğini etkiler. Bu sebeple bazı plakalar önerilen metoda uygun olarak eksiltilmiştir. Yapının nihai şekli, ısıtma ve aydınlatma sağlamak için güneşten daha fazla enerji almamızı sağlayacaktır. Çözümleri göstermek için fiziksel bir model de yapılmıştır.

Anahtar Kelimeler: rijit origami, Miura-Ori, küresel mekanizmalar, serbestlik derecesi.

To my mother Mahizer,
To my father Elxan,
with love.

TABLE OF CONTENTS

LIST OF FIGURES.....	ix
LIST OF TABLES.....	vii
CHAPTER 1. INTRODUCTION.....	13
1.1. Motivation.....	13
1.2. Problem Statement.....	19
1.3. Previous Studies Related to Origami-Inspired Deployable Structures.....	19
1.4. Methodology.....	21
CHAPTER 2. REVIEW OF THE LITERATURE.....	23
2.1. History of Origami.....	23
2.2. Terminology.....	24
2.3. Theorems.....	27
2.3.1. Huzita- Hatori Axioms.....	28
2.3.2. Toshikazu Kawasaki's Theorem.....	30
2.3.3. Maekawa's Theorem.....	30
2.3.4. Sufficiency Control.....	30
2.4. Type Classification with Most Famous Origami Examples.....	32
2.4.1. Traditional Origami.....	32
2.4.2 Action Origami.....	33
2.4.3 Rigid Origami.....	34
2.4.4. Origami Tessellation.....	36
2.4.5. Kirigami (and Pop Up).....	37
2.4.6. Unit Origami.....	38
2.4.7. 3d Geometric Origami.....	39
2.4.8 Wet Folding.....	39
CHAPTER 3. GEOMETRIC ANALYSIS OF THE MIURA-ORI PATTERN AND ITS DERIVATIONS.....	41

3.1. Geometric Approach to Miura-Ori Pattern.....	46
3.1.1. Rotation Angle (δ).....	46
3.1.2. Unit Length (k).....	47
3.2. Geometric Approach to Arc-Miura Pattern.....	48
3.2.1. Rotation Angles of a Unit (δ_1, δ_2).....	50
3.2.2. External Angle (γ).....	52
3.2.3. Unit Angle (θ).....	53
3.2.4. The Length of a Unit (k).....	53
3.2.5. The Radius of the Pattern (r).....	53
3.3. Geometric Approach to Tapered Miura and Tapered Arc-Miura Pattern.....	54
3.4. Validity of the Developed Formulas	55
3.4.1. Review of the Miura-Ori.....	55
3.4.2. Review of the Arc-Miura.....	57
3.4.3. Review of the Tapered Miura Pattern.....	60
3.4.4. Review of the Tapered Arc-Miura Pattern.....	61
3.4.5. Conclusion.....	63
 CHAPTER 4. MOBILITY ANALYSIS OF MIURA ORI PATTERN.....	67
4.1. Determining DoF of Miura-Ori Pattern.....	68
4.2. Determining the Excessive Plates and Joints of Miura-Ori.....	72
4.2.1 Excessive Plates and Joint Studies on the Six Derivations.....	75
 CHAPTER 5. CASE STUDY.....	82
5.1. Example Problem.....	82
 CHAPTER 6. CONCLUSION.....	95
 REFERENCES.....	96

LIST OF FIGURES

<u>Figure</u>	<u>Page</u>
Figure 1. Origami in Science.....	14
Figure 2. Glass Pavilion.....	14
Figure 3. Experimental Timber Cover.....	15
Figure 4. Stadium and Sports Complex.....	15
Figure 5. Glanerburg customs building.....	16
Figure 6. One-way Colour Tunnel.....	16
Figure 7. Accordeon Recover Shelter.....	17
Figure 8. Hyposurface.....	18
Figure 9. Al-Bahar Tower Façade.....	18
Figure 10. Test of the Timber Folding Patterns Prototype.....	20
Figure 11. Crease Patterns and Folding Steps for the Preliminary Base and Waterbomb Base.....	25
Figure 12. Origami Vertex.....	25
Figure 13. Inside Reverse, Outside Reverse, Crimp and Pleat fold.....	26
Figure 14. The Six Standard Origami Bases.....	27
Figure 15. Huzita- Hatori axioms.....	29
Figure 16. Application of Kawasaki's Theorem in a Foldable Paper Crane.....	30
Figure 17. Two Origamis with the Same MV-Assignment	31
Figure 18. Inconsistency of Flat Folding (Bern, 1996).....	31
Figure 19. Possibility of Flat Folding	32
Figure 20. Yoshizawa`s Butterfly.....	33
Figure 21. Shafer`s “Venus Fly Trap” is an Example of Action Origami.....	34
Figure 22. Origami Shopping Bag.....	35
Figure 23. A Corrugated Vault Used as a Transformable Architecture that Connects Two Existing Buildings.....	35
Figure 24. Tessellation.....	36
Figure 25. A Kirigami House Made in Cardstock.....	37
Figure 26. Duomo Milan.....	38
Figure 27. Mind-Blowing Modular Origami Model of St. Basil Cathedral.....	38
Figure 28. Masu Box.....	39

Figure 29. Wet Folding.....	40
Figure 30. Miura-Ori pattern.....	42
Figure 31. Arc-Miura Patterns.....	43
Figure 32. Tapered Miura patterns.....	44
Figure 33. Tapered Arc-Miura Patterns.....	45
Figure 34. Assistance Angle ε on the Unfolded Miura-Ori Pattern.....	46
Figure 35. Parameters in the Folded Position of the Miura-Ori Pattern.....	48
Figure 36. Parameters in the Folded Position of the Arc-Miura Pattern.....	50
Figure 37. Assistance Angles ε and φ on the Unfolded Arc-Miura Pattern.....	51
Figure 38. Piece of Pattern for Developing the External Angles.....	52
Figure 39. Creating of Tapered Miura and Tapered Arc-Miura Pattern.....	54
Figure 40. Miura-Ori Folded Patterns where α is Equal to 30° , 45° and 60°	55
Figure 41. Type 1 Patterns.....	58
Figure 42. Type 2 Patterns.....	59
Figure 43. Miura-Ori Folded Patterns.....	61
Figure 44. Tapered Miura Folded Pattern with Same Span Lengths.....	63
Figure 45. Curvature Distinction of Folded Arc-Miura Pattern.....	64
Figure 46. Numbered Folded Patterns.....	66
Figure 47. A Spherical Four-Bar Mechanism.....	67
Figure 48. Miura-Ori Unit as a Spherical Mechanism.....	68
Figure 49. An Unfolded Miura-Ori Unit.....	68
Figure 50. Miura-Ori Patterns Consist of Two Columns.....	70
Figure 51. Miura-Ori Patterns in Three Columns.....	70
Figure 52. Miura-Ori Patterns in Four Columns.....	71
Figure 53. Pattern with Two Excessive Plates.....	72
Figure 54. Double Arrangement Rule (DAR).....	74
Figure 55. Correct and Wrong Determination of Excessive Plates and Joints.....	75
Figure 56. Determination of Excessive Plates and Joints on the Pattern of Fig.51(2b)....	76
Figure 57. Determination of Excessive Plates and Joints on the Pattern of Fig.51(2c)....	77
Figure 58. Determination of Excessive Plates and Joints on the Pattern of Fig.51(2d)....	78
Figure 59. Determination of Excessive Plates and Joints on the Pattern of Fig.52(3b)....	79
Figure 60. Determination of Excessive Plates and Joints on the Pattern of Fig.52(3c)....	79
Figure 61. Determination of Excessive Plates and Joints on the Pattern of Fig.52(3d)....	80

Figure 62. Draft Path of the Example Problem.....	83
Figure 63. Curve ₁ Pattern.....	87
Figure 64. Curve ₃ Pattern.....	87
Figure 65. Curve ₂ Pattern.....	87
Figure 66. Curve ₃ Pattern.....	88
Figure 67. Line ₂ Pattern.....	88
Figure 68. Combination of Different Parts.....	88
Figure 69. Example of the Unfolded Whole Pattern.....	91
Figure 70. Pattern of the Shelter.....	91
Figure 71. First Excessives.....	92
Figure 72. Samples of Removing 174 th Excessives.....	92
Figure 73. Folded Shelter.....	93
Figure 74. Shelter Visualizations.....	94

LIST OF TABLES AND SCHEMES

<u>Table</u>	<u>Page</u>
Scheme 1. Developed State and Flat-Folded State.....	27
Table 1. Comparison of the Unit Lengths Caused by Different Vertex Angles.....	55
Table 2. Checking for Calculation of Type 1.....	56
Table 3. Checking for Calculation of Type 2.....	58
Table 4. Comparison of Tapered Patterns.....	60
Table 5. Checking for Calculation of Tapered Arc-Miura.....	61

CHAPTER 1

INTRODUCTION

1.1 Motivation

Origami is the art of folding paper. Although it started to be used as a hobby by the ancient Japanese, recently origami is applied to different areas, such as architecture, engineering, medicine, electronics, astronomy, manufacturing & packing industry. Brigham Young University mechanical engineers, Larry Howell and his team designed compact solar array (Figure 1(a)) that developed into space to get power for space stations in 2013 (Zirbel et al., 2013). Wyss Institute (Harvard) researcher– Shawn Douglas and colleagues used Origami DNA in 2012 (Figure 1(b)) to create 3D shapes (Douglas, Bachelet, & Church, 2012). In 2013 Arizona State University researchers constructed a deployable paper-based lithium-ion battery (Figure 1(c)) that can be folded as Miura-Ori pattern (Cheng et al., 2013).

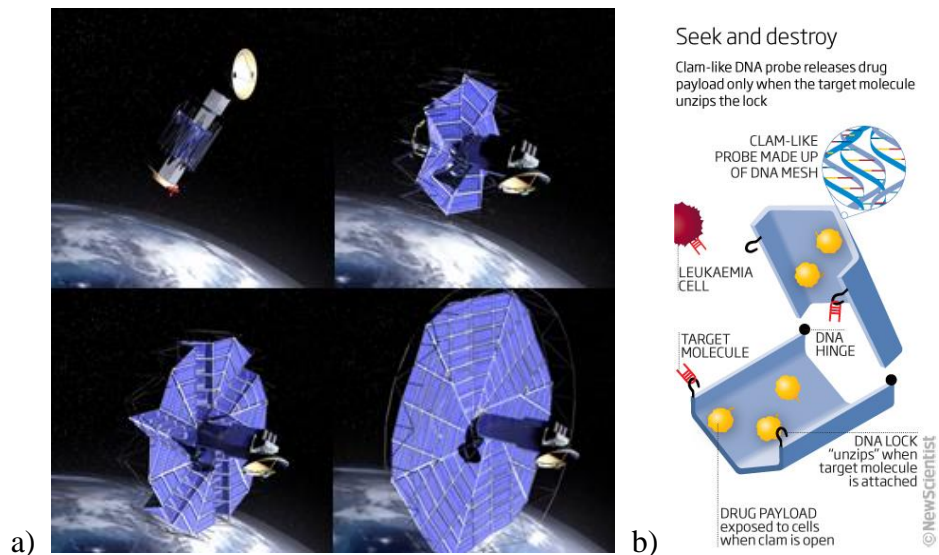


Figure 1. a) Solar Array (Source: Zirbel et al., 2013); b) Origami DNA (Source: Douglas et al., 2012); c) Paper-Based Lithium-Ion Battery (Source: Cheng et al., 2013).

(cont. on next page)

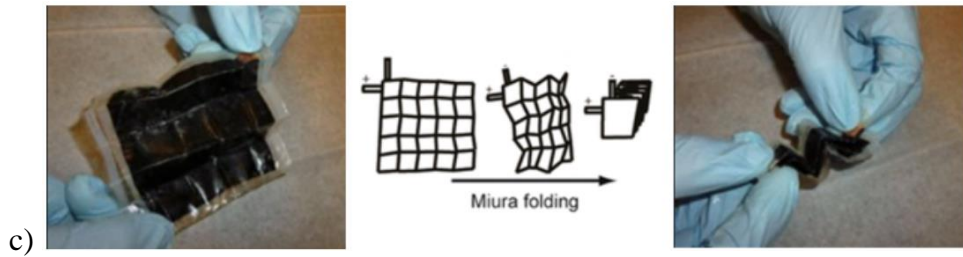


Figure 1. (cont.)

Designing and construction of folded plate structures began at the beginning of the twentieth century. Bruno Taut applied origami as facade detail in Berlin–Grunau in 1912 (Figure 2), Eduardo Torroja as decks of the dining room in Tarragona in 1956, Renzo Piano as mobile structure for Sulfur Extraction in Italy in 1966 (Figure 3), Jørn Utzon for stadium and sports complex in Jeddah in 1967 (Figure 4), Mats Karlsson as foldable plastic tube in Stockholm in 2008 (Vyzoviti & de Souza, 2012).



Figure 2. Glass Pavilion, Bruno Taut
(Source: L. S. d. Lang, 2015.)

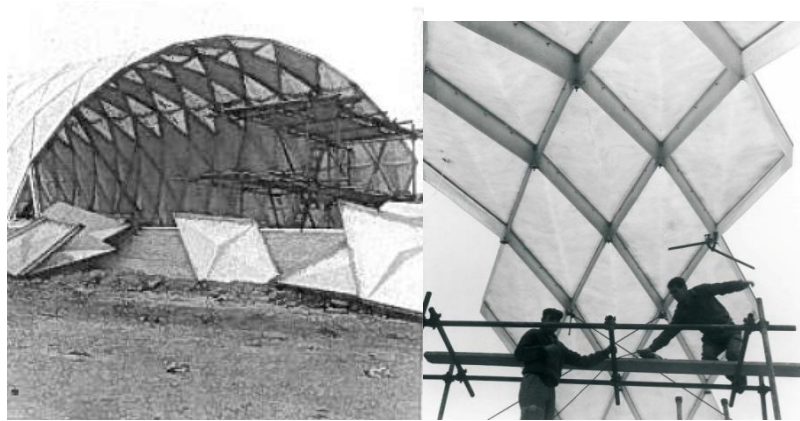


Figure 3. Mobile Structure for Sulfur Extraction, Renzo Piano
(Source: Piano, 1966.)

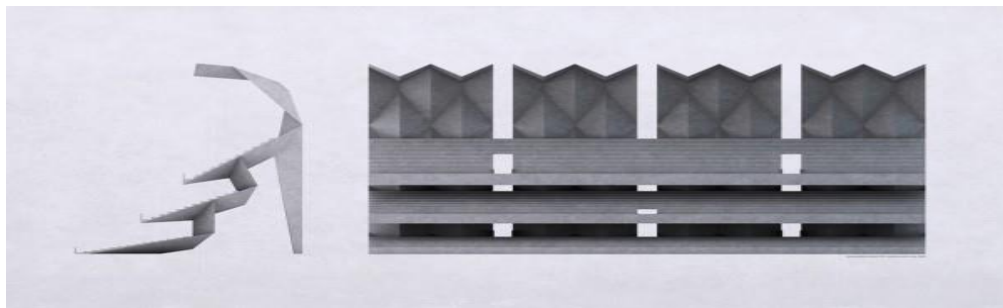


Figure 4. Stadium and Sports Complex, Jørn Utzon
(Source: Mariano, 2012.)

In architecture origami progress in three ways, such: folded plate roofs or façades; deployable architectural structures; transformable or kinetic architecture (Schenk, 2012).

Origami **folded** plate roofs or façades are stable in folded position. Several applied examples involve basic V-shaped folded roofs and also special or freeform complicated patterns in architecture. An early sample is customs building at Glanerburg covered with continuous folded plates (Figure 5). The façades of US Air Force Academy Cadet Chapel is enclosed with folded aluminum plates in 1954 (Gordon, 1954). One-way Colour Tunnel (Figure 6) with glass plate in 2007 is also folded plate structures base on origami. Mark Schenk described the main points of plate roofs or façades with mechanical advantage, visual appeal, materiality (timber, glass, etc.), approximation to curved surfaces (Schenk, 2012).

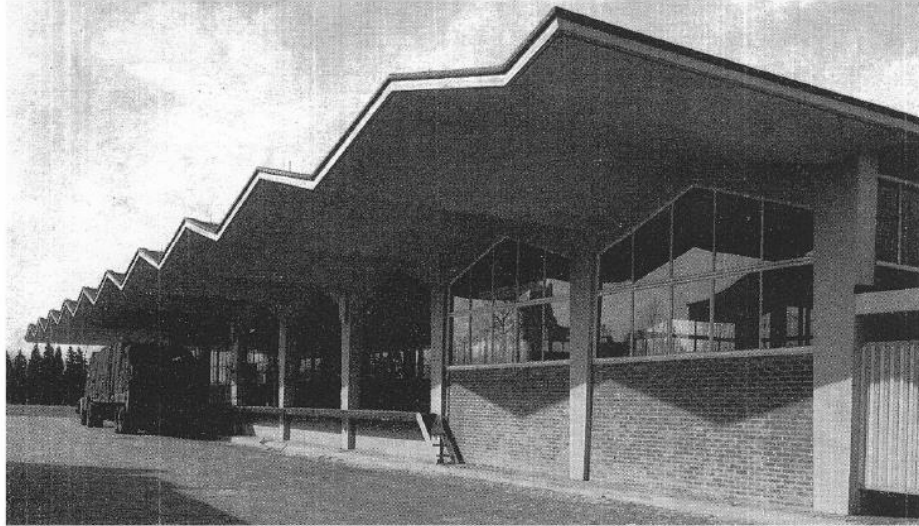


Figure 5. Glanerburg Customs Building
(Source: Beltman & Spit, 1962.)



Figure 6. One-way Colour Tunnel
(Source: Schenk, 2012.)

Unlike folded structures, **deployable and transformable** structures are developable. Andre James stated developable objects, in his thesis, such as turning, wrapping, enfolding piercing, hinging, knotting, weaving, compressing, balancing and unfolding, and he declared that all these manipulations together with each other or separately generate a developable object (James, 2008). **Deployable** structures are easily

transported in its fully folded state. To activate the deployable system, whole structure should be unfolded. On the other hand, the system of transformable (or kinetic) structures active both folded and unfolded states, every position has own duty. Accordion recover shelter which designed for disaster in 2008 by Matthew Malone, origami inspired bamboo house (Figure 7) in 2008 by Ming Trang, deployable shelter in 2009 by Tachi and etc. are the proposed examples for deployable structures (Schenk, 2012). Hypo surface moving wall is a kinetic architecture sample, which is controlled by sound and movement (Figure 8). It was designed in 2000 by Mark Goulthorpe and etc (Burry, 2006). Moving origami facade cover is also kinetic architecture samples, has shading function for the Al-Bahar Tower facade (Figure 9).

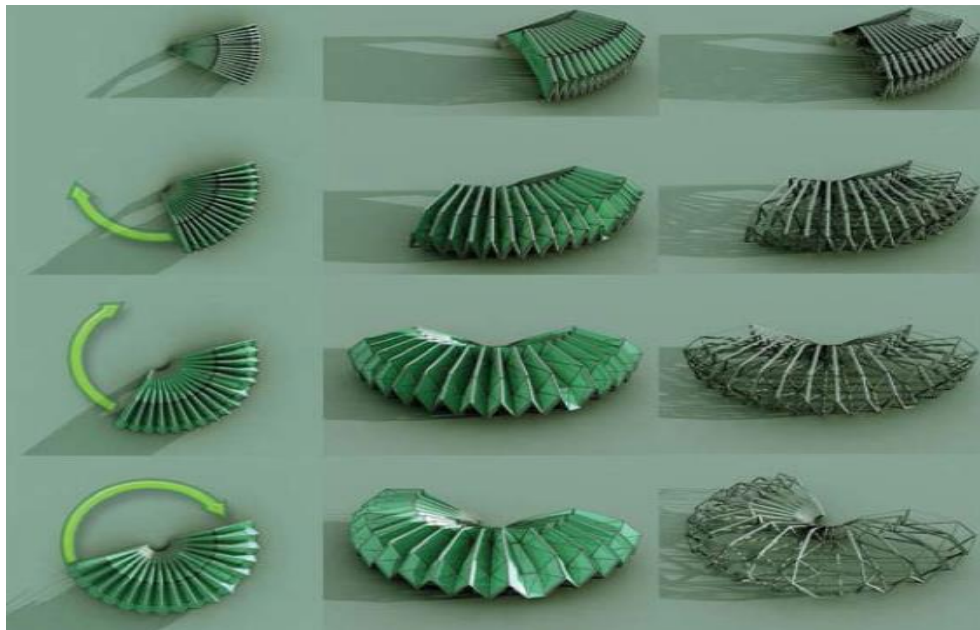


Figure 7. Accordion Recover Shelter
(Source: Schenk, 2012.)



Figure 8. Hypo surface
(Source: Burry, 2006.)

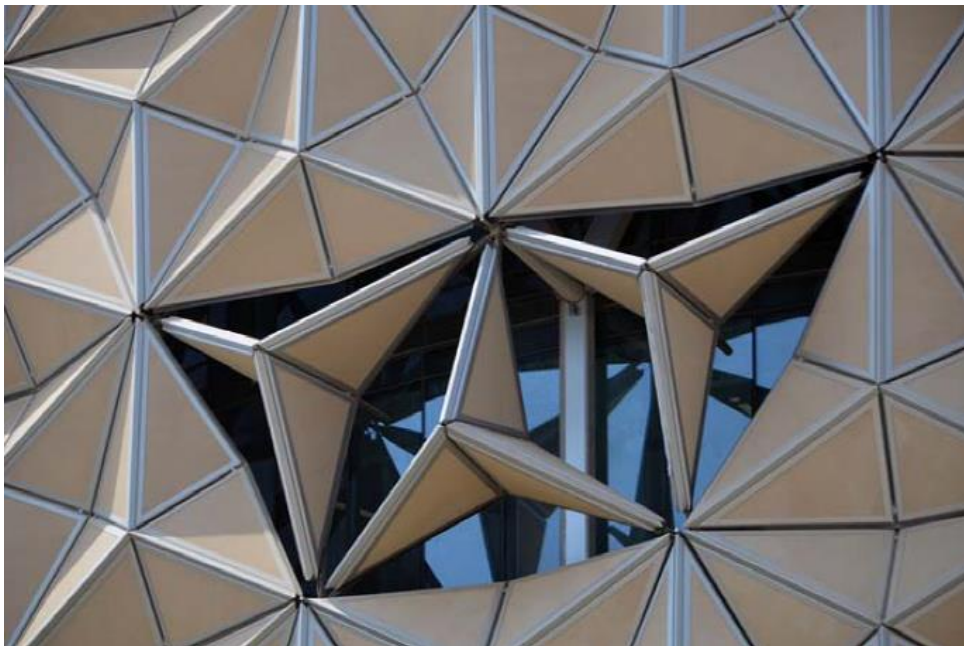


Figure 9. Al-Bahar Tower Façade
(Source: Boake, Bes, & Arch, 2014.)

1.2. Problem Statement

The thesis consists of two main problems: geometric analysis and mobility analysis of the Miura pattern (Chapter 3. and 4.).

Architectural plate structures which are designed with origami patterns as roofs, facades, buildings, have specific and complex geometries. Because of its complex configuration, it is difficult to apply such structures to a given area or cover a building part. There are hundreds of origami patterns, and each origami pattern requires special geometry calculation according to its shape. The first problem area is the geometric possibilities of rigid Miura patterns and its derivations. These patterns have some parameters, such as span lengths (a or b), vertex angles (α or δ). Third chapter includes research of geometric characteristics of the rigid Miura pattern with these basic parameters.

Origami based architectural structures are fully surrounded with plates. Rigid plates strengthen mechanism and increase the durability of the structure. Although this configuration has beneficial side, the placement of the plates make space fully covered, so structures could not be adequately illuminated with daylight. These deployable structures may also require energy consumption. The second problem is around the mobility aspect of Miura pattern by the analysis of degrees of freedom. With this concept, number of excessive plates and excessive joints are obtained and number of placement of excessive alternatives are analyzed.

1.3. Previous Studies Related to Origami-Inspired Deployable Structures

There are several studies on origami-inspired structures. Arzu Gönenç and et al., Ulrich Buri, Martin Trautz and Ralf Herkrath, Tomohiro Tachi have discussed different origami patterns which are applied to architecture.

Arzu Gönenç and et al. proposed development of 2-D diagram to understand the mathematical relations of the patterns in order to explore solid modeling in computational media. The researchers noted: "This relation between 2-D diagrams and the resulting 3-D solid models have also clues for the manufacturing/ fabrication of these models from simple sheets of raw materials to complex forms" (Sorguç, Hagiwara, & Selçuk, 2009).

The researchers discussed several student workshops on origami structures. Students obtained "mesh networks" of structural forms with using diagram method. By the mesh networks, Middle East Technical University (METU) students experienced shell structure, The University of Cambridge students designed cardboard structure, and built "Packaged" pavilion (Sorguç et al., 2009).

Martin Trautz and Ralf Herkrath studied the development of folded plate principles on spatial structures. Researchers analyzed free-form geometry details of the structures with a Finite Element Method (FEM) programme. The program was set some parameters to change variables of the free-form geometry structures. These parameters are height, frequency of the folding, thickness of a metal element (Trautz & HERKRATH, 2009).

Ulrich Buri investigated new methods of designing folded structures which could be built with timber plates (Figure 10). He was convinced that a design method which rapidly generates and modifies folded plate structures is of great interest, and can form the basis of a productive collaboration between architects and engineers. He proposed modeling in a 3D CAD software for regular folding patterns. To analyze the geometry of the folds, classical representations of architectural drawings (plans and sections) were used (Buri, 2010).

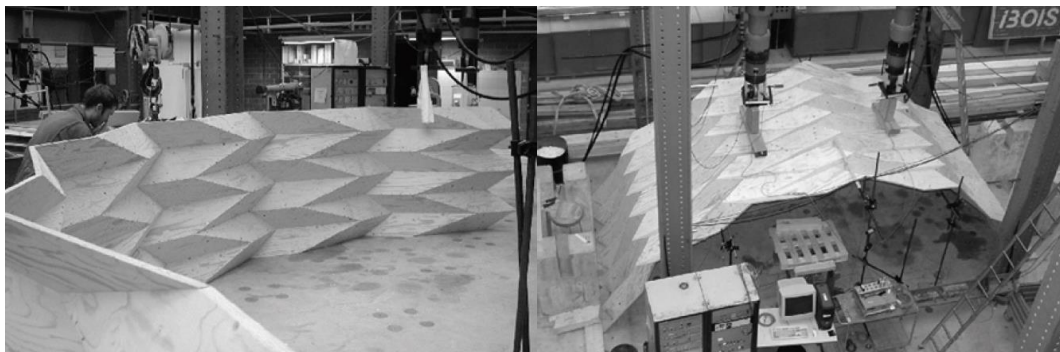


Figure 10. Test of the Timber Folding Patterns Prototype
(Source: Buri, 2010.)

Tomohiro Tachi developed a method to design free-form variations of Resh-like origami tessellations with Japan Science and Technology (JST) Presto program. They optimized the surface to make it developable and also non-intersecting at the vertices (Tachi, 2013).

If we look at the studies that relates origami mechanisms, we can recognize that the most of the themes are form generation of the Miura-Ori. Joseph M. Gattas and Zhong You described parametrizations of curved-crease geometries of Miura-ori (Gattas, Wu, & You, 2013), Jianguo Cai and et al. analyzed geometry and motion of origami-based deployable shelter structures (Cai, Deng, Xu, & Feng, 2015). Marcelo A. Dias et al. worked on mechanics of curved crease origami with analyzing multiple curved structures (Dias, Dudte, Mahadevan, & Santangelo, 2012).

The previous studies presented in the second part of the thesis review such topics, as: degrees of freedom origami inspired structures and mobility of origami. L.A. Bowen et al. worked on a position analysis of action origami vertex observing relationship between input and output angles. The researchers suggest future work to demonstrate this method for mechanisms which allow spherical centers to move (Bowen et al, 2014). Tarek AlGeddawy's et al. studied design model of regular product to help designers connect foldability and mobility (AlGeddawy, Abbas, & ElMaraghy, 2014).

1.4. Methodology

The first part of the study is based on calculations in order to design desired Miura Pattern. In this part parameters are identified to analyze and define geometric variations. Miura derivative patterns are demonstrated with several trigonometric formulas and theorems. Studied patterns are drawn in Autocad and calculated with Microsoft Excel to determine validity of the analysis.

The second part of the study investigates to remove excessive plates from the structure considering mobility factors to let daylight into the structure. In order to investigate mobility, 12 different Miura-Ori patterns are analyzed. During the investigation excessive plates and its joints are determined without changing the mobility. A new method is developed to pick relevant excessives. This part is procured with perception and analytical thinking on the behavior of the patterns and some calculations.

In the both parts, several paper model of the Miura derivative patterns are made to observe the geometric and mechanical behavior. Rigid Origami Simulator which was introduced by Tomohiro Tachi, is used to simulate kinematics of the Miura derivative patterns.

In the case study, a designed pattern is proposed as a deployable shelter to show the real-world application. The origami shelter is visualized in the 3ds MAX and Lumion.

CHAPTER 2

REVIEW OF THE LITERATURE

2.1. History of Origami

Origami (折り紙) from *ori* - "folding", and *kami* - "paper" is the ancient Japanese art of paper folding (Dureisseix, 2011). The process of folding doesn't require stretching, cutting, or gluing and crossing (E. Demaine, 2010).

"Origami involves the creation of paper forms usually entirely by folding" (Katz, 2001-2014)

There is an ongoing debate as to who were the first paper folders. Certainly, paper folding is a part of Chinese culture: perhaps they were the first. When people are buried, replicas of items are folded and included in their tombs. Also, the Chinese have always been frugal people who would not waste something that could be reused. So, a paper that has served its original purpose now can be recycled for origami. Many origami toys were developed by the Chinese. The most famous of these is the "waterbomb". Children make balloons out of paper, fill them with water and throw them down with a loud splat.

It is believed that paper has been invented by Ts'ai Lun, a Chinese court official, in 105 AD. By the invention of paper, origami spread out several countries primarily in China and Japan, then Uzbekistan, Egypt, Spain, France, England, Italy and etc. (Smith, 2005).

In Japan Origami was developed in special period, as follows:

794-1185 A.D. Heian Period- evolution of ceremonial fold and some basic origami models;

1185-1333 A.D. Kamakura Period- Origami extension everywhere in Japan;

1333-1573 A.D. Muromachi Period- development of "Modern" origami;

1603-1867 A.D. Edo Period- Origami had become an entertainment;

1868-1912 A.D. Meiji Period- Gaining popularity of origami usage in schools (E. O. E. Demaine, Joseph 2007).

The first famous origami book "*The Secret of One Thousand Cranes Origami*" or "How to Fold a Thousand Cranes" was published in 1797. The book name is the

translation of "Hiden Senbazuru Oriката". In Japanese language *Sen nen* (千年) is 'one thousand years' and *Senba zuru* (千羽鶴) is 'one thousand cranes' (Ishii, 2013).

Akira Yoshizawa (1911-2005) is known as a master of origami. When he was just three years old, he started working with origami as a hobby and at the age of 26, Yoshizawa worked full time on origami and published several books. In 1935 he developed universal symbols to help people understand diagrams, without understanding his native language (Hoover, 2006-2014).

2.2. Terminology

After unfolding a fold trace is formed on paper, that trace is a **crease** (R. J. Lang, 2004-2014b).

Crease pattern is a collection of creases which presents an origami model on a flat piece of paper. Note that there can be dual crease patterns (Figure 11.) that shows different origami models. It is easy to define crease pattern in traditional origami (Figure 11), as, creases starting from corners and create angles by connecting with vertex. (Dureisseix, 2011).

"A fold is an action and a crease is the product of that action" (Greenberg, 2011). If we look at a crease pattern with unfolded paper, we can see that there are two main folds: **mountain** and **valley** folds. They are dual of each other because they can interchange by changing the face of the paper. In spatial position, mountain folds follow concave 3D shapes and valley folds follow convex 3D shapes (Dureisseix, 2011).

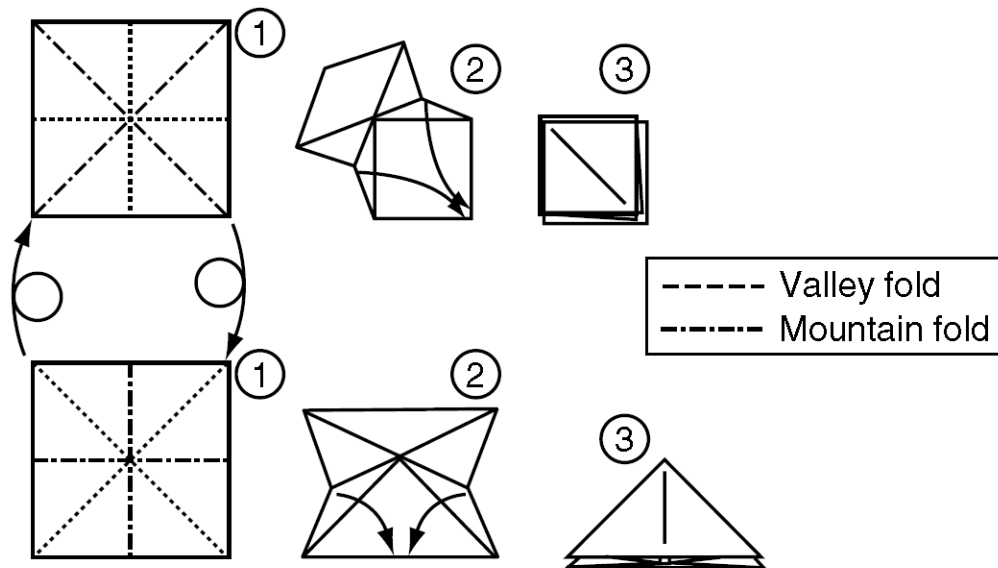


Figure 11. Crease Patterns and Folding Steps for the Preliminary Base (top) and Waterbomb Base (bottom) (Source: Dureisseix, 2011.)

"**Vertex** : a point in a crease pattern where multiple creases come together" (R. J. Lang, 2004-2014b). **Vertex** is the point where several folds meet (Figure 12).

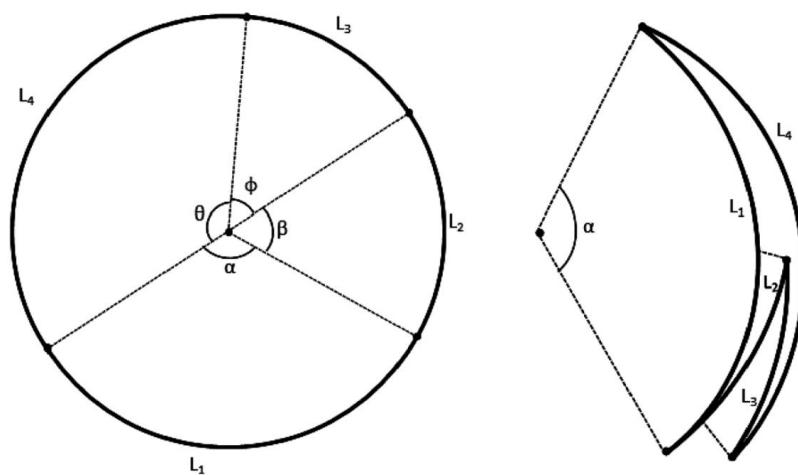


Figure 12. Left: Unfolded Origami Single Vertex. Right: Partially Folded Origami Vertex (Source: Lang J., 2013.)

Apart from mountain and valley fold, there are other four folds mostly using as a term (Figure 13.):

- **Inside reverse fold.** Open edges of the paper is turned inside-out.

- **Outside reverse fold.** Open edges of the paper is turned outside-out.
- **Crimp fold.** A pair of valley folds and mountain folds converge at one point.
- **Pleat fold.** Mountain and valley fold are parallel, or near. They are folded together (Engel, 2011).

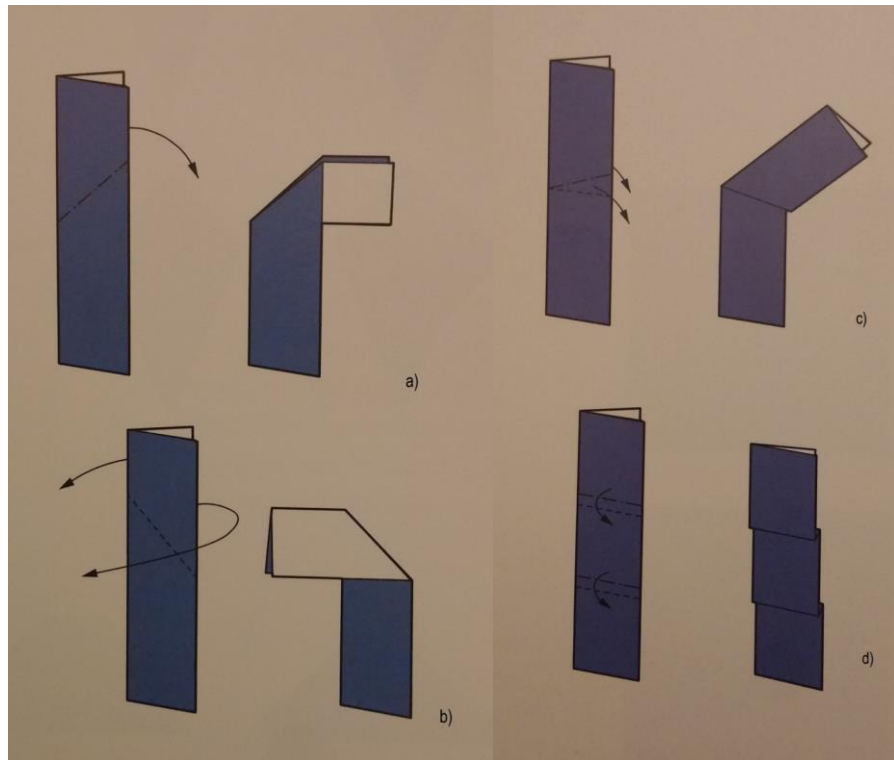


Figure 13. (a) Inside reverse fold; (b) Outside reverse fold; (c) Crimp fold; (d) Pleat fold.

Most origamists decompose the folding process into two stage: base and shape (R. J. Lang, 2004-2014c). "**Base** : a regular geometric shape that has a structure similar to that of the desired subject" (R. J. Lang, 2004-2014b). Lang`s tree method focuses on the design of the origami base. "The usage of a base has many benefits; the folding sequence will be easier to remember and create diagrams for". (WikiBooks, 2014). **Shape** is the end of transforming a base into the actual origami model (E. O. E. Demaine, Joseph 2007). In Figure 14, there is *Standard Origami Bases*:

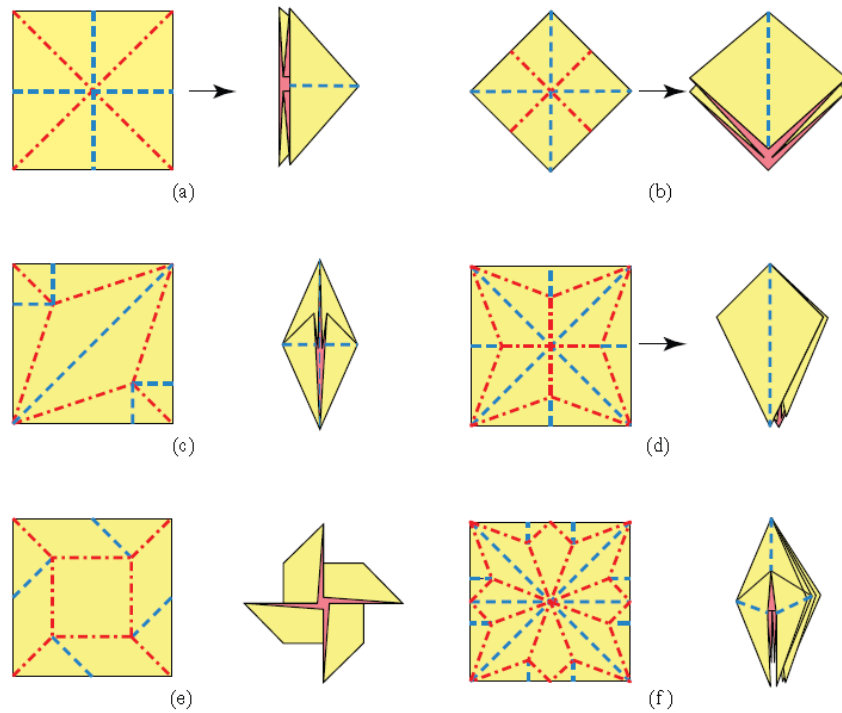
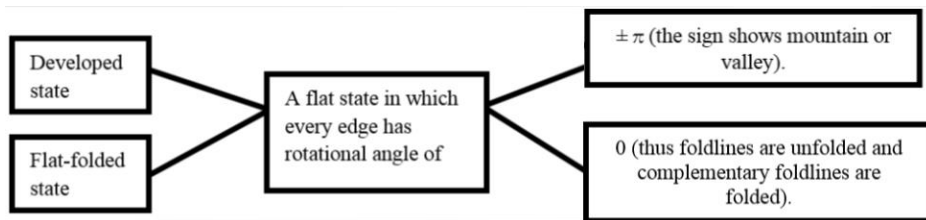


Figure 14. The Six Standard Origami Bases; (a) Waterbomb; (b) preliminary; (c) fish; (d) bird; (e) windmill; (f) frog (Source: E. O. E. Demaine, Joseph 2007)

2.3. Theorems

According to unfolding process four type of behaviours are possible for the conditions of origami shapes: (non) developable and (non) flat-foldable.

“Developed state” and “flat-folded state” are defined as follows in Tachi’s paper (Scheme 1.)



Scheme 1. Developed State and Flat-Folded State (Source: Tachi, 2010.)

In order to prove flat vertex folds condition several theorems were achieved. Mathematical approaches about origami are on the three main bases:

Huzita-Hatori axioms;

Kawasaki's Theorem;

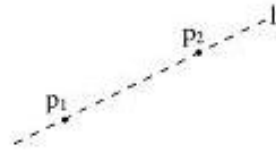
Maekawa's theorems.

2.3.1. Huzita- Hatori axioms

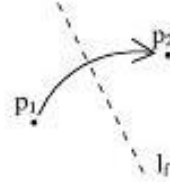
Huzita- Hatori axioms firstly discovered by Jacques Justin in 1989, then in 1991 recovered by Humiaki Huzita. These 7 axioms were finalized by Koshiro Hatori, Justin and Robert Lang in 2001 (Fei, 2013).

The axioms are (Figure 15):

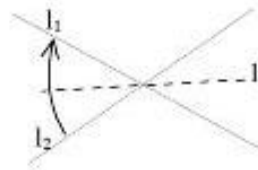
(O1) Given two points p_1 and p_2 , we can fold a line connecting them.



(O2) Given two points p_1 and p_2 , we can fold p_1 onto p_2 .



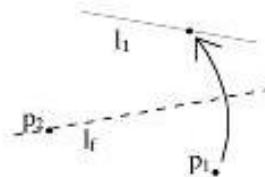
(O3) Given two lines l_1 and l_2 , we can fold line l_1 onto l_2 .



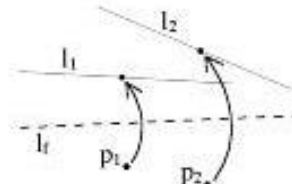
(O4) Given a point p_1 and a line l_1 , we can make a fold perpendicular to l_1 passing through the point p_1 .



(O5) Given two points p_1 and p_2 and a line l_1 , we can make a fold that places p_1 onto l_1 and passes through the point p_2 .



(O6) Given two points p_1 and p_2 and two lines l_1 and l_2 , we can make a fold that places p_1 onto line l_1 and places p_2 onto line l_2 .



(O7) Given a point p_1 and two lines l_1 and l_2 , we can make a fold perpendicular to l_2 that places p_1 onto line l_1 .

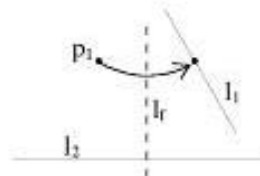


Figure 15. Huzita- Hatori axioms
(Source: R. J. Lang, 2004-2014a.)

2.3.2. Toshikazu Kawasaki's Theorem

Kawasaki Theorem explains that for affirming a given crease pattern is foldable, all the sequences of angles around each (interior) vertex must be summed to 180° as given in eq. (1) and eq. (2) and showed in Fig. 16 (Fei, 2013).

$$\alpha_1 - \alpha_2 + \alpha_3 - \alpha_4 + \dots - \alpha_{2n} = 0 \quad (2.1)$$

$$\alpha_1 + \alpha_3 + \dots + \alpha_{2n-1} = \alpha_2 + \alpha_4 + \dots + \alpha_{2n} = 180^\circ \quad (2.2)$$

$\alpha_1, \alpha_2, \dots, \alpha_{2n}$ is the consecutive angles between the creases (Lim, 2007).

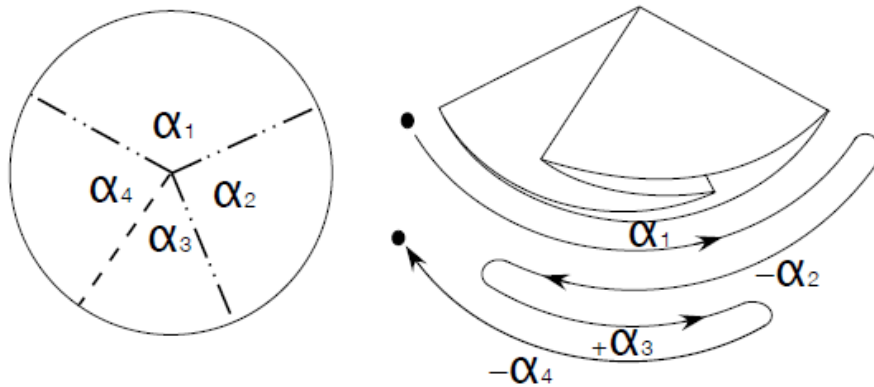


Figure 16. Application of Kawasaki's Theorem in a Foldable Paper Crane (Source: Fei, 2013.)

2.3.3. Maekawa's Theorem

If the difference between the number of mountain creases and valley creases are equal to 2, origami crease pattern is a flat, shown in eq. (3) (Fei, 2013).

$$M - V = \pm 2 \quad (2.3)$$

where, M is the number of mountain creases; V is the number of valley creases.

2.3.4 Sufficiency Control

According to the Maekawa's theorem flat origami can be described by its MV assignment. In Figure 17. we can recognize that Maekawa's description is not enough for flat-foldability. Origami patterns may overlap differently with the same MV-assignment (Figure 17).

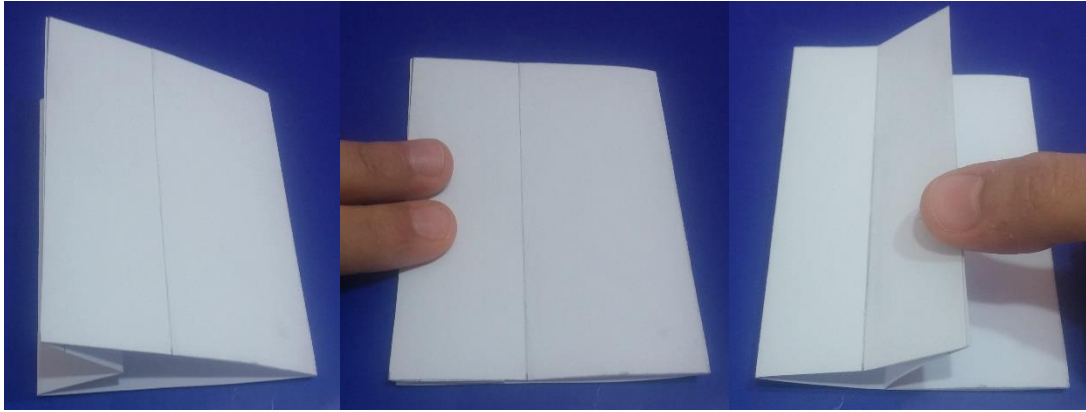


Figure 17. Two Origamis with the Same MV-Assignment but Different Overlap Maps

In the Figure 17, same patterns are folded differently. Hence, first sample is valid MV assignment, while another still fails to fold flat. M. Bern and B. Hayes showed that assigning mountain and valley folds for flat origami is NP-hard (Non-deterministic Polynomial acceptable problems).

Figure 18 is the alteration of Figure 19. Each vertex has equal number of creases, but one is flat foldable, another is not. In figure 19 Bern and et al. were omitted NP hardness proofs, and modified vertex angles from 90° to 35° (Bern, 1996).

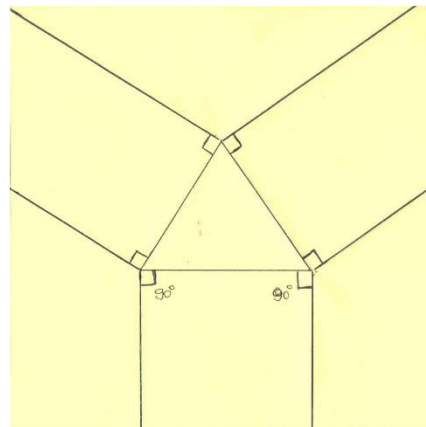


Figure 18. Inconsistency of Flat Folding (90°)

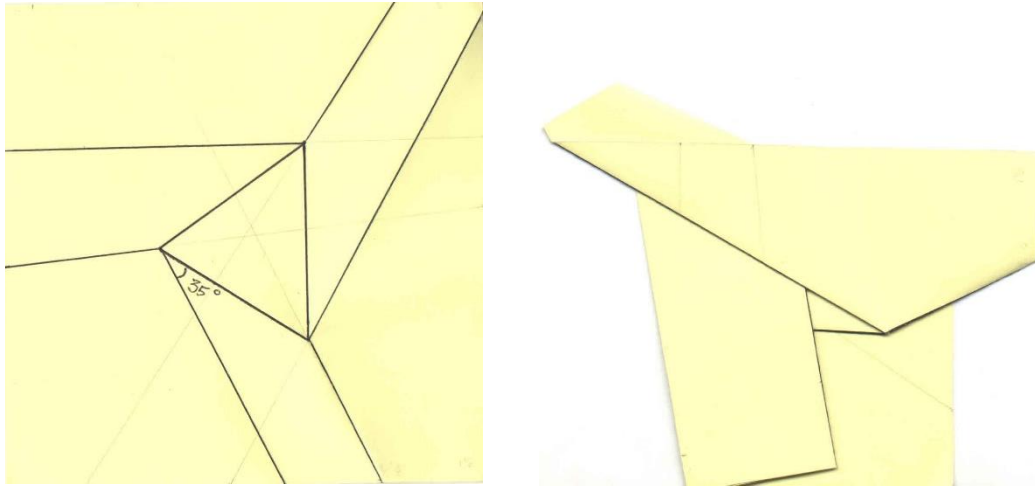


Figure 19. Possibility of Flat Folding (35°)

Crease patterns can be *locally* flat-foldable but that have no *global* flat folding that works for the whole crease pattern at once (Hull, 2011).

"Because global flat foldability depends on the whole structure not only the point, you should consider some area, not a point" (Lim, 2007).

Schneider proposed four conditions in his study. He proposed four conditions for flat-foldability:

- "1. All crease lines must be straight line segments.
2. All interior vertices in the crease pattern must be of even degree.
3. At each interior vertex, the sum of every other angle must be 180° .
4. There must exist a superposition ordering function that does not violate the non-crossing condition" (Schneider, 2004).

2.4. Type Classification with Most Famous Origami Examples

2.4.1. Traditional origami

"Traditional designs are designs of uncertain origin. Nobody knows where they were first folded, when, by whom and sometimes why. Some may be a thousand years old or more" (Jackson, 1990).

Traditional origami is a straight fold on a square, planar piece of paper (Figure 20). During that process tearing, cutting or gluing are not allowed. It is commonly static and representational (Greenberg, 2011).

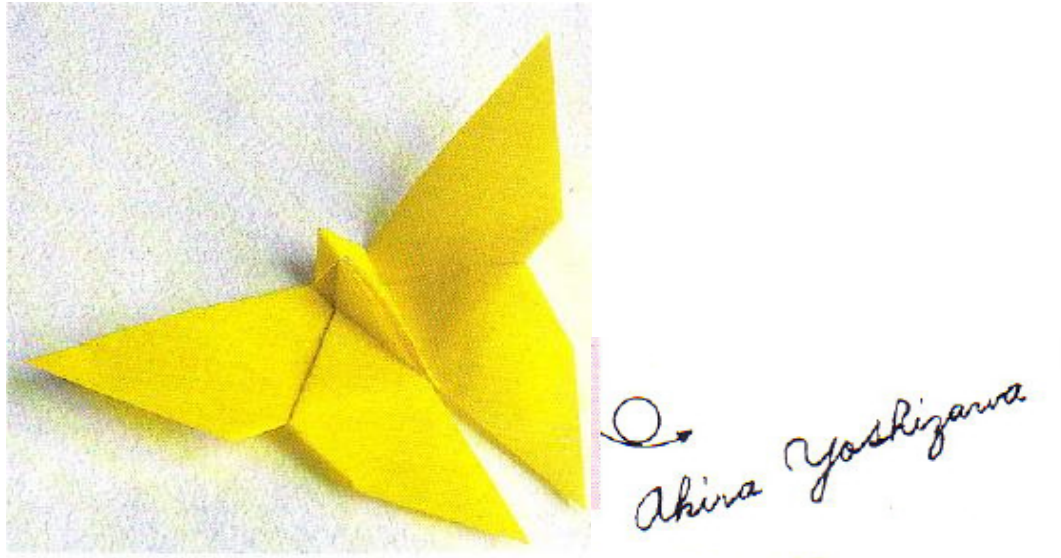


Figure 20. Yoshizawa`s Butterfly
(Source: Jackson, 1990.)

“Traditional origami models were often developed from similar patterns. While some of them are rarely used, there are six that are used quite frequently (Fig. 14): the waterbomb base, preliminary fold, kite base, fish base, bird base and frog base“ (WikiBooks, 2014). They also called as the classic bases, share the same symmetry, and certain structural properties, were used until the 1960s (WikiBooks, 2014).

2.4.2. Action Origami

"Action origami (Fig. 21) is a field of origami dealing with models that are folded so that they exhibit motion in their final, deployed state" (Lang J., 2013). Motion is not observed from folded state to unfolded state in action origami. Action origami models mostly have been improved as children`s toys: flapping cranes, tops, and paper airplanes. There are in fact hundreds of action origami models. From a single flat sheet of paper, engineers use many of complicated patterns to accomplish act, with one manufacturing

process- folding (Lang J., 2013). Engineers introduce the term “action origami” as "kinetic origami" (Greenberg, 2011).

Action origami (Figure 21) models have been created by various origami artists. The primary sources of action origami is in Lang and Shafer’s book (Lang J., 2013).

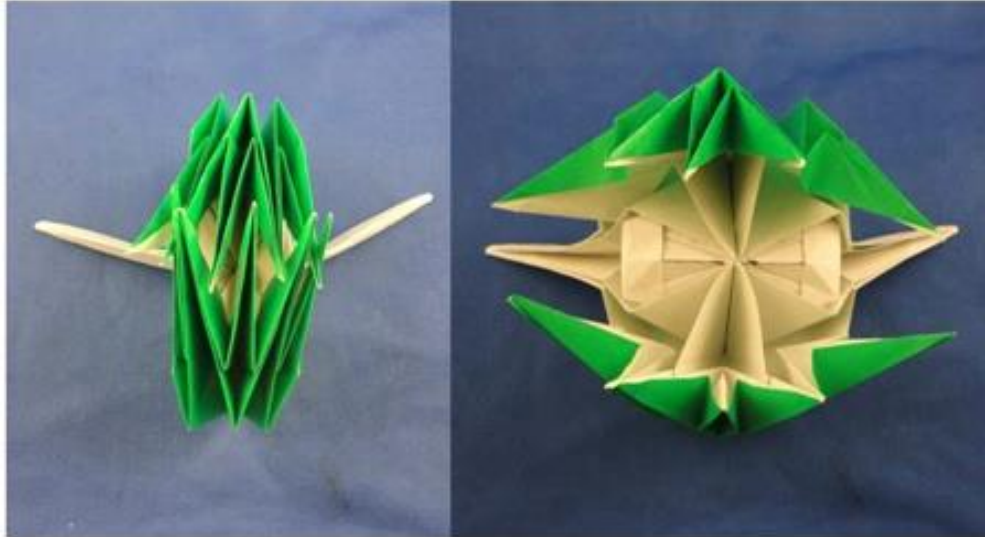


Figure 21. Shafer’s “Venus Fly Trap” is an Example of Action Origami (Source: Lang J., 2013.)

2.4.3. Rigid Origami

Rigid origami is a type of origami where all surfaces are rigid, except the crease lines. "If the plates could be replaced with nonflexible material and the creases with hinges while maintaining motion, the origami is considered **rigid**" (Lang J., 2013). Commonly rigid origami is used in manufacturing and packaging industry. A basic example is a shopping bag (Figure 22). Benefit of the material maintains self-folding of the origami structures. It transforms without the deformation of each facet (Figure 23). Folding process does not require bending or twisting (Greenberg, 2011).

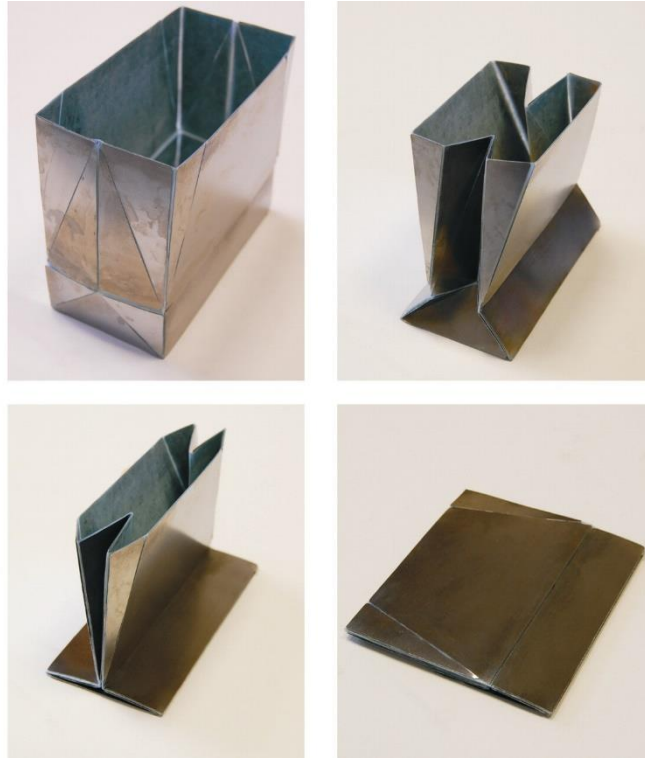


Figure 22. Origami Shopping Bag
(Source: Wu & You, 2011.)

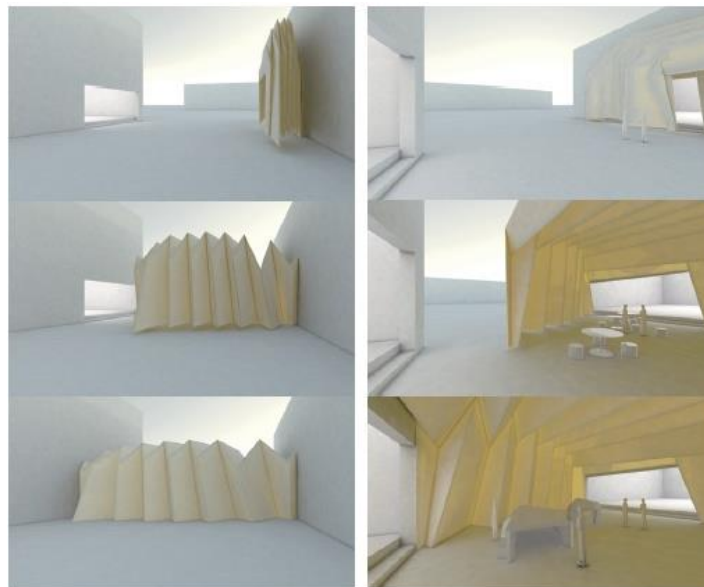
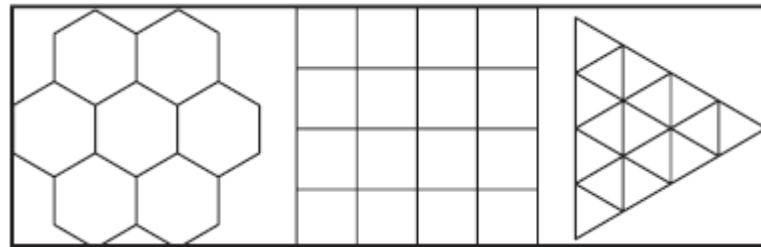


Figure 23. A Corrugated Vault Used as a Transformable Architecture that Connects Two Existing Buildings (Source: Tachi, 2010.)

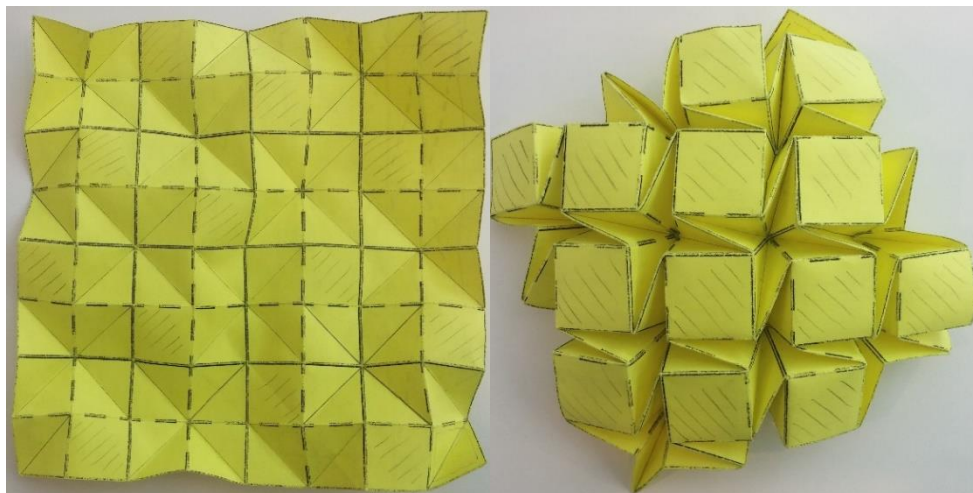
2.4.4. Origami Tessellation

Tessellations is repetition patterns of specific shapes (Figure 24 (a)). "The word "tessellation" comes from the Latin "tessella" meaning "small square" - which the Romans used for making mosaics and tile designs" (Gjerde, 2007).

In origami tessellation from a single sheet of paper, a complex repeating pattern of shapes are made. It was extended from simple square tilings to various pieces inspired by Islamic art. "There are three basic tessellation patterns, called "regular tessellations" which tile infinitely using only one shape" (Gjerde, 2007) These tilings are equilateral triangles, squares, and hexagons (Gjerde, 2007). It is clear that during developed acts from folded to unfolded forms tiles rotate Figure 24 (b)).



a)



b)

Figure 24. a) Hexagon, Square and Triangle- Basic Tessellation Patterns (Source: Gjerde, 2007); b) A Tessellation from a Square Twist Fold.

2.4.5. Kirigami (and Pop Up)

Kirigami is a variation of origami (Figure 25 and 26). The Japanese word Kirigami came from "*Cyrus*" or "kiru" means "to cut", "kami" means "paper". In order to make kirigami pattern, folded base is used and then it is cut. The cuts are opened and flattened to make the finished kirigami. It is defined as the art of folding and cutting paper (Hart, 2007). Kinetic kirigami models are often made planar materials, especially kirigami pop-up models (Greenberg, 2011).

Pop-up is similar to kirigami, but they have also a difference. Kirigami is made from a single piece of paper. Otherwise pop ups can be made of several pieces glued together (Carrek, 2014).



Figure 25. A Kirigami House Made in Cardstock
(Source: Greenberg, 2011.)

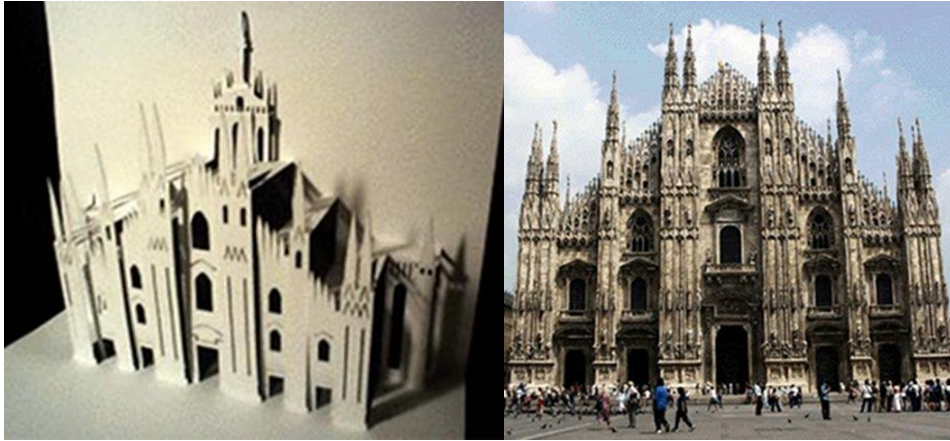


Figure 26. Duomo Milan
(Source: Carrek, 2014.)

2.4.6. Unit Origami (Modular Origami)

As the name emphasised, different numbers of units are prepared and assembled to produce many forms in unit origami folding method (Fuse, 1990).

"Because no adhesives are used, sometimes assemblies are unstable" (Fuse, 1990). But it never reduce interest of unit origami. There are also reasons for that curiosity. First it is easy. Second, folding process is like some of puzzles.

In 2012, 42-year-old Sergei Tarasov, a school teacher from the Russian village of Tigritskoe, has recently completed an incredibly detailed modular origami model of Moscow's St. Basil cathedral (Figure 27), 1.5 meter tall.



Figure 27. Modular Origami Model of St. Basil Cathedral
(Source: Spooky, 2012.)

2.4.7. 3D Geometric Origami

Much of the previous origami examples can be unfolded flat. In 3D origami main works focus on polyhedral structures (Dureisseix, 2011). That geometric foldings are created with Platonic or Archimedean solids by interlocking modules to each other. Module types and the base shape of the paper depend on the design of the solid (Karaveli, 2014).

"The Masu box (Figure 28) is a traditional Japanese design. It is a classic folded box; strong, adaptable, functional, and elegant in construction and final form" (Jackson, 2011).



Figure 28. Masu Box.

2.4.8. Wet Folding

Wet folding was a secret folding technique of the great Japanese master Akira Yoshizawa. In the latter half of the twentieth century, during the West tour Akira's audiences were impressed by his organic creation. The difference and effect of this folding is rather than making every crease sharp, soft, curved and rounded creases are obtained when the paper dries (R. J. Lang, 2004-2014d). For the wet folding, usually the heavier, stiffly art paper is suggested. A common problem occurred when beginners add too much water to paper (Figure 29).



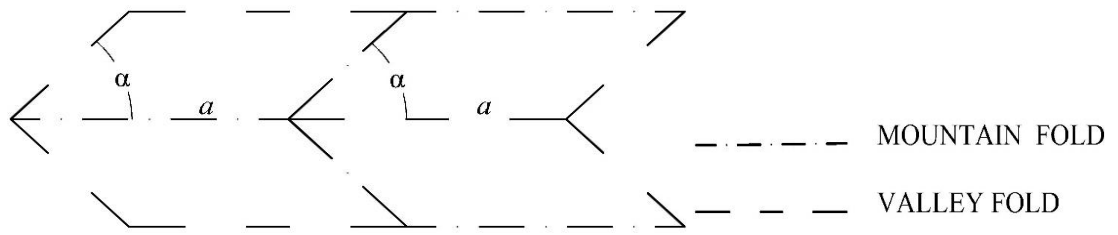
Figure 29. Wet Folding
(Source: Origami, 2014.)

CHAPTER 3

GEOMETRIC ANALYSIS OF THE MIURA-ORI PATTERN AND ITS DERIVATIONS

The Miura-Ori is a rigid foldable origami pattern that is formed from a tessellated arrangement of a single repeated unit geometry. The unit consists of four identical parallelogram plates. It can fold by rotation of rigid plates about hinged creases without twisting or stretching of the plates. **Miura unit** has a basic geometry with single vertex angle (α) and single span length (a) (Figure 30). Joseph M. Gattas and et al. introduced some derivative patterns by modifying single characteristic of the base Miura pattern. In this chapter, three samples are studied: Miura, Arc-Miura and Tapered Miura patterns (Gattas et al., 2013).

Arc-Miura pattern has common parameters with Miura pattern, just plus one more constant as vertex angle β for Arc-Miura (Figure 31). The specific feature of **Tapered Miura** pattern is its tapered lines spread out from a common center point (Figure 32). It has also one vertex angle. In this section, a new derivation of Miura-Ori is introduced by adding second vertex angle to Tapered Miura pattern. It is called as **Tapered Arc-Miura pattern** (Figure 33). Unlike Miura and Arc-Miura, Tapered Miura and Tapered Arc-Miura has one more angle parameter (taper angle ω), where in Miura and Arc-Miura this angle is zero and the straight crease lines are parallel.



a)

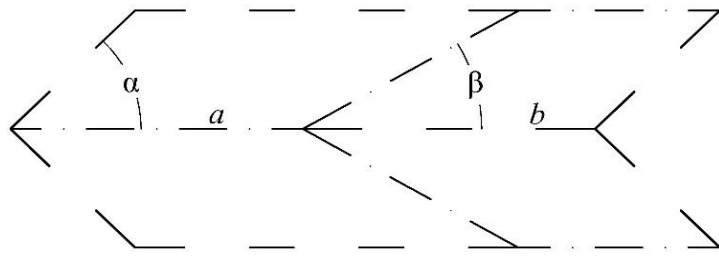


b)



c)

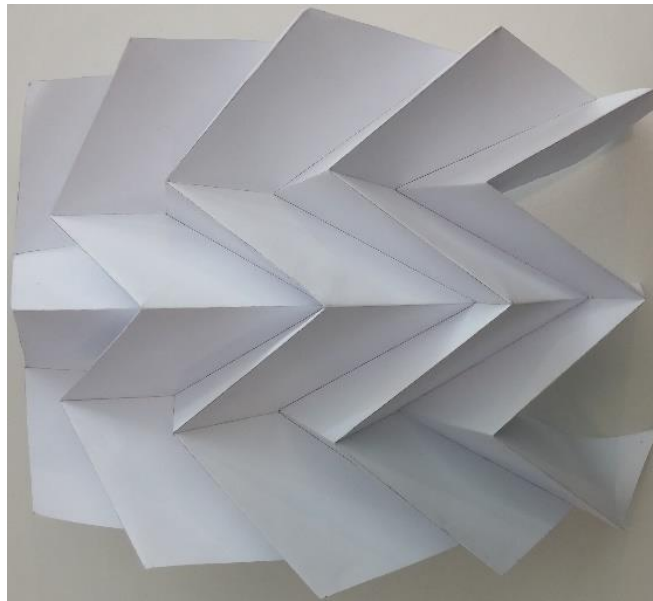
Figure 30. Miura-Ori pattern: a) Miura-Ori unit; b) Flat-Folded Miura-Ori Pattern; c) Partly Folded Miura-Ori Pattern.



a)

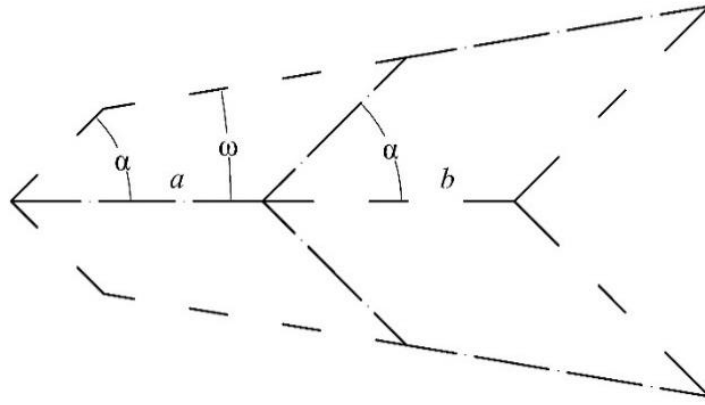


b)



c)

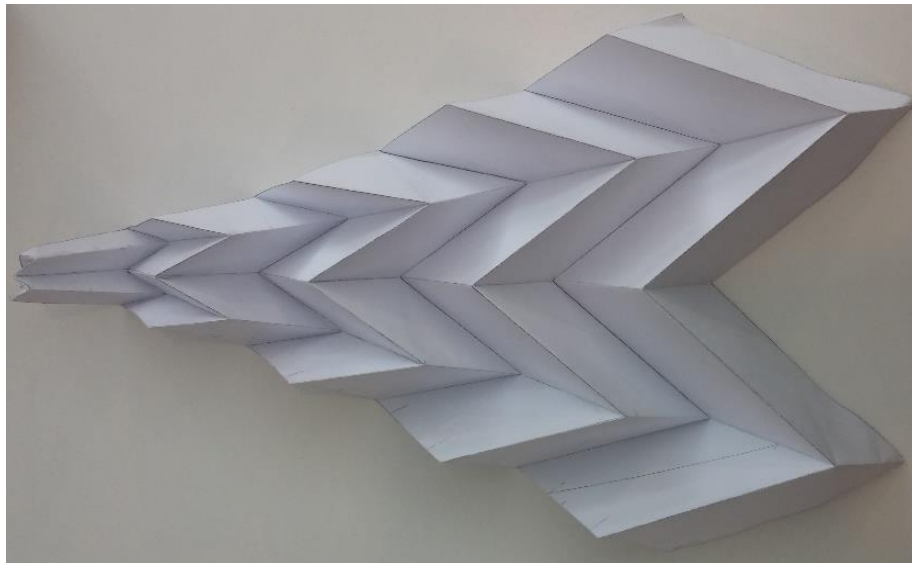
Figure 31. Arc-Miura Patterns: a) Arc-Miura Unit; b) Flat-Folded Arc-Miura Pattern; c) Partly Folded Arc-Miura Pattern.



a)

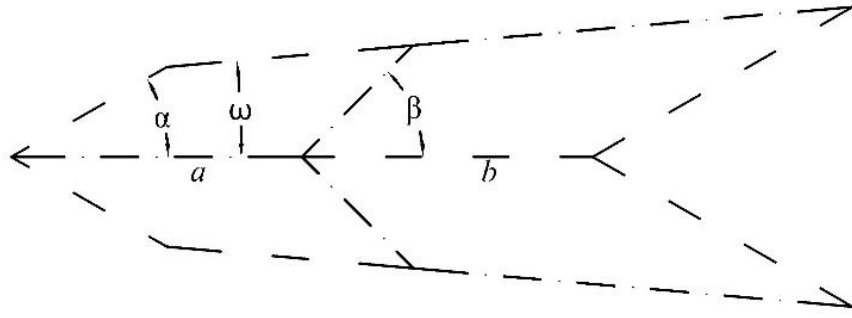


b)

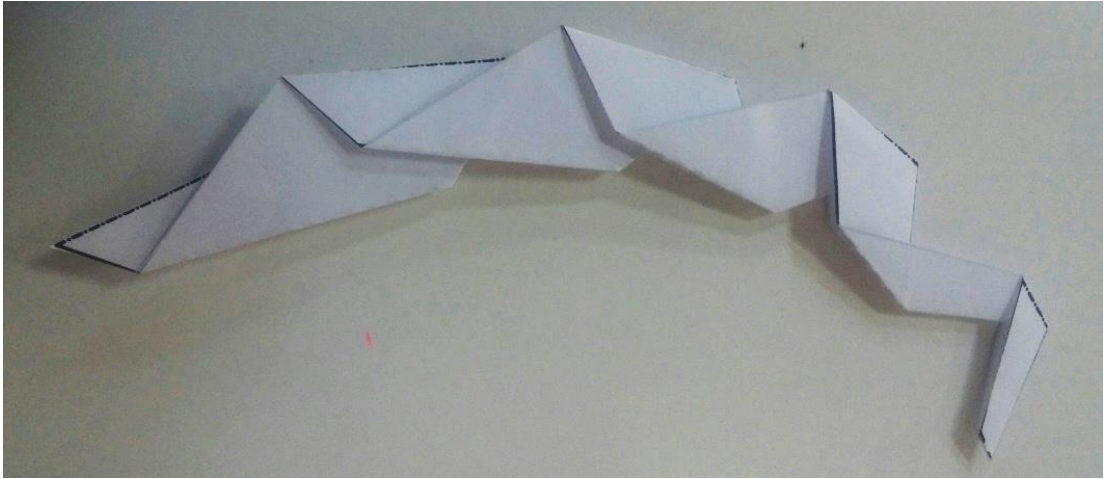


c)

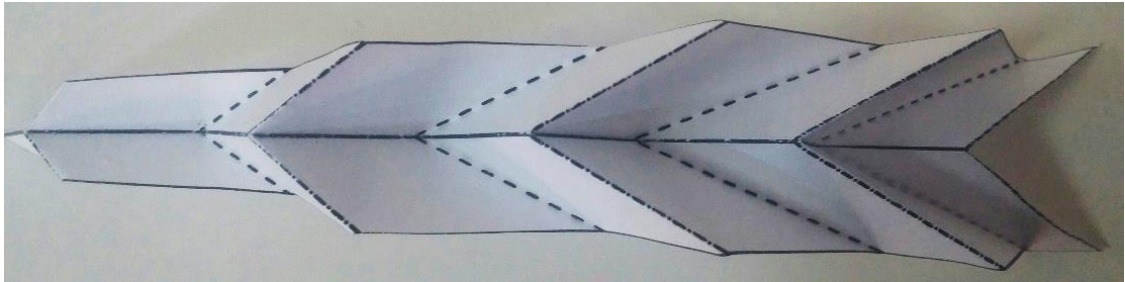
Figure 32. Tapered Miura patterns: a) Tapered Miura Unit; b) Flat-Folded Tapered Miura Pattern; c) Partly Folded Tapered Miura Pattern.



a)



b)



c)

Figure 33. Tapered Arc-Miura Patterns (left unfolded, right folded pattern): a) Tapered Arc-Miura Unit; b) Flat-Folded Tapered Arc-Miura Pattern; c) Partly Folded Tapered Arc-Miura Pattern.

As shown in the figures above, unfolded geometry of the pattern units involves vertex angles and span lengths. Miura pattern has single vertex angle α , however Arc-Miura and introduced Tapered Arc-Miura pattern has two vertex angles α , β that follows each other. Span lengths are equal in the all three patterns. During the analysis, the

possibility of different span lengths are also considered, so b is included as a second span length. The flat-folded forms of the patterns indicate main differences. Flat-folded Miura and Tapered Miura patterns illustrate as straight form, however Arc-Miura and Tapered Arc-Miura illustrate an arc form.

3.1. Geometric Approach to Miura-Ori Pattern

The geometry of the Miura-Ori pattern is analyzed by specified parameters. Vertex angle of Miura-Ori is always constant (Figure 30 (a)).

Specified parameters are expressed below,

$$\text{Vertex angle} = \alpha$$

$$\text{Span length}_1 = a$$

$$\text{Span length}_2 = b$$

Rotation angle (δ) and length of one unit (k) are another parameters will help to analyze the geometry (Figure 35). As,

$$\text{Rotation angle} = \delta$$

$$\text{Length of one unit} = k$$

3.1.1. Rotation Angle (δ)

In this step the rotation angle (δ) need to be calculated. Rotation angle is the turning value of a unit.

The angle ε is assistance angle for arranging relationship between vertex angle α and rotation angle δ (Figure 35). Using figure 34. the angle can be calculated as, below

$$\varepsilon = 180^\circ - \alpha \tag{3.1}$$

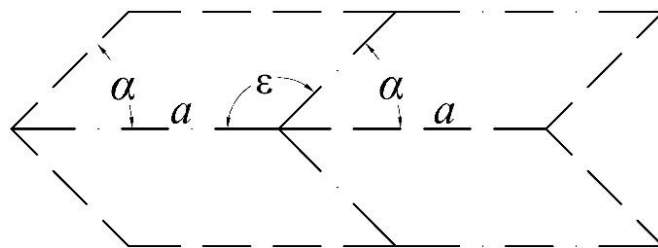


Figure 34. Assistance Angle ε on the Unfolded Miura-Ori Pattern.

To define the rotation angle δ in folded position (Figure 35), we refer flat position of the mechanism.

$$\delta = \varepsilon - \alpha = (180^\circ - \alpha) - \alpha = 180^\circ - 2\alpha \quad (3.2)$$

3.1.2. Unit Length (k)

The unit length of Miura-Ori pattern k_{ssl} (with same span length) is obtained by sine theorem.

$$\begin{aligned} k_{ssl} / \sin \delta &= a / \sin \alpha \\ k_{ssl} &= a \sin \delta / \sin \alpha = a \sin (180^\circ - 2\alpha) / \sin \alpha \end{aligned} \quad (3.3)$$

The unit length Miura-Ori pattern k_{dsl} (different span length) is obtained specially. The simple definition of the k_{dsl} is (Figure 35 (b))

$$k_{dsl} = c + y \quad (3.4)$$

And,

$$y = (d - c) / 2 \quad (3.5)$$

Using eq. (3.4.) and eq. (3.5.),

$$\begin{aligned} k_{dsl} &= c + y = c + (d - c) / 2 \\ k_{dsl} &= (d + c) / 2 \end{aligned} \quad (3.6)$$

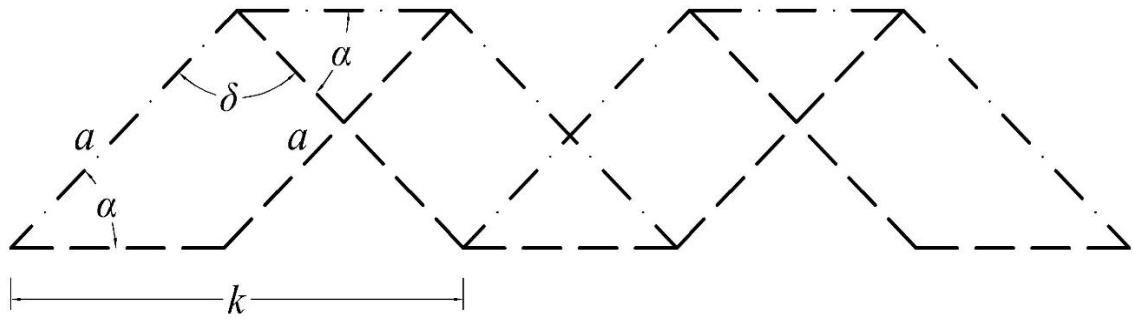
d is the base side of the triangle which consists of a , a , d sides and c is the base side of the triangle which consists of b , b , c sides. With the sine theorem c and d is expressed as,

$$d = a \sin \delta / \sin \alpha \quad (3.7)$$

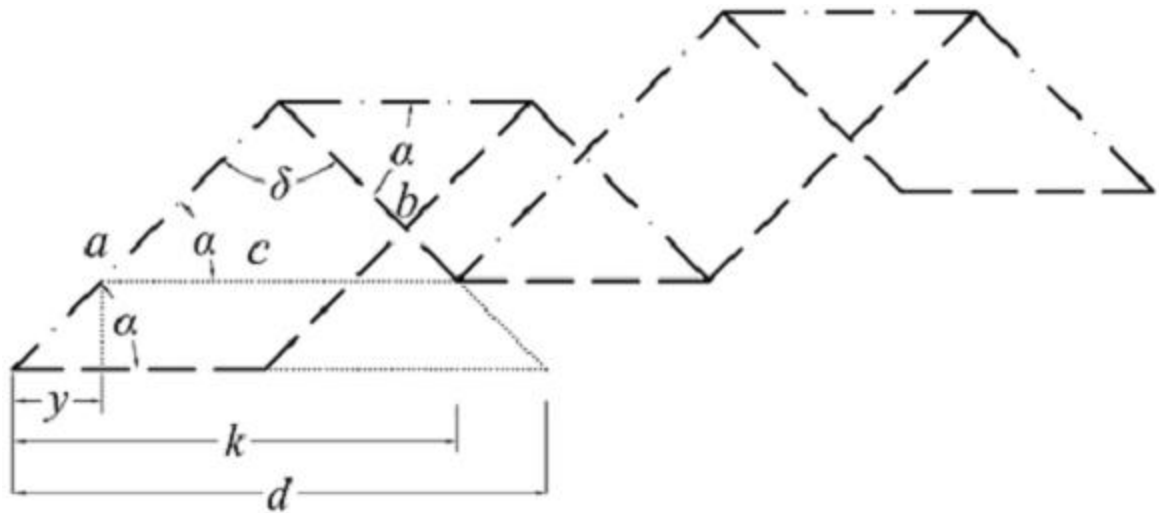
$$c = b \sin \delta / \sin \alpha \quad (3.8)$$

Thus, the final definition of the k_{dsl} is expressed with leading eq. (3.6.)

$$\begin{aligned} k_{dsl} &= (d + c) / 2 = (a \sin \delta / \sin \alpha + b \sin \delta / \sin \alpha) / 2 \\ k_{dsl} &= (a + b) \sin \delta / 2 \sin \alpha \end{aligned} \quad (3.9)$$



a)



b)

Figure 35. Parameters in the Folded Position of the Miura-Ori Pattern: a) flat-folded position with same span length ($a=b$); b) flat-folded position with different span length ($a \neq b$).

3.2. Geometric Approach to Arc-Miura Pattern

Geometric possibilities of Arc-Miura pattern are analyzed using specified parameters of vertex angles α , β , and span lengths a and b . The measurement module for the geometric analysis is the unit that is composed of 4 facets. In the first stage we have only four specified parameters (Figure 31 (a)), expressed as below

$$\text{Vertex angle}_1 = \alpha$$

$$\text{Vertex angle}_2 = \beta$$

$$\text{Span length}_1 = a$$

$$\text{Span length}_2 = b$$

Geometric analysis is developed on the flat-folded position of the pattern. The next step is to calculate other parameters δ_1 , δ_2 , γ , k , r , θ that are necessary to analyze whole pattern. The constants of c , d , x , y are assistant parameters (Figure 36). To extend and calculate parameters flat and folded positions of the pattern are observed and opposed. These parameters expressed as below

$$\text{Rotation angle}_1 = \delta_1$$

$$\text{Rotation angle}_2 = \delta_2$$

$$\text{External angle} = \gamma$$

$$\text{Unit Angle} = \theta$$

$$\text{Length of one unit} = k$$

$$\text{Radius of the Pattern} = r$$

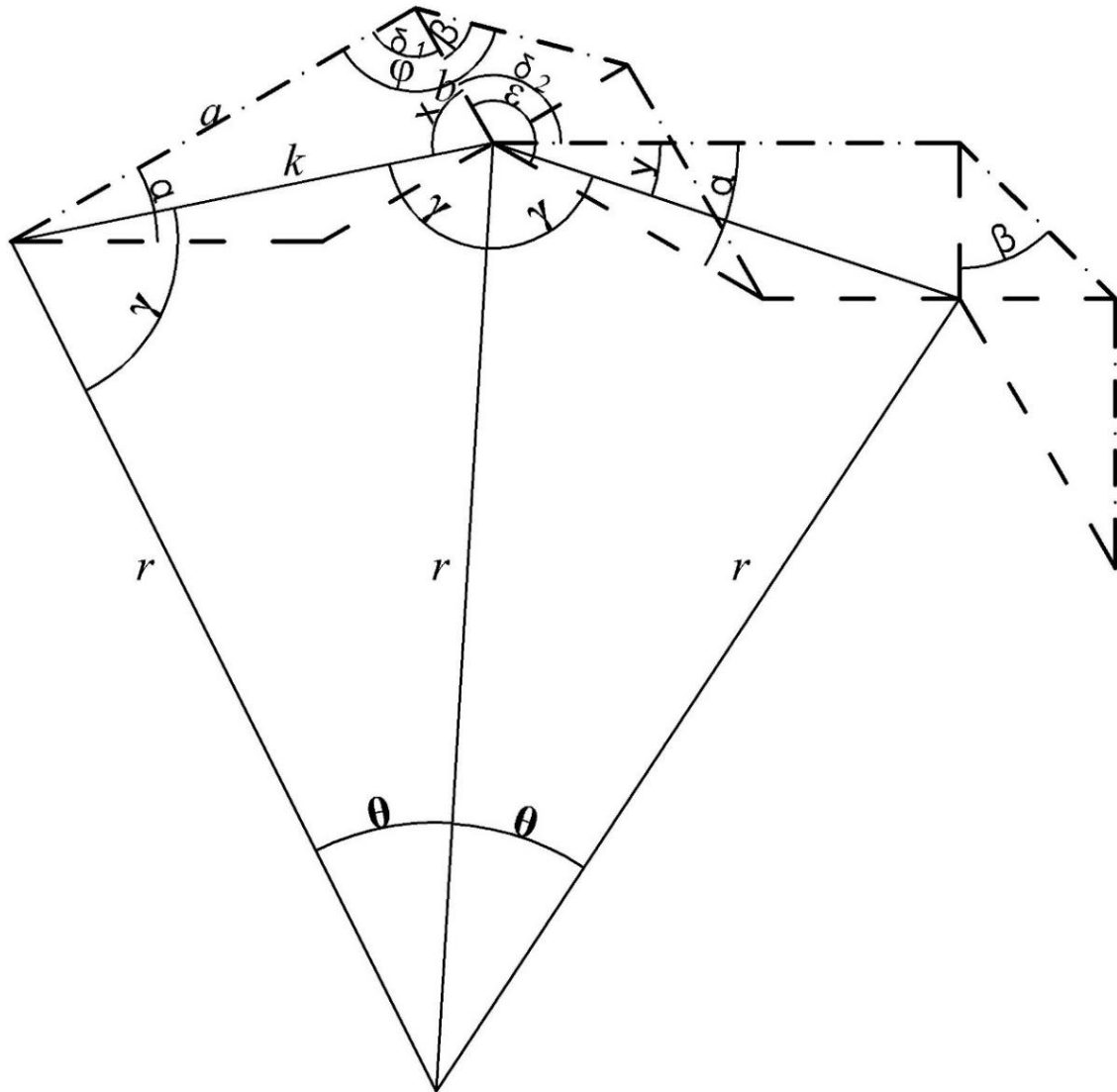


Figure 36. Parameters in the Folded Position of the Arc-Miura Pattern.

3.2.1. Rotation Angles of a Unit (δ_1, δ_2)

Calculation of second rotation angle δ_2 of Arc-Miura is same with rotation angle of Miura-Ori pattern. According to eq (3.2), δ_2 is expressed below

$$\delta_2 = \varepsilon - \alpha = (180^\circ - \alpha) - \alpha = 180^\circ - 2\alpha \quad (3.10)$$

The first rotation angle δ_1 is specified by another assistance angle φ (Figure 37). Using figure 37. the angle can be calculated as, below

$$\varphi = 180^\circ - \beta \quad (3.11)$$

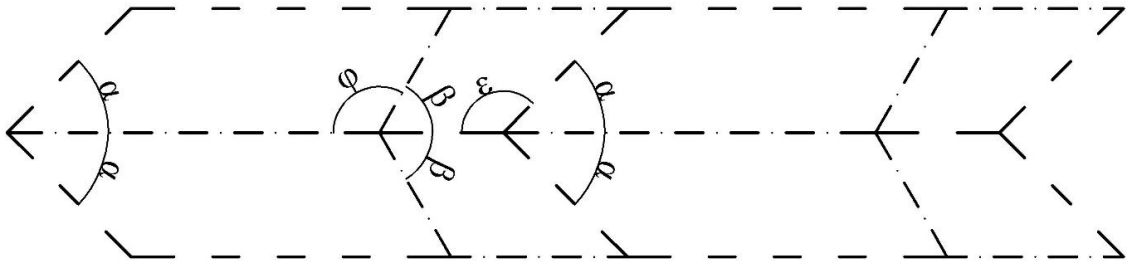


Figure 37. Assistance Angles ε and φ on the Unfolded Arc-Miura Pattern.

Then first rotation angle δ_1 is obtained according to folded position of the pattern (Figure 36), we refer flat position of the mechanism.

$$\delta_1 = \varphi - \beta = (180^\circ - \beta) - \beta = 180^\circ - 2\beta \quad (3.12)$$

3.2.2. External Angle (γ)

The external angle γ is obtained by the formula for the sum of the x , δ_2 , y , 2γ is equal 360° (Figure 38).

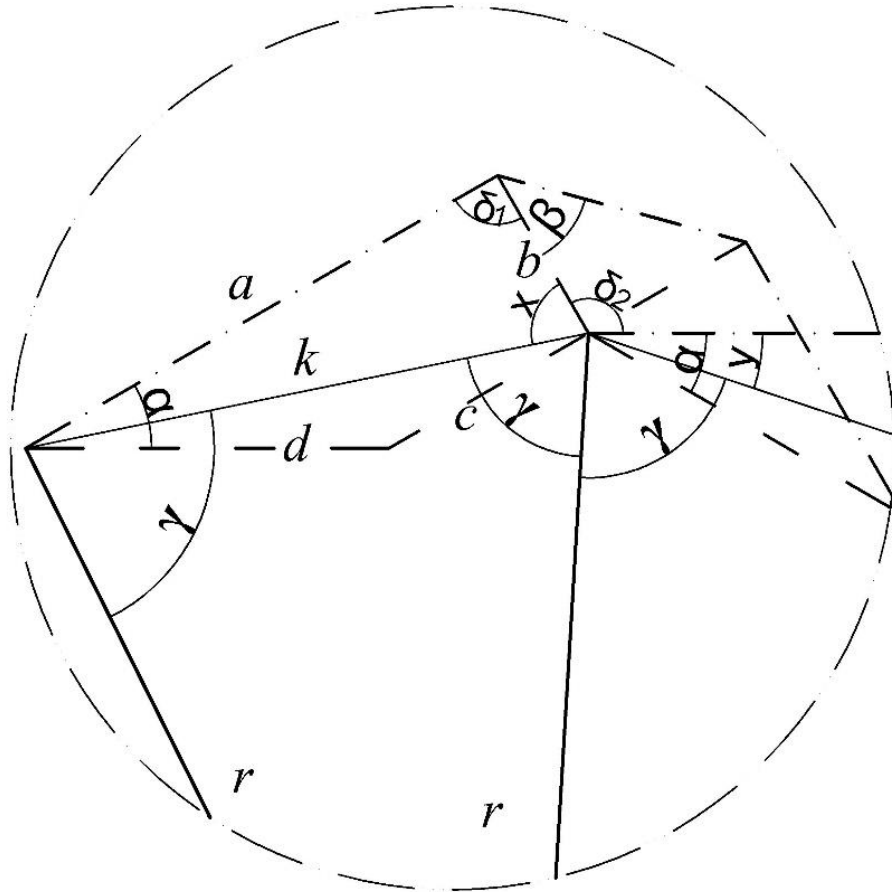


Figure 38. Piece of Pattern for Developing the External Angles.

According to figure 38, external angles can be expressed as below, eq (3.5).

$$x + \delta_2 + y + 2\gamma = 360^\circ \quad (3.13)$$

Using sum of the interior angles of a triangle helps to identify the x and y angles.

$$x + \delta_1 + y = 180^\circ$$

where $x+y$ is

$$x + y = 180^\circ - \delta_1 \quad (3.14)$$

After defining the sum of angles, the external angle γ can be calculated with using the eq. (3.13 and 3.14).

$$\begin{aligned}
\gamma &= (360^\circ - (x + \delta_2 + y))/2 = (360^\circ - (180^\circ - \delta_1 + \delta_2))/2 \\
&= (360^\circ - 180^\circ + \delta_1 - \delta_2)/2 = 90^\circ + \delta_1/2 - \delta_2/2 \\
&= 90^\circ + 90^\circ - \beta - 90^\circ + \alpha = 90^\circ - \beta + \alpha
\end{aligned} \tag{3.15}$$

There is a special condition;

$$\text{If } \beta > \alpha, \gamma = 90^\circ - \beta + \alpha;$$

$$\text{If } \beta < \alpha, \gamma = 90^\circ - \alpha + \beta;$$

The external angle γ helps to find radius r of the full pattern and unit angle θ .

3.2.3. Unit Angle (θ)

The unit angle can be calculated after γ is known. The formula for the *sum* of the angles in a *triangle helps to define* the unit angle θ . According to the triangle with r , k and r sides (Figure 36), θ can be specified as

$$\begin{aligned}
2\gamma + \theta &= 180^\circ \\
\theta &= 180^\circ - 2\gamma = 180^\circ - 180^\circ + 2\beta - 2\alpha = |2\beta - 2\alpha|
\end{aligned} \tag{3.16}$$

The formulation is presented in a module because of α and β amount.

3.2.4. The Length of a Unit (k)

k is the length of one unit and is also the base side of the triangle *which consists of* a , k and b sides. There, span lengths a , b and the rotation angle δ_1 are the specified parameters. In this triangle, k is obtained by using cosine theorem.

$$\begin{aligned}
k^2 &= a^2 + b^2 - 2ab \cos \delta_1 \\
k &= \sqrt{a^2 + b^2 - 2ab \cos \delta_1}
\end{aligned} \tag{3.17}$$

3.2.5. The Radius of the Pattern (r)

r is the radius of the pattern and obtained by the triangle *which consists of* r , k and r sides, with sine theorem.

$$r / \sin \gamma = k / \sin \theta$$

where r is

$$r = k \sin \gamma / \sin \theta = k \sin \gamma / \sin (180^\circ - 2\gamma) \tag{3.18}$$

3.3. Geometric Approach to Tapered Miura and Tapered Arc-Miura Pattern

Tapered Miura is basically similar with Miura pattern as seen in figure 39. The added lines create new angle that is called taper angle ω . Taper angle is also the starting vertex angle of Tapered Miura. Pattern starts with taper angle ω , then first vertex angle α and second vertex angle β . Tapered Arc-Miura has the same characters with Arc-Miura. As a consequence, Miura and Tapered Miura, Arc-Miura and Tapered Arc-Miura are similar patterns of each other. Because of these resemblances, these patterns do not have special geometric studies. Taper angle is an independent variable and does not affect the analysis. Taper angle is obtained according to the number of plates.

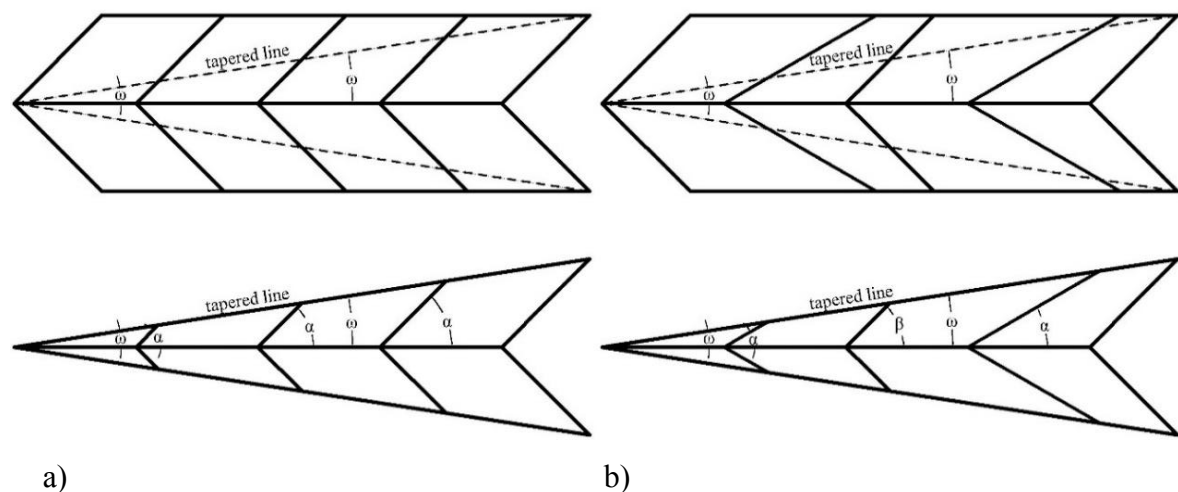


Figure 39. Creating of Tapered Miura and Tapered Arc-Miura Pattern: a) From Miura Pattern to Tapered Miura; b) From Arc-Miura to Tapered Arc-Miura Pattern.

3.4. Validity of the Developed Formulas

Miura-Ori and its derivations are reviewed with three different vertex angles and same span lengths. In order to testify the validity of the developed formulas Microsoft Excel is used. Derived formulas are placed into the cells. According to assigned values of the specified parameters, rest parameters are calculated. Then flat-folded positions of the

patterns are drawn in Autocad. This software helps to measure exact values of the drawings.

3.4.1. Review of the Miura-Ori

Three different Miura-Ori are analyzed. These patterns have 30° , 45° , 60° vertex angles. Span length a is 4 and equal to b in all three. (Table 1. and Figures 40).

Table 1. below shows Excel calculations of all the studied constants. Vertex angle α is different in all three examples.

Table 1. Comparison of the Unit Lengths Caused by Different Vertex Angles.

Vertex Angles (α)	Span length ₁ (a)	Span length ₂ (b)	Rotation angle (δ)	Unit Length (k)
30	4	4	120	6,928
45	4	4	90	5,657
60	4	4	60	4

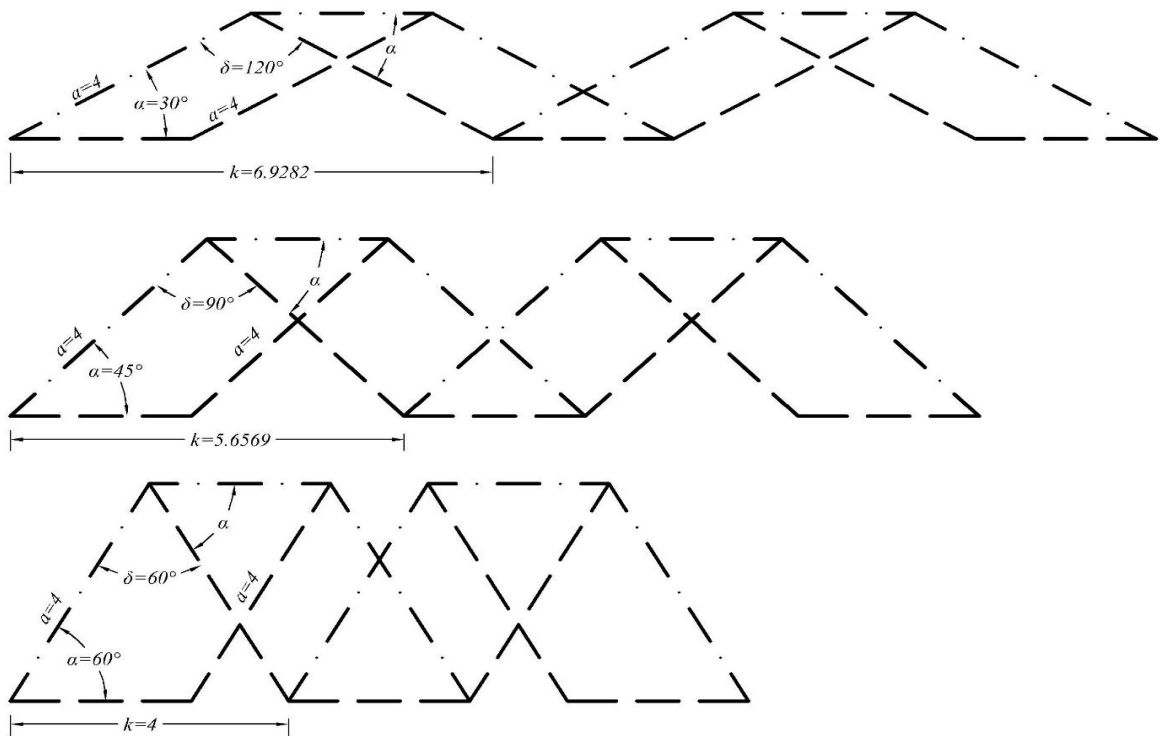


Figure 40. Miura-Ori folded patterns where α is equal to 30° , 45° and 60° .

Figure 40. is Autocad drawings of the analyzed patterns. The measurement of the constants on the drawings validates the study.

The research on Miura-Ori result the distinction in folded position of the patterns (Figure 40). The vertex angles affect the pattern rotations and cause the distinction of the unit lengths.

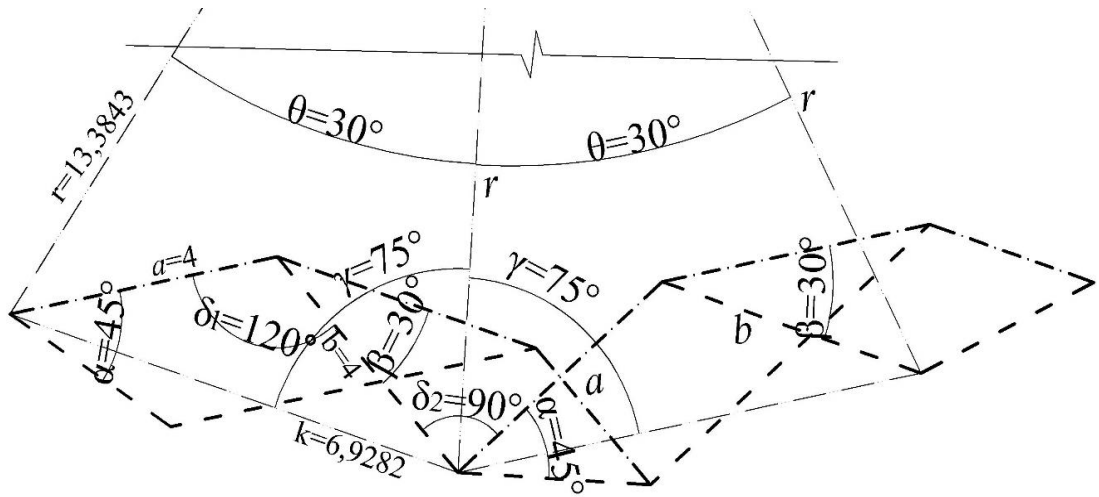
According to figure 40. we can explain relations between vertex angles and unit lengths. In the first example, the folded pattern with 30° vertex angles has 6.93 cm unit length. The unit length of the second pattern ($\alpha=45^\circ$) is 5.65 cm, and third pattern ($\alpha=60^\circ$) is 4 cm. Three examples verify that vertex angle α is inversely proportional to unit length k . The increase of the vertex angles cause the decrease of the unit lengths of the patterns.

3.4.2. Review of the Arc-Miura

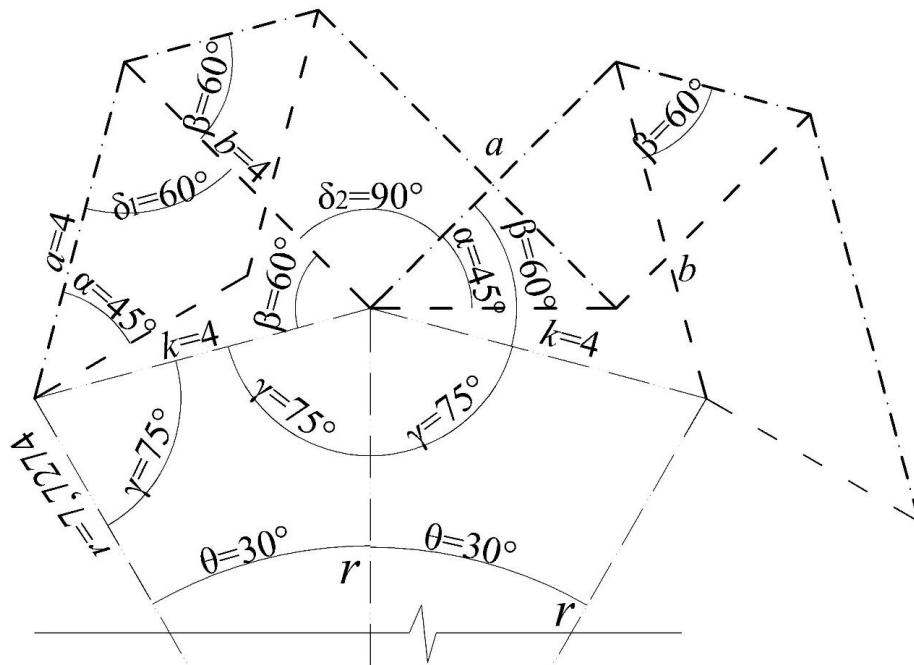
Type 1. Three different type 1 Arc-Miura are analyzed. These arcs have 45° & 30° , 45° & 60° , 45° & 75° vertex angles. Span length a is 4 cm and equal to b . (Table 2. and Figure 41).

Table 2. Checking for Calculation of Type 1.

Vertex angle ₁ α	Vertex angle ₂ β	Span length ₁ a	Span length ₂ b	Rotation angle ₁ δ_1	Rotation angle ₂ δ_2	External angle γ	Unit angle θ	Unit length k	Radius r
45	30	4	4	120	90	75	30	6,9282	13,384
45	60	4	4	60	90	75	30	4	7,7274
45	75	4	4	30	90	60	60	2,0706	2,0706



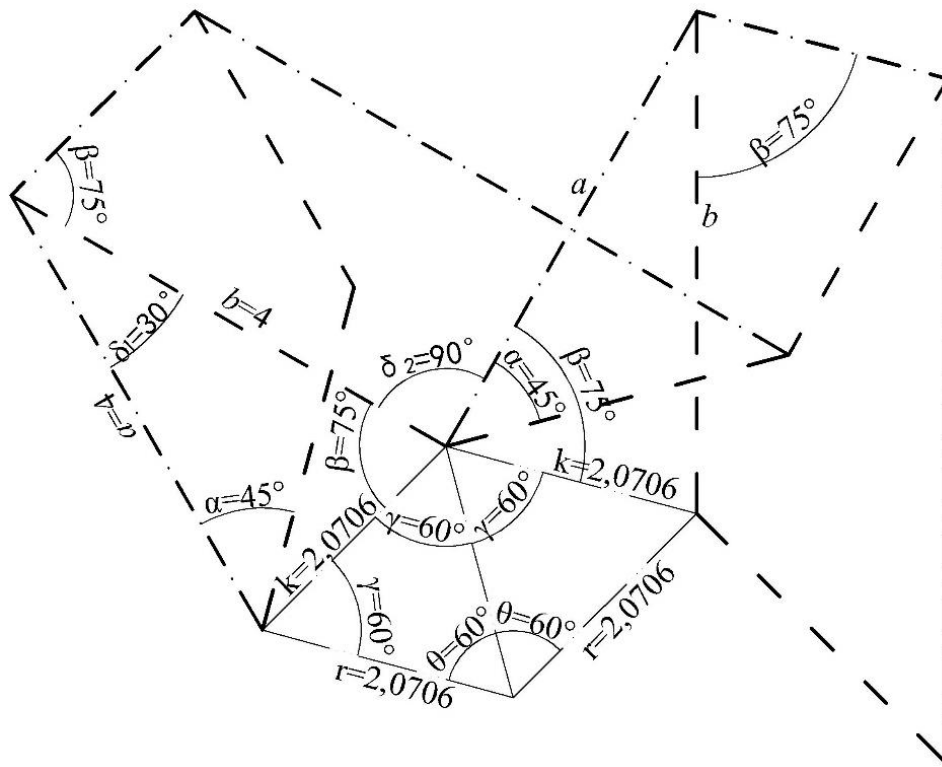
a)



b)

Figure 41. Type 1 Patterns. a) The Arc-Miura unit with 45°&30° vertex angles; b) The Arc- Miura unit with the 45°&60° Vertex Angles; c) The Arc-Miura unit with 45°&70° vertex angles.

(cont. on next page)



c)

Figure 41. (cont.)

Type 2. Three different type 2 Arc-Miura are analyzed. These arcs have 45° & 30° , 45° & 60° , 45° & 75° vertex angles. Span length a is 4 cm and equal to b . (Table 3. and Figure 42).

Table 3. Checking for Calculation of Type 2.

Vertex Angles	α	β	a	b	δ_1	δ_2	γ	θ	k	r
30° & 15°	30	15	4	4	150	120	75	30	7,7274	14,928
30° & 45°	30	45	4	4	90	120	75	30	5,6569	10,928
30° & 60°	30	60	4	4	60	120	60	60	4	4

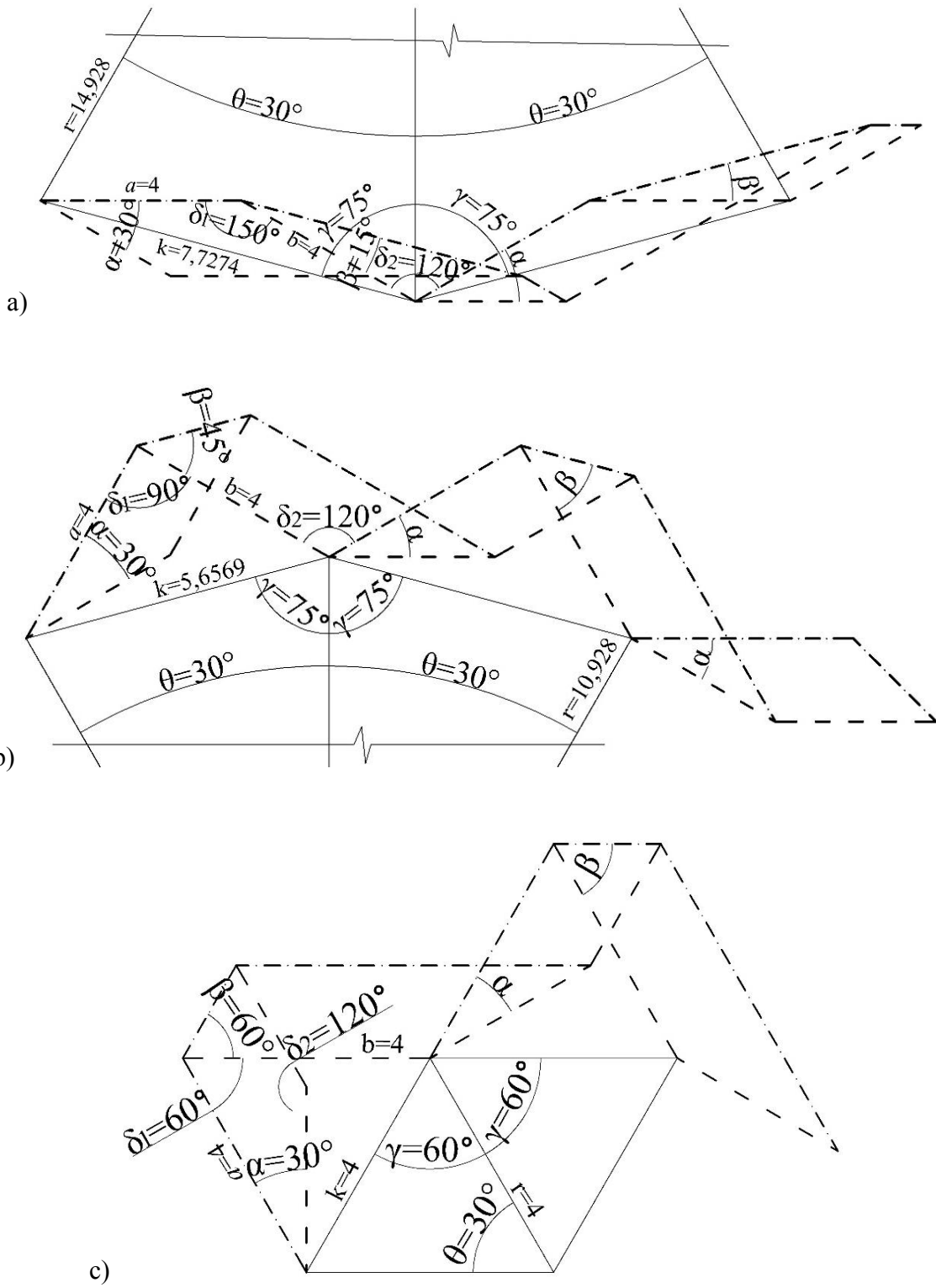


Figure 42. Type 2 Patterns. a) Arc-Miura unit with the 30°&15° vertex angles; b) Arc-Miura unit with the 30°&45° vertex angles; c) The 30°&60° Vertex Angles Pattern.

The table 2. and table 3. show Excel calculations of all the studied constants. Each vertex angle α is equal for its three examples and second rotation angle δ_2 , and first vertex angles α are dependent to each other. Thus the second rotation angle (δ_2) of all three samples are equal. In the first and second samples, unit angle θ are equal, because they were specified by the relationship of vertex angles β and α . Furthermore, the values of the γ are also equal. In the Figure 41 (c). equilateral triangle and in the Figure 42 (c). isosceles triangle is shown which consists of r , k and r sides.

Figure 41. and b26. are Autocad drawings of the studied patterns. The validity of the calculation is approved after measurement of the constants on the drawings.

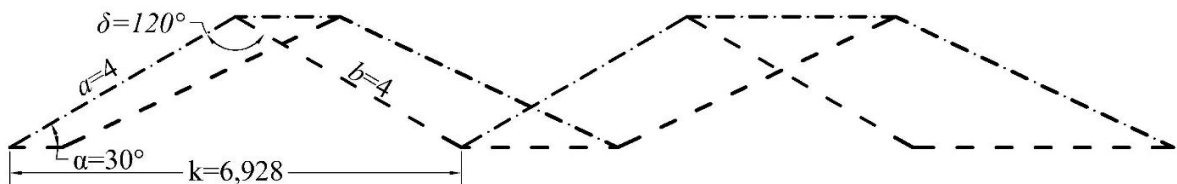
3.4.3. Review of the Tapered Miura Pattern

Three different Tapered Miura patterns are analyzed. These patterns have 30° , 45° and 60° vertex angles. In these patterns, a is 4 and equal to b . (Table 4. and Figures 43).

Tapered pattern has only one vertex angle α is different in all examples. Table 4. Below shows Excel calculations of all the studied constants which is exactly same with Miura pattern calculation (same with Table 1).

Table 4. Comparison of Tapered Patterns.

Vertex Angles (α)	Span length ₁ (a)	Span length ₂ (b)	Rotation angle (δ)	Unit Length (k)
30	4	4	120	6,928
45	4	4	90	5,657
60	4	4	60	4



a)

Figure 43. Miura-Ori Folded Patterns. a) The Piece of the 30° Vertex Angles; b) The Piece of the 45° Vertex Angles; c) The Piece of the 60° Vertex Angles.

(cont. on next page)

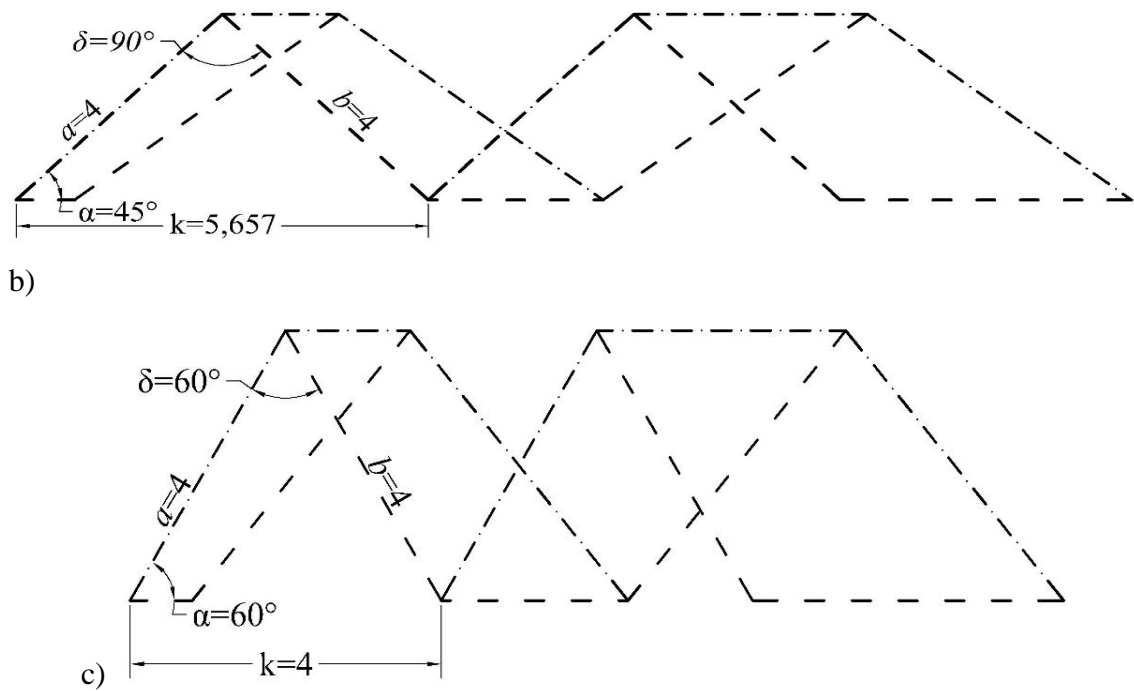


Figure 43. (cont.)

Figure 43. is Autocad drawings of the studied patterns. The measurement of the constants on the drawings validates the study.

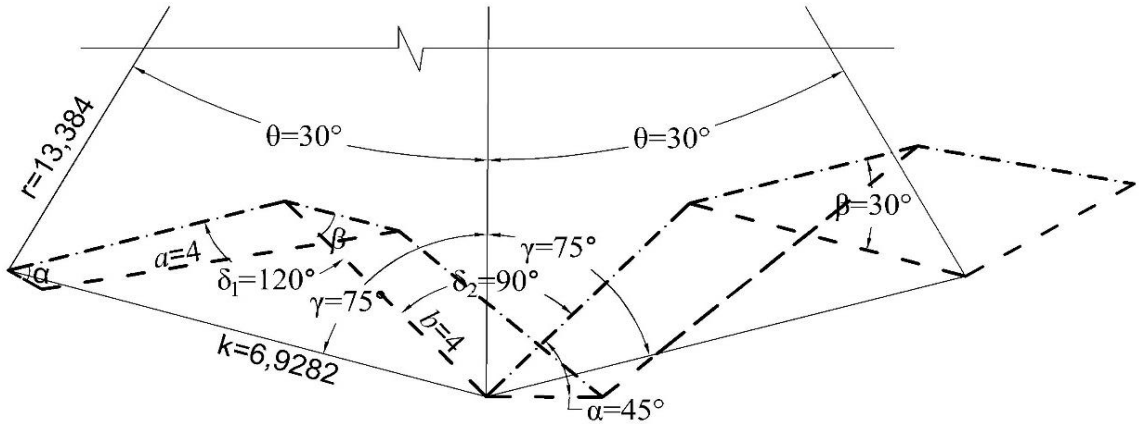
3.4.4. Review of the Tapered Arc-Miura Pattern

Three different Tapered Arc-Miura will be analyzed. These arcs have 45°&30°, 45°&60°, 45°&75° vertex angles. Span length a is also 4 cm and equal to b . (Table 5. and Figure 44).

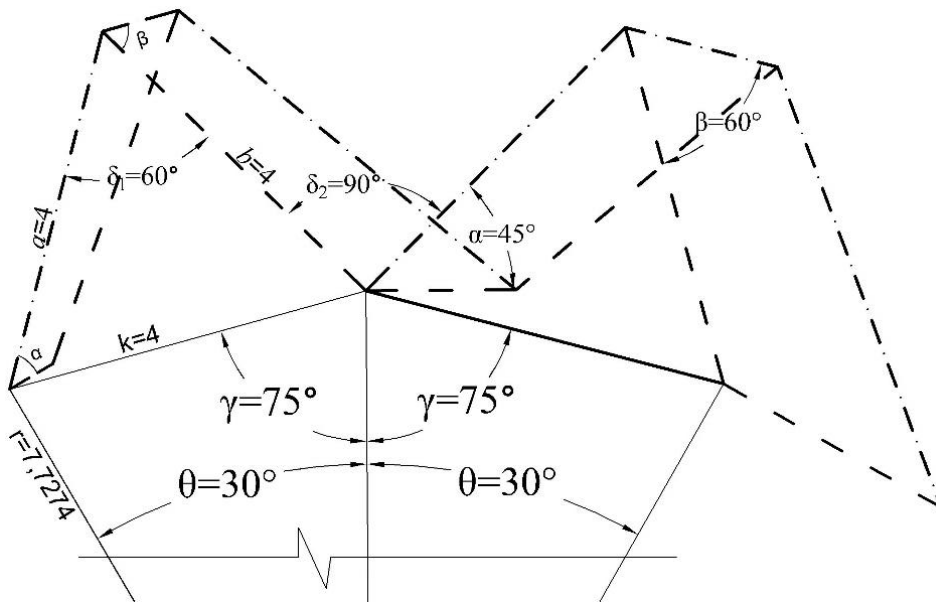
Table 5. shows Excel calculations of all the studied constants. It is exactly same with Arc-Miura pattern calculation (same with Table 2).

Table 5. Checking for Calculation of Tapered Arc-Miura.

Vertex angle1 α	Vertex angle2 β	Span length1 a	Span length2 b	Rotation angle1 δ_1	Rotation angle2 δ_2	External angle γ	Unit angle θ	Unit length k	Radius r
45	30	4	4	120	90	75	30	6,9282	13,384
45	60	4	4	60	90	75	30	4	7,7274
45	75	4	4	30	90	60	60	2,0706	2,0706



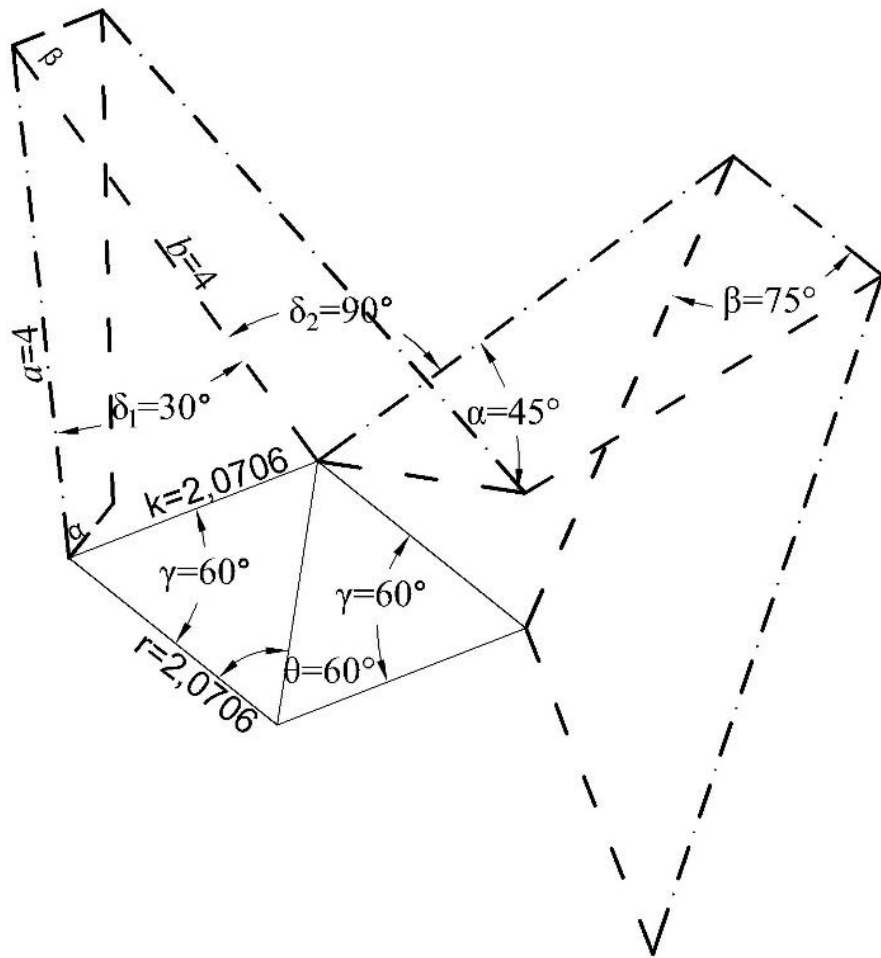
a)



b)

Figure 44. Tapered Miura folded pattern with Same Span Lengths. a) The Piece of the 45°&30° Vertex Angles; b) The Piece of the 45°&60° Vertex Angles; c) The 45°&75° Vertex Angles Pattern.

(cont. on next page)



c)

Figure 44. (cont.)

Figure 44. is Autocad drawing of the studied patterns. The validity of the calculation is approved after measurement of the constants on the drawings.

3.4.5. Conclusion

During the research of Arc-Miura, the curvature distinctions are recognized in folded position of the patterns (Figure 45). The vertex angles affect the pattern rotations.

Considering figure 45. we can explain relations between the vertex angles and the folded forms. In the first example, the folded pattern with 45° & 30° vertex angles takes a convex form. Second example with 45° & 45° vertex angles presents a straight form. Third example with 45° & 60° vertex angles, and fourth example with 45° & 75° vertex angles take

concave forms. As a consequence of the curvature distinction (Figure 45), three circumstances can be investigated, as below

- 1) if $\alpha > \beta$, folded pattern takes convex form;
- 2) if $\alpha = \beta$, folded pattern takes straight form;
- 3) if $\alpha < \beta$, folded pattern takes concave form.

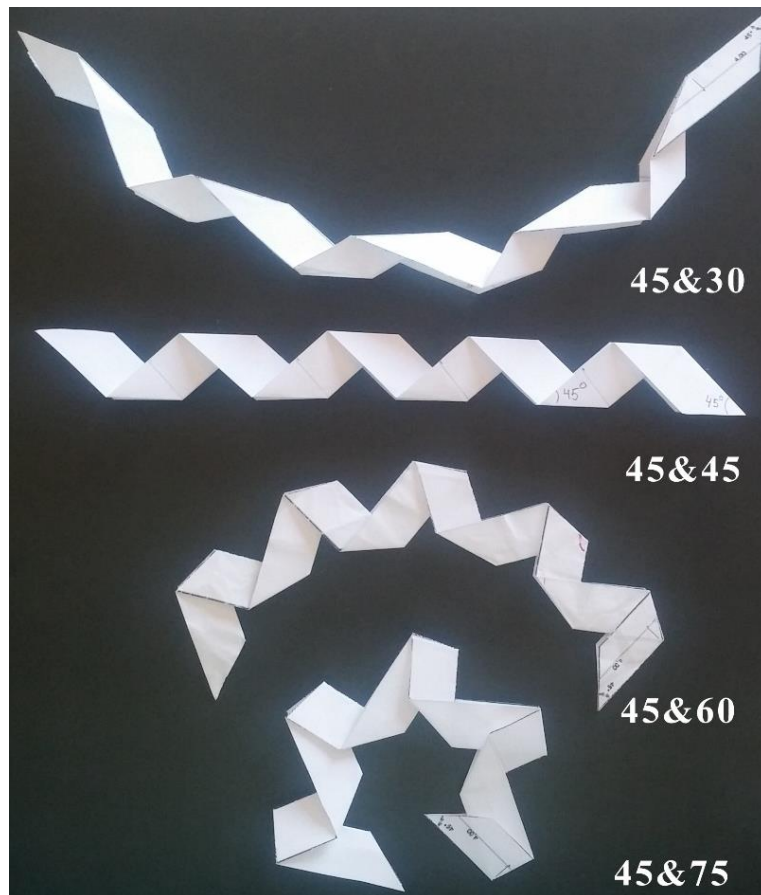


Figure 45. Curvature Distinction of Folded Arc-Miura Pattern.

The difference between the vertex angles determine the radius of the folded pattern. If the difference between the angles decrease, the radius increase or vice versa.

Although the span lengths of the patterns are equal, $45^\circ&30^\circ$ and $45^\circ&60^\circ$ angle patterns complete full surroundings with 12 units, however $45^\circ&75^\circ$ pattern with 6, numbered in figure 46 (a). The angle difference in the $45^\circ&30^\circ$ and $45^\circ&60^\circ$ patterns are $\pm 15^\circ$, while it is $\pm 30^\circ$ in the $45^\circ&75^\circ$ pattern. The result is also same for type 2.; if vertex angle difference is $\pm 15^\circ$, circle complete with 12 units and if it is $\pm 30^\circ$, circle complete with 6 units (Figure 46 (b)).

Unit number can be obtained by the difference of vertex angles,

$$360^\circ / (\beta - \alpha) = n_{link} \quad (3.19)$$

Type 1. and type 2. have different vertex angles, but the vertex angle difference is similar in each first, second and third example. Some similarities are observed as: δ_2 in each parts are equal, γ and θ in all types are equal (Table 2. and 6).

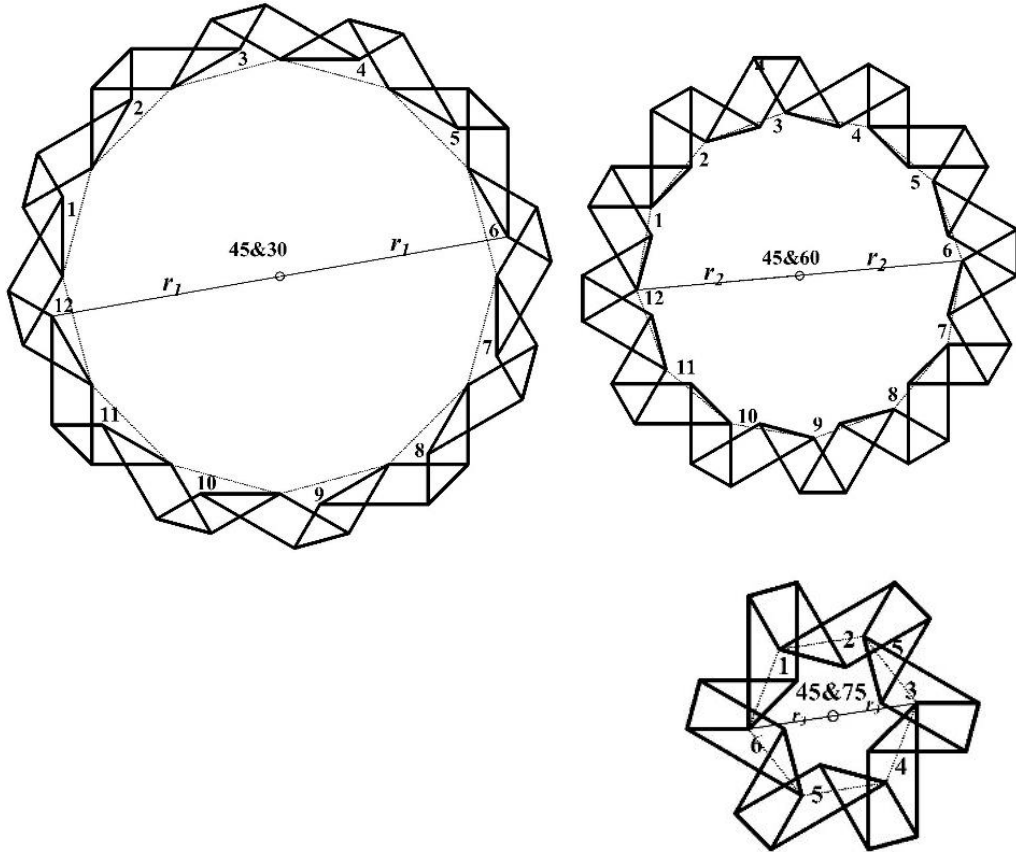
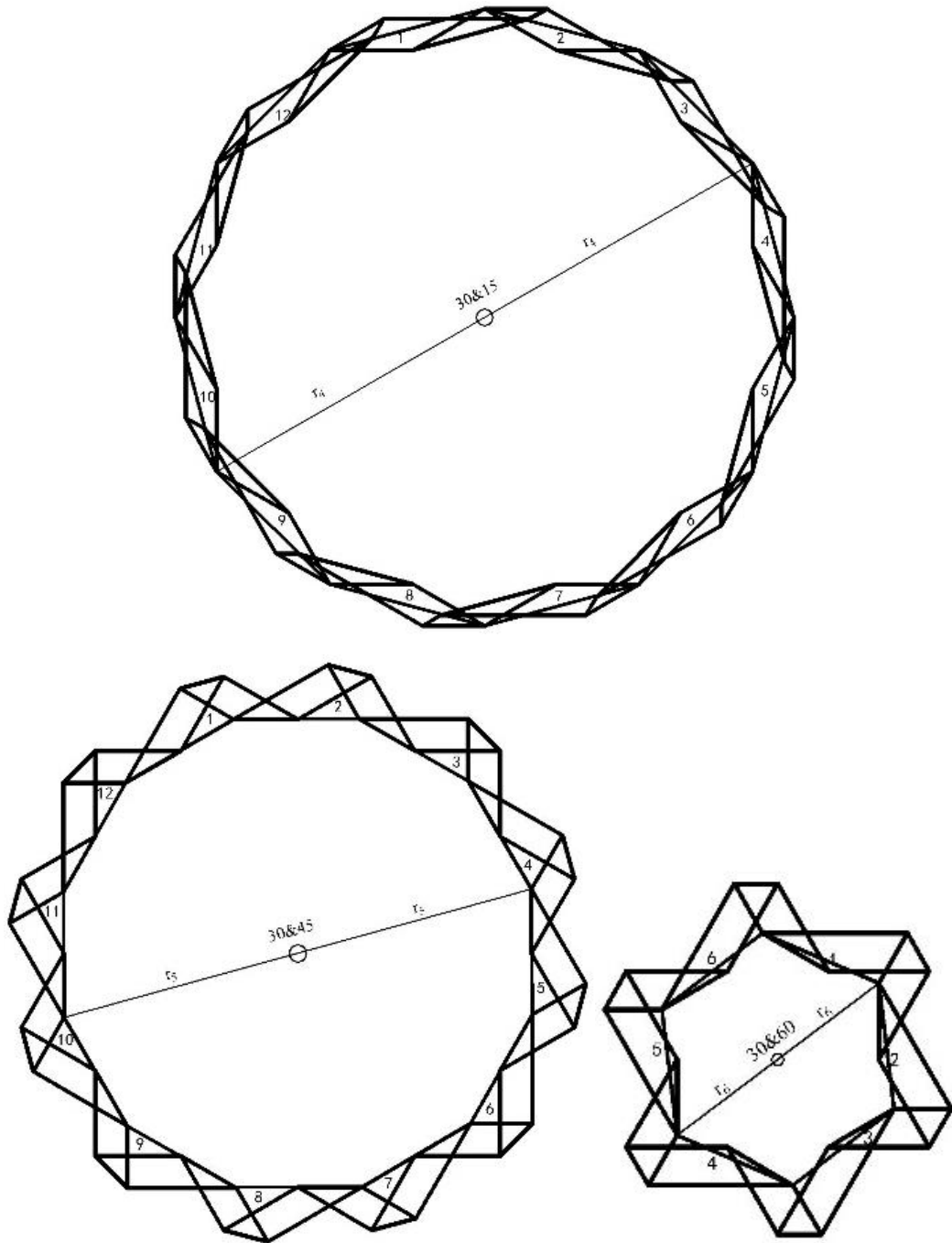


Figure 46. Numbered folded patterns. a) Type 1. Pattern; b) Type 2. Pattern.

(cont. on next page)



b)

Figure 46. (cont.)

CHAPTER 4

MOBILITY ANALYSIS OF MIURA ORI PATTERN

The Miura-Ori unit is composed of a symmetrical degree-4 vertices. Degree-4 vertex consists of four intersecting crease lines which are symmetric about a horizontal centerline. This unit is a four bar spherical mechanism with a single degree of freedom (DOF). A four bar spherical mechanism is a rotational manipulator with all axes intersecting at the center of the sphere (Lum, Rosen, Sinanan, & Hannaford, 2006). The axes indicate the directions of all revolute joints. A spherical four-bar mechanism is shown in figure 47.

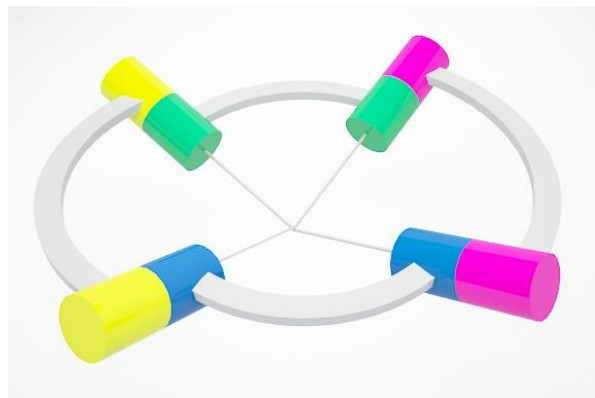


Figure 47. A Spherical Four-Bar Mechanism.

Figure 48 illustrates the similarity between a Miura-Ori unit and a spherical mechanism. The origami creases are analogous to hinges and the facets are analogous to rigid plates. Note that four creases intersect at a vertex.



Figure 48 Miura-Ori Unit as a Spherical Mechanism
(Source: Mooth, 2014.)

4.1. Determining DoF of Miura-Ori Pattern

Miura-Ori unit is a spherical mechanism with its rigid plates and revolute joints. An unfolded unit of the Miura-Ori pattern, constructed from four identical parallelogram plates and four revolute joints, is shown in Fig. 49. Each vertex has four crease lines and the mechanism works with one degree of freedom.

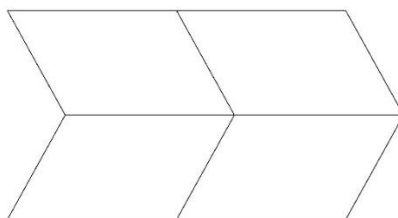


Figure 49. An Unfolded Miura-Ori Unit.

Considering Miura-Ori origami as a mechanism, the mobility of the unit can be calculated with Grubler Kutzbach formula (Phillips, 2006) as (4.1.),

$$M = \lambda(n-1) - \sum_{i=1}^5 (\lambda-i)j_i \quad (4.1.)$$

where λ is the DoF of space in which the mechanism operates ($\lambda = 3$ for spherical mechanisms), n is number of plates and j_i is number of joints having i DoFs.

The dimension of active motion of rigid body for spherical mechanism is RRR. The dimension of subspace is $\lambda=3$. So, the formula is given, as

$$M = 3(n-1) - 2j_1 - j_2 \quad (4.2.)$$

where j_1 is the number of single degree of joints, j_2 is the number of two degree of freedom joints.

The joints of the Miura-Ori are all revolute. Revolute joints have one degree of freedom, so j_2 is reduced from eq. (4.2.). Mobility of a Miura-Ori can be calculated as follows,

$$M = 3(n-1) - 2j_1 \quad (4.3)$$

$$M = 3(4-1) - 2 \times 4 = 1$$

The sum of plates in Miura-Ori pattern can be calculated by eq. (4.4.),

$$\sum \text{plate} = a \times b \quad (4.4)$$

where $\sum \text{plate}$ is the number of plates, a is the number of columns and b is the number of rows.

The sum of joints can be calculated by eq. (4.5.),

$$\sum j = a(b-1) + b(a-1) \quad (4.5)$$

where $\sum j$ is the sum of joints.

Developing a mobility analysis on Miura-Ori involves studying twelve items (Figure 50, 51 and 52). These patterns are established with adding new facets to the base pattern. Patterns in the numbered steps line up horizontally. Numbered steps differ by column numbers, each one has one more column facets. The derivations are needed to check whether there are mobility variations or not. Following steps are recovered by mobility calculations on the classified examples.

1) Miura-Ori patterns consist of two columns. All four examples have *one* degree of freedom.

$$a) M = 3(4-1) - 2 \times 4 = 1$$

$$b) M = 3(6-1) - 2 \times 7 = 1$$

$$c) M = 3(8-1) - 2 \times 10 = 1$$

$$d) M = 3(10-1) - 2 \times 13 = 1$$

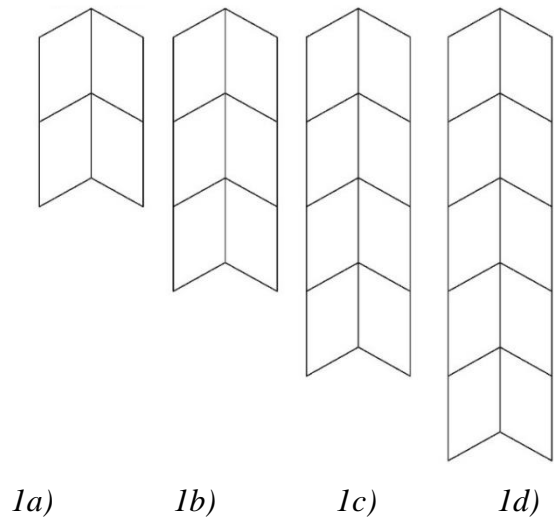


Figure 50. Miura-Ori Patterns Consist of Two Columns.

2) Miura-Ori patterns consist of three columns:

$$a) M = 3(6-1) - 2 \times 7 = 1$$

$$b) M = 3(9-1) - 2 \times 12 = 0$$

$$c) M = 3(12-1) - 2 \times 17 = -1$$

$$d) M = 3(15-1) - 2 \times 22 = -2$$

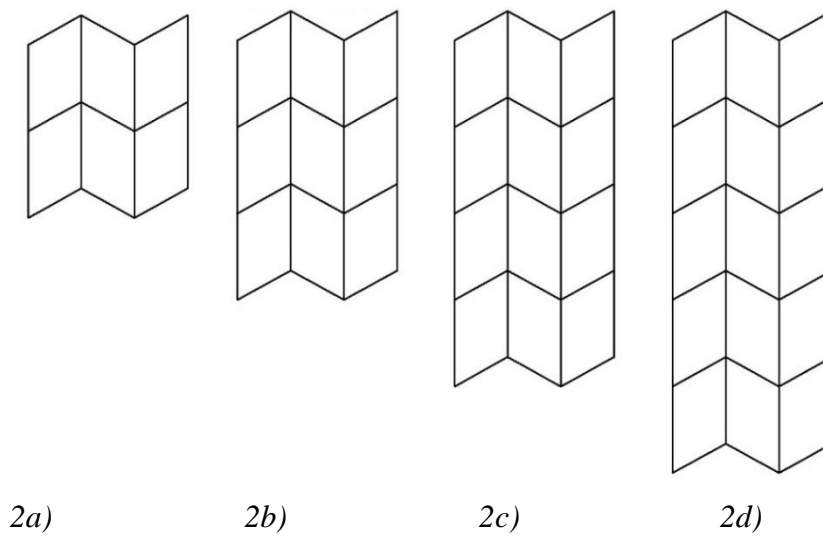


Figure 51. Miura-Ori Patterns in Three Columns.

3) Miura-Ori patterns consist of four columns.

$$a) M = 3(8-1) - 2 \times 10 = 1$$

$$b) M = 3(12-1) - 2 \times 17 = -1$$

$$c) M = 3(16-1) - 2 \times 24 = -3$$

$$d) M = 3(20-1) - 2 \times 31 = -5$$

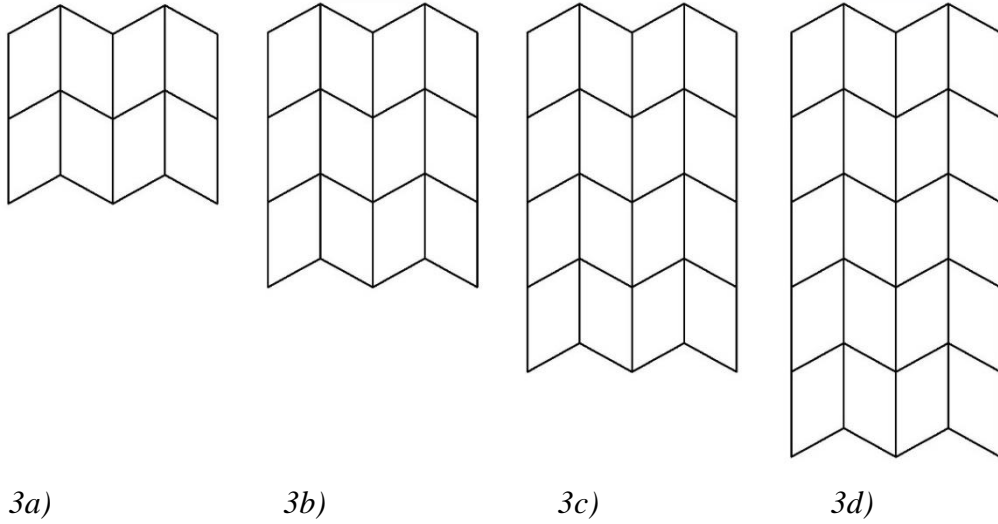


Figure 52. Miura-Ori Patterns in Four Columns.

It is known that deployable Miura-Ori pattern is a single DoF mechanism. However, Grubler Kutzbach formula fails above examples. While the derivation processes, mobility calculations variate with zero and negative values in the examples. The patterns are single DoF but the equation fails in some generated Miura-Ori patterns. Zero and negative amount of mobility can be explained with excessive plates in Miura-Ori patterns. In that case, how many and where are they situated in the pattern?

In order to find exact solution with Grubler Kutzbach formula, a new parameter (q_{\max}) is necessary. q_{\max} is the number of maximum excessive plates. It helps to find number of excessive plates for each mechanisms in Miura-Ori generations. Modified Grubler Kutzbach formula is given below

$$M = 3(n-1) - 2j_l + q_{\max} = 1 \quad (4.6)$$

It is known that all the generated Miura-Ori patterns are single DoF mechanisms. Thus, there is not any excessive plate in the pattern shown in figure 49.

$$M = 3(n-1) - 2j_l + q_{\max} = 1$$

$$M = 3(4-1) - 2 \times 4 + q_{max} = 1$$

$$q_{max} = 0$$

4.2. Determining the Excessive Plates and Joints of Miura-Ori

Mobility results except one state presence of excessive plates. The aim of this subchapter is to find the number of excessive plates and joints. Additionally, determining the place of excessive plates is another aim of the subchapter.

Modified Grubler Kutzbach formula in eq. (4.6.) helps to find maximum number of excessive plates.

Figure 53 shows a single DoF pattern with excessive plates. According to the calculation, the number of maximum excessive plates are two.

$$M = 3(n-1) - 2j_1 + q_{max} = 1$$

$$M = 3(12-1) - 2 \times 17 + q_{max} = 1$$

$$q_{max} = 2$$

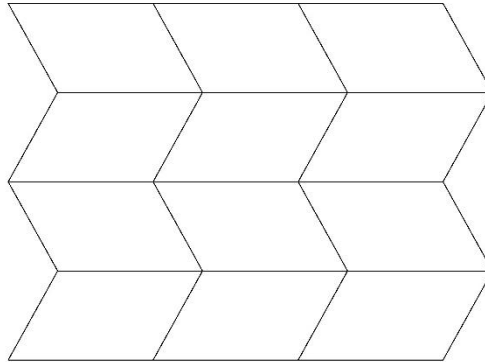


Figure 53. Pattern with Two Excessive Plates.

In figure 53 there are two excessive plates. But these plates are not determined randomly. To eliminate excessive plates from proper place, the number of excessive joints is also necessary. Finding the number of excessive joints helps us to pick up proper plates.

$$\left\{ \begin{array}{l} q_1 = q_{max} ; \\ q_2 = q_1 - 2 ; \\ q_3 = q_2 - 2 ; \\ q_4 = q_3 - 2 ; \end{array} \right. \quad \left\{ \begin{array}{l} j_{exc.1} = 2 \times q_{max} ; \\ j_{exc.2} = j_{q1} - 3 ; \\ j_{exc.3} = j_{q2} - 6 ; \\ j_{exc.4} = j_{q3} - 9 . \end{array} \right.$$

So,

$$q_1 = q_{max} \quad (4.7)$$

$$j_{exc.1} = 2 \times q_{max} \quad (4.8)$$

$$q_n = q_{n-1} - 2 \quad (4.9)$$

$$j_{exc.n} = j_{exc.n-1} - 3 \quad (4.10)$$

To find desired number of excessive plates and joints (q_n, j_n) without determining number of previous one (q_{n-1}, j_{n-1}), arithmetic sequence rule is used. The n^{th} term of an arithmetic sequence is below, where n is the number of terms and d is the common difference (Boyer & Merzbach, 2011).

$$a_n = a_1 + (n-1)d \quad (4.11)$$

The common difference for arithmetic sequence is obtained below,

$$d = a_{n+1} - a_n \quad (4.12)$$

For the excessive plates, if $a_{n+1} = q_n$ and $a_n = q_{n-1}$, and using eq. 4.9.

$$d_q = q_n - q_{n-1} = (q_{n-1} - 2) - q_{n-1} = -2 \quad (4.13)$$

So the n^{th} term of a plate is obtained,

$$q_n = q_1 - 2(n-1) \quad (4.14)$$

For the excessive joints, if $a_{n+1} = j_{exc.n}$ and $a_n = j_{exc.n-1}$, and using eq. 4.10.

$$d_j = j_{exc.n} - j_{exc.n-1} = -j_{exc.n-1} - 3 - j_{exc.n-1} = -3 \quad (4.15)$$

So the n^{th} term of a joint is obtained,

$$j_n = j_1 - 3(n-1) \quad (4.16)$$

To check the excessive plate equations, figure 53 is used.

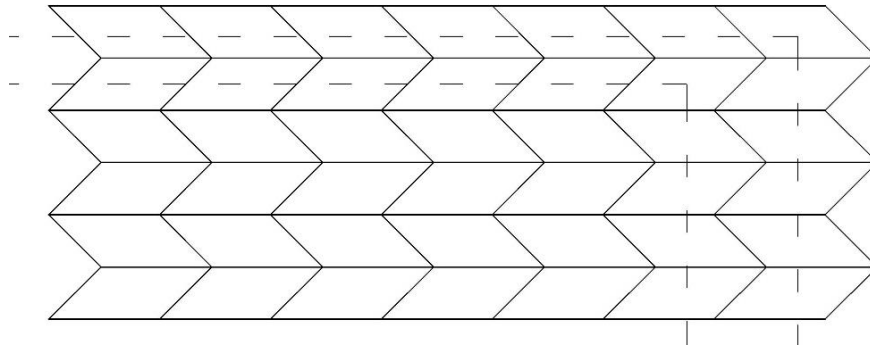
$$q_{max} = 2,$$

$$I \text{ exc. plate} = 2 \text{ and } I \text{ exc. joint} = 4;$$

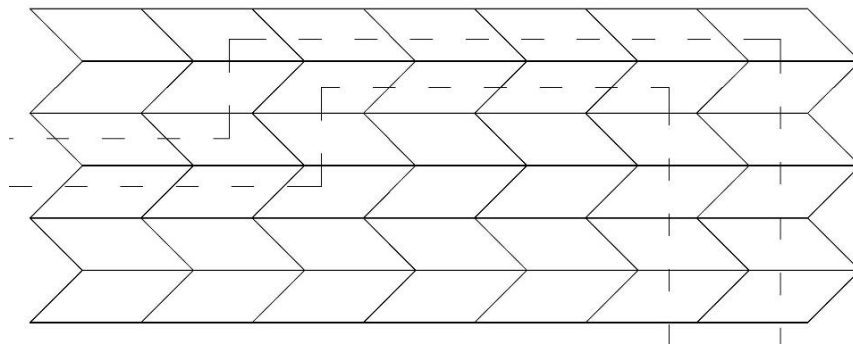
$$II \text{ exc. plate} = 0 \text{ and } II \text{ exc. joint} = 1.$$

It means, one of the excessive variation is 2 plates and 4 joints, another is 0 plate and 1 joints.

Modified Grubler Kutzbach formula is not enough to determine the proper excessive plates. A Method of Double Arrangement (MoDA) should be concerned. The Method of Double Arrangement is demand of two-line plates for both two concurrent edge. As figure 54, MoDA involves the plates which are along the dashed lines.



a)



b)

Figure 54. A Method of Double Arrangement (MoDA) examples. a) Maximum 20 excessive plates; b) 22 excessive plates.

After the calculation and determination of number of excessive plates and joints, if the placement of necessary plates are not conformed with the MoDA, the pattern does not deploy. There are determination examples in figure 55. The pattern has 3 excessive plates and 6 excessive joints. Three placement variations are designated. First two examples are correct, the Method of Double Arrangement have been fitted in the edges of left and top side. Third variation is wrong, because the hatched plate is single, the MoDA is not provided.

$$M = 3(n-1) - 2j_1 + q_{max} = 1$$

$$M = 3(15-1) - 2 \times 22 + q_{max} = 1$$

$$q_{max} = 3$$

$$3L6j$$

$$M = 3(12-1) - 2 \times 16 = 1$$

1) $3L6j \checkmark$

2) $3L6j \checkmark$

3) $3L6j \times$

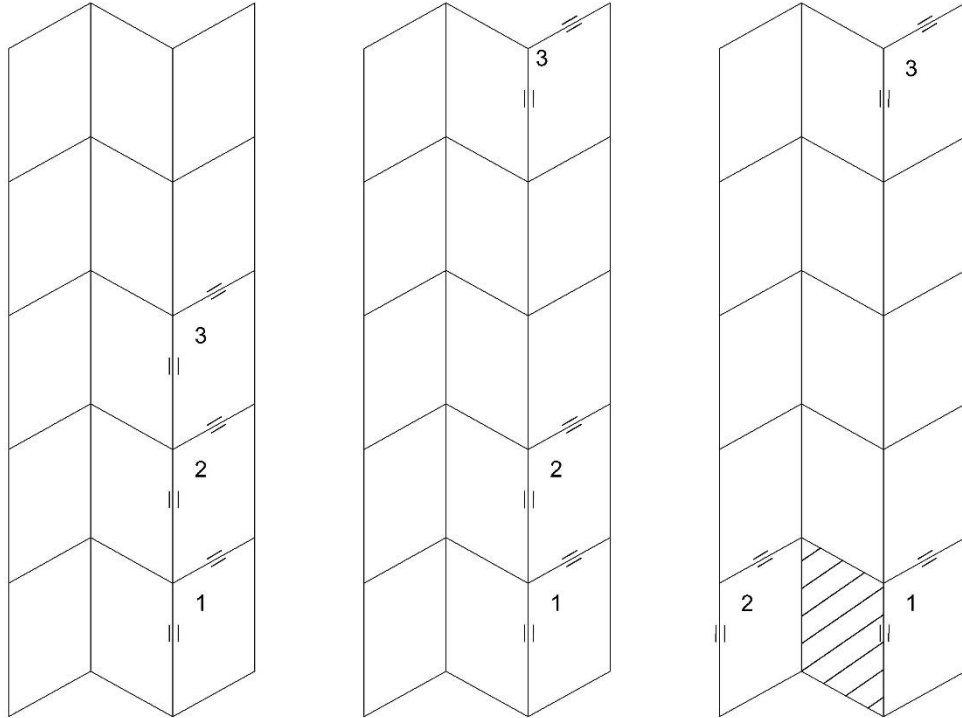


Figure 55. Correct and Wrong Determination of Excessive Plates and Joints.

4.2.1 Excessive Plates and Joint Studies on the Six Derivations

Following step focuses on the excessive plates and joints layout designs of 6 derivations. The 6 derivations with single DoF are studied again with Modified Grubler Kutzbach formula to find excessive plates. With the eq. From 4.7. to 4.10. the excessive plates and joints are obtained. Then, the locations of excessive plates and joints are chosen (Fig. 56-60).

$$2b) M = 3(9-1) - 2 \times 12 + q_{max} = 1$$

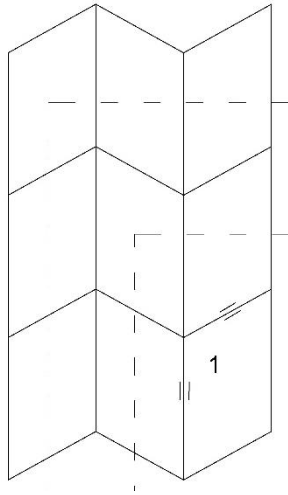
$$q_{max} = 1$$

2b₁) **1L2j**

$$q_1 = 1;$$

$$j_{exc.1} = 2.$$

$$M = 3(8-1) - 2 \times 10 = 1$$



2b₁)

Figure 56. Determination of Excessive Plates and Joints on the Pattern of Fig. 51 (2b).

$$2c) M = 3(12-1) - 2 \times 17 + q_{max} = 1$$

$$q_{max} = 2$$

2c₁) **2L4j**

$$q_1 = 2;$$

$$j_{exc.1} = 4.$$

$$M = 3(10-1) - 2 \times 13 = 1$$

2c₂) **0L1j**

$$q_1 = 0;$$

$$j_{exc.1} = 1.$$

$$M = 3(12-1) - 2 \times 16 = 1$$

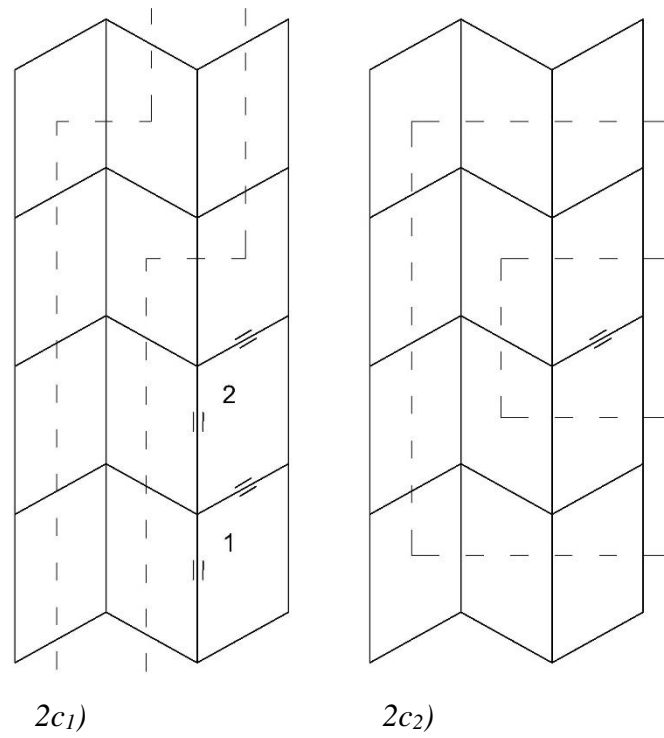


Figure 57. Determination of Excessive Plates and Joints on the Pattern of Fig. 51 (2c).

$$2d) M = 3(15-1) - 2 \times 22 + q_{max} = 1$$

$$q_{max} = 3$$

$$2d_1) \mathbf{3L6j}$$

$$q_1 = 3;$$

$$j_{exc.1} = 6.$$

$$M = 3(12-1) - 2 \times 16 = 1$$

$$2d_2) \mathbf{1L3j}$$

$$q_1 = 1;$$

$$j_{exc.1} = 3.$$

$$M = 3(14-1) - 2 \times 19 = 1$$

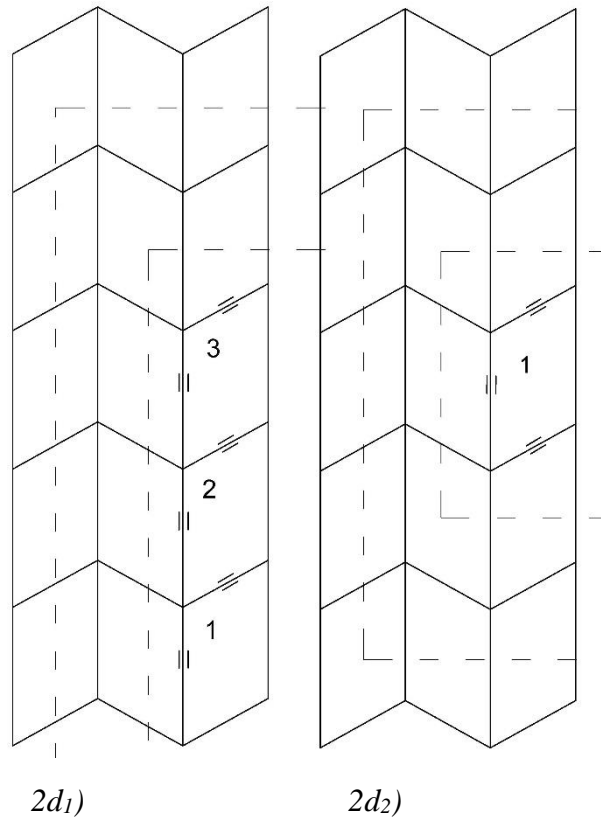


Figure 58. Determination of Excessive Plates and Joints on the Pattern of Fig. 51 (2d).

$$3b) M = 3(12-1) - 2 \times 17 + q_{max} = 1$$

$$q_{max} = 2$$

$$3b_1) \mathbf{2L4j}$$

$$q_1 = 2;$$

$$j_{exc.1} = 4.$$

$$M = 3(10-1) - 2 \times 13 = 1$$

$$3b_2) \mathbf{0L1j}$$

$$q_2 = 0;$$

$$j_{exc.2} = 1.$$

$$M = 3(12-1) - 2 \times 16 = 1$$

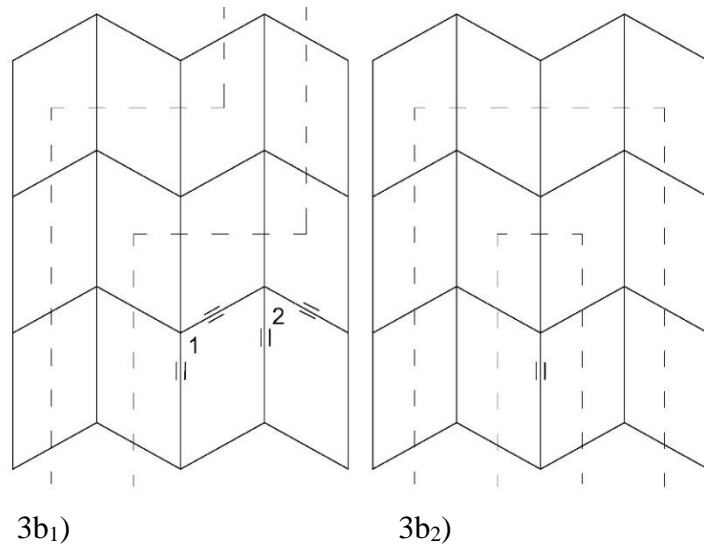


Figure 59. Determination of Excessive Plates and Joints on the Pattern of Fig. 52 (3b).

$$3c) M = 3(16-1) - 2 \times 24 + q_{max} = 1$$

$$q_{max} = 4$$

$$3c_1) \mathbf{4L8j}$$

$$3c_2) \mathbf{2L5j}$$

$$3c_3) \mathbf{0L2j}$$

$$q_1 = 4;$$

$$q_2 = 2;$$

$$q_3 = 0;$$

$$j_{exc.1} = 8.$$

$$j_{exc.2} = 5.$$

$$j_{exc.3} = 2.$$

$$M = 3(12-1) - 2 \times 16 = 1$$

$$M = 3(14-1) - 2 \times 19 = 1$$

$$M = 3(16-1) - 2 \times 22 = 1$$

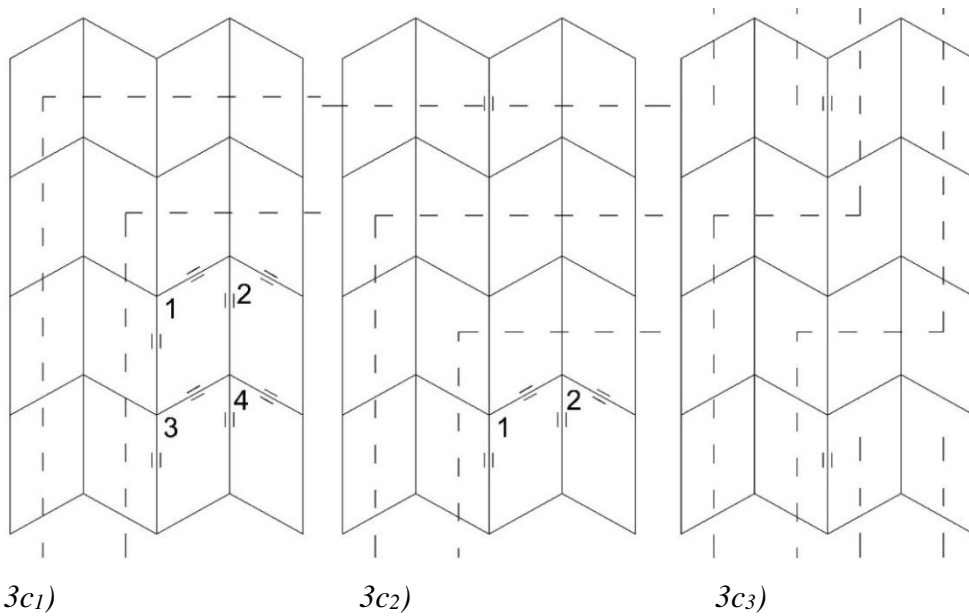


Figure 60. Determination of Excessive Plates and Joints on the Pattern of Fig. 52 (3c).

$$3d) M = 3(20-1) - 2 \times 31 + q \max = 1$$

$$q \max = 6$$

3d₁) 6L12j

$$q_1 = 6;$$

$$j_{exc.1} = 12.$$

$$M = 3(14-1) - 2 \times 19 = 1$$

3d₂) 4L9j

$$q_2 = 4;$$

$$j_{exc.2} = 9.$$

$$M = 3(16-1) - 2 \times 22 = 1$$

3d₃) 2L6j

$$q_3 = 2;$$

$$j_{exc.3} = 6.$$

$$M = 3(18-1) - 2 \times 25 = 1$$

3d₄) 0L3j

$$q_4 = 0;$$

$$j_{exc.4} = 3.$$

$$M = 3(20-1) - 2 \times 28 = 1$$

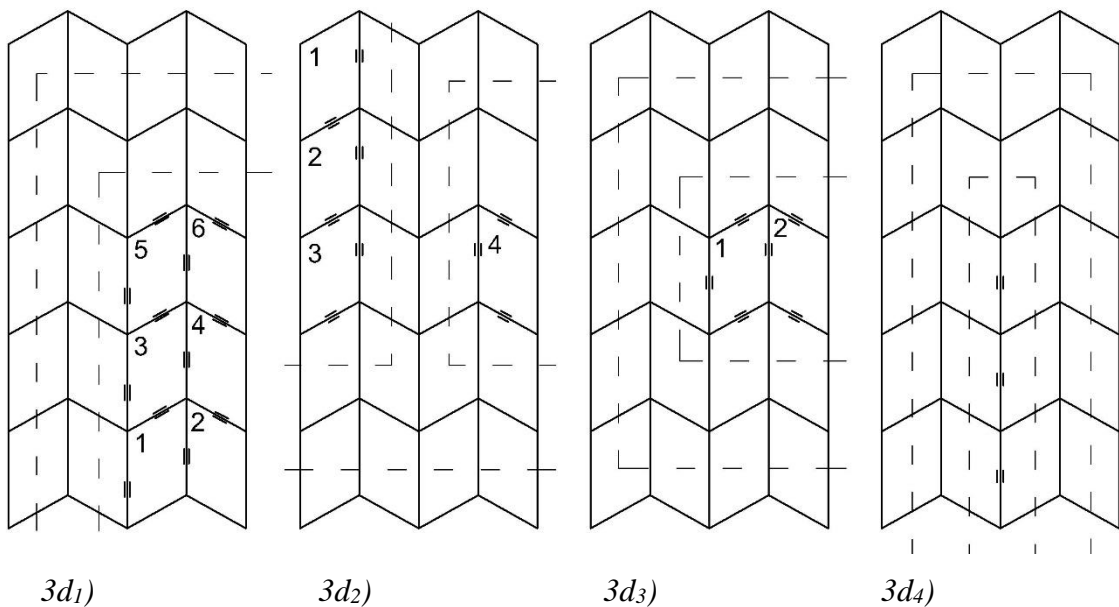


Figure 61. Determination of Excessive Plates and Joints on the Pattern of Fig. 52 (3d).

Miura-Ori derivations share common mechanical features with Miura-Ori. Miura-Ori (Figure 30 (a)), Arc-Miura (Figure 31 (a)), Tapered Miura (Figure 32 (a)) and Tapered-Arc Miura (Figure 33 (a)) patterns can be characterized commonly, as:

-Unit (of each patterns) is composed of a symmetrical degree-4 vertices.

-Unit (of each patterns) is a four bar spherical mechanism with a single degree of freedom (DOF).

-Unit (of each patterns) is consisted from 4 revolute joints on the axes, which intersect at the sphere center of mechanism.

Because of common mechanical features only Miura-Ori has been analyzed in this chapter. The same calculations and results can be applied to other Miura patterns (derivations).

CHAPTER 5

CASE STUDY

In this section, a design is proposed to show the application and possibility of the analyzed Miura-Ori pattern and its derivatives.

5.1. Example Problem

Example problem starts with a short geometric description of the design. It is a path of a folded origami pattern (figure 62 bold line) which is consisted from three curves and two straight lines. Here some specific conditions are given for calculation:

a) The radii of the draft curves are given

$$curve_1 = 180 \text{ cm};$$

$$curve_2 = 135 \text{ cm};$$

$$curve_3 = 90 \text{ cm}.$$

b) Curve angles are 150° , 96° and 99° .

c) Straight line measurements are 220 cm and 150 cm. And,

$$\alpha_{\text{line1}} = \alpha_{\text{curve1}}$$

$$\alpha_{\text{line2}} = \beta_{\text{curve3}}$$

d) Span length is preferred equal ($a=b$) as 60 cm.

The problem is to design Arc-Miura pattern shelter according to the draft path and remove excessive plates and joints.

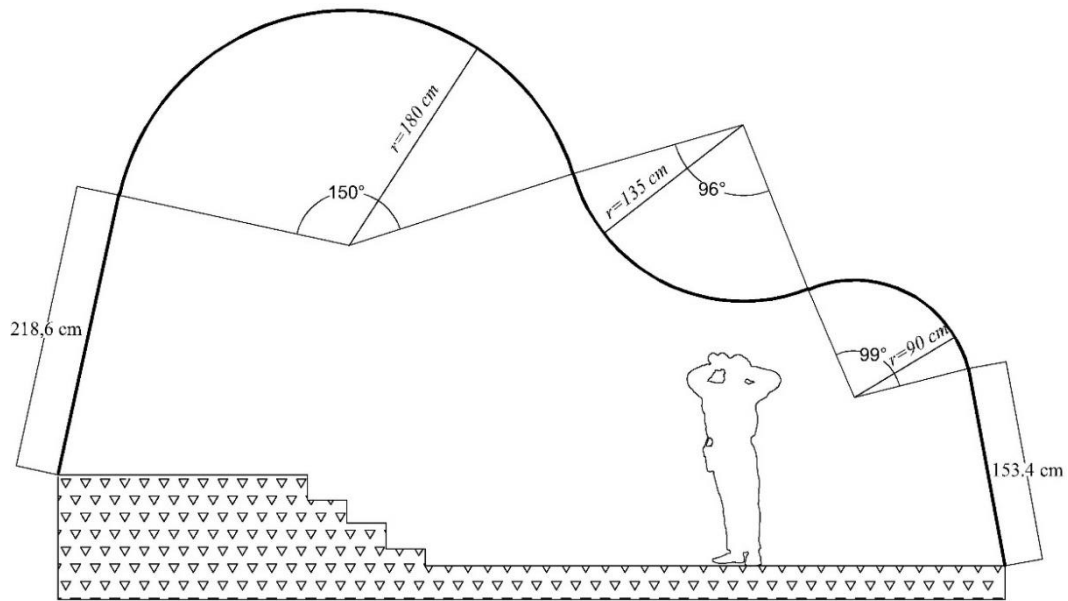


Figure 62. Draft Path of the Example Problem.

Following steps include solution of the problem sequentially.

1. Identify the vertex angles of curves

Defined parameters for the curves are written below

$$r_1 = 180 \text{ cm};$$

$$r_2 = 135 \text{ cm};$$

$$r_3 = 90 \text{ cm},$$

$$a=b=60 \text{ cm},$$

To calculate vertex angles radius formula is used.

$$r = k \sin \gamma / \sin (180^\circ - 2\gamma) \quad (3.18)$$

Hence, indefinite parameters should be calculated,

$$\gamma = 90^\circ - \beta + \alpha \text{ (for } \beta > \alpha)$$

$$\gamma = 90^\circ - \alpha + \beta \text{ (for } \beta < \alpha) \quad (3.15)$$

$$k = \sqrt{a^2 + b^2 - 2ab \cos (180^\circ - 2\beta)} \quad (3.17)$$

There are three different curves, so three different calculations are necessary. In the third chapter, angle relation with curve was described. Thus, if α is bigger than β the curve is convex, if not the curve is concave. In there, first and third curves are concave, second is convex. According to this condition, vertex angles are obtained for all types.

In curve 1. (concave $\beta > \alpha$)

$$r = 180 \text{ cm}$$

$$a = 60 \text{ cm}$$

$\beta - \alpha$ is accepted as 15°

$$\gamma = 90^\circ - \beta + \alpha = 90^\circ - \alpha - 15^\circ + \alpha = 75^\circ$$

$$k = \sqrt{a^2 + b^2 - 2ab \cos(180^\circ - 2\beta)} = \sqrt{a^2 + a^2 - 2a^2 \cos(180^\circ - 2\beta)} = \sqrt{2a^2(1 - \cos(180^\circ - 2\beta))} = \sqrt{7200(1 - \cos(180^\circ - 2\beta))} = \sqrt{7200(1 + \cos 2\beta)}$$

So with eq (3.10),

$$r = k \sin \gamma / \sin(180^\circ - 2\gamma)$$

$$180 = \sqrt{7200(1 + \cos 2\beta)} \sin 75^\circ / \sin 30^\circ = \sqrt{7200(1 + \cos 2\beta)} \times 1.93$$

$$93.26 = \sqrt{7200(1 + \cos 2\beta)}$$

$$8698.2 = 7200(1 + \cos 2\beta)$$

$$0.21 = \cos 2\beta$$

$$\beta = 39^\circ 22'$$

$$\alpha = \beta - 15^\circ = 24^\circ 22'$$

In curve 2. (convex $\alpha > \beta$)

$$r = 135 \text{ cm}$$

$$a = 60 \text{ cm}$$

$\alpha - \beta$ is accepted as 16°

$$\gamma = 90^\circ - \alpha + \beta = 90^\circ - \beta - 16^\circ + \beta = 74^\circ$$

$$k = \sqrt{7200(1 + \cos 2\beta)}$$

So with eq (3.10),

$$r = k \sin \gamma / \sin(180^\circ - 2\gamma)$$

$$135 = \sqrt{7200(1 + \cos 2\beta)} \sin 74^\circ / \sin(180^\circ - 2\gamma)$$

$$5538.2055 = 7200(1 + \cos 2\beta)$$

$$\cos 2\beta = -0.231$$

$$2\beta = 103^\circ 21' 21.431''$$

$$\beta = 51^\circ 40'$$

$$\alpha = \beta + 16^\circ = 67^\circ 40'$$

In curve 3. (concave $\beta > \alpha$)

$$r = 90 \text{ cm}$$

$$a = 60 \text{ cm}$$

$\beta - \alpha$ is accepted as $16^\circ 30'$

$$\gamma = 90^\circ - \beta + \alpha = 90^\circ - \alpha - 16^\circ 30' + \alpha = 73^\circ 30'$$

$$k = \sqrt{7200 (1 + \cos 2\beta)}$$

So with eq (3.10),

$$r = k \sin \gamma / \sin (180^\circ - 2\gamma)$$

$$90 = \sqrt{7200 (1 + \cos 2\beta)} \sin 73^\circ 30' / \sin 33^\circ$$

$$2613.2697 = 7200 (1 + \cos 2\beta)$$

$$\cos 2\beta = -0.637$$

$$2\beta = 129^\circ 34' 6.525''$$

$$\beta = 64^\circ 47'$$

$$\alpha = \beta - 16^\circ 30' = 48^\circ 17'$$

2. Identify number of the units and plates of curves

For curve 1. ($\beta = 39^\circ 22'$; $\alpha = 24^\circ 22'$),

The angles of curve 1. is 150° . To identify unit number unit angle are necessary.

$$\theta = 180^\circ - 2\gamma \tag{3.16}$$

$$\theta = 180^\circ - 150^\circ = 30^\circ$$

Pattern angle is 150° , so unit number is

$$150^\circ / \theta = 150^\circ / 30^\circ = 5$$

As described in third chapter, each unit has 4 plates. Plates number is obtained as

$$A \text{ unit number} \times a \text{ unit plates} = 5 \times 4 = 20$$

For curve 2. ($\beta = 51^\circ 40'$; $\alpha = 67^\circ 40'$),

$$\theta = 180^\circ - 148^\circ = 32^\circ$$

Pattern angle is 96° , so unit number is

$$96^\circ / \theta = 96^\circ / 32^\circ = 3$$

Plates number is obtained as

$$A \text{ unit number} \times a \text{ unit plates} = 3 \times 4 = 12$$

For curve 3. ($\beta = 64^\circ 47'$; $\alpha = 48^\circ 17'$),

$$\theta = 180^\circ - 147^\circ = 33^\circ$$

Pattern angle is 99° , so unit number is

$$99^\circ / \theta = 99^\circ / 33^\circ = 3$$

Plates number is obtained as

$$A \text{ unit number} \times a \text{ unit plates} = 3 \times 4 = 12$$

3. Identify the vertex angles of lines

Given angle conditions is below,

$$\alpha_{\text{line1}} = \alpha_{\text{curve1}} = 24^{\circ} 22'$$

$$\alpha_{\text{line2}} = \beta_{\text{curve3}} = 64^{\circ} 47'$$

4. Identify number of the units and plates of lines

Defined parameters for the lines are written below

$$l_1 = 218,6 \text{ cm}; l_2 = 153.4 \text{ cm}$$

$$a = b = 60 \text{ cm}$$

$$\alpha_{\text{line1}} = 24^{\circ} 22'$$

$$\alpha_{\text{line2}} = 64^{\circ} 47'$$

Unit length formula is used to obtain number of the units and plates.

$$k_{sst} = a \sin (180^{\circ} - 2\alpha) / \sin \alpha \quad (3.3)$$

Hence,

In line 1.

$$k_{sst} = a \sin (180^{\circ} - 2\alpha) / \sin \alpha = 60 \times \sin 131^{\circ} 16' / \sin 24^{\circ} 22' = 60 \times 0.7516 / 0.4126 = 109.3$$

In line 2.

$$k_{sst} = a \sin (180^{\circ} - 2\alpha) / \sin \alpha = 60 \times \sin 50^{\circ} 26' / \sin 64^{\circ} 47' = 60 \times 0.771 / 0.905 = 51.12$$

To identify unit number line length is divides by unit length.

In line 1.

$$l_1 / k = 220 / 109.3 = 2.01 \sim 2$$

In line 2.

$$l_2 / k = 150 / 51.12 = 2.93 \sim 3$$

Unit numbers of line₁ and line₂ are fractional numbers. To fold the example pattern number should be integer. So, these fractions are simplified by rounding off. And, line lengths are changed (Figure 73).

$$\text{Line 1. } 2 \times k = 218.6$$

$$\text{Line 2. } 3 \times k = 153.4$$

Each unit has 4 plates. Plates number is obtained as

In line 1.

$$\text{number of units} \times \text{number of unit plates} = 2 \times 4 = 8$$

In line 2.

$$\text{number of units} \times \text{number of unit plates} = 3 \times 4 = 12$$

5. Draw crease pattern

The example shelter has 5 pattern parts; line₁, curve₁, curve₂, curve₃, line₂. These parts are drawn according to obtained vertex angles and defined parameters. Then mountain and valley folds are assigned (Figure 63-67).

Line₁. Vertex angle of the line₁ are $24^{\circ} 22'$. Span length is 60 cm. Line₁ is composed of 8 plates.

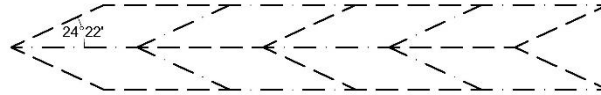


Figure 63. Curve₁ Pattern.

Curve₁. Vertex angles of the curve₁ are $\alpha = 24^{\circ} 22'$ and $\beta = 39^{\circ} 22'$. Span length is 60 cm. Curve₁ is composed of 20 plates.

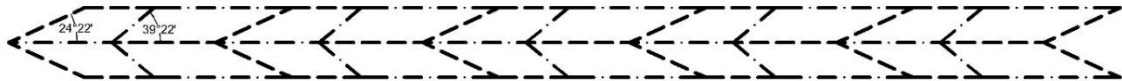


Figure 64. Curve₃ Pattern.

Curve₂. Vertex angles of the curve₂ are $\alpha = 67^{\circ} 40'$ and $\beta = 51^{\circ} 40'$. Span length is 60 cm. Curve₂ is composed of 12 plates.

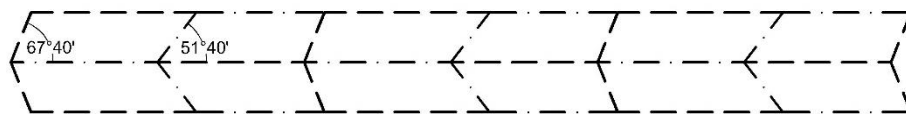


Figure 65. Curve₂ Pattern.

Curve₃. Vertex angle of the curve₃ are $\alpha = 48^{\circ} 17'$ and $\beta = 64^{\circ} 47'$. Span length is 60 cm. Curve₃ is composed of 12 plates.

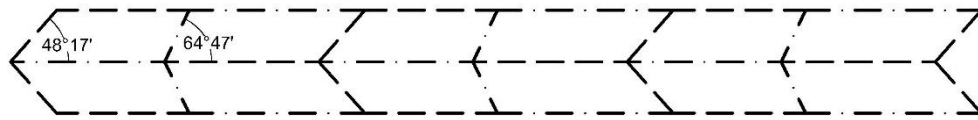


Figure 66. Curve₃ Pattern.

Line₂. Vertex angle of the line₂ are $\alpha = 64^\circ 47'$. Span length is 60 cm. Line₁ is composed of 12 plates.

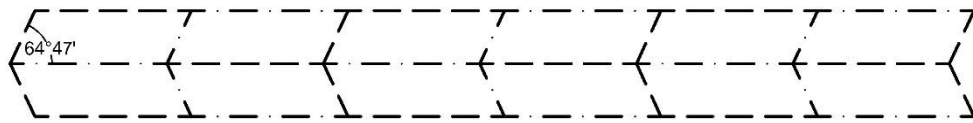
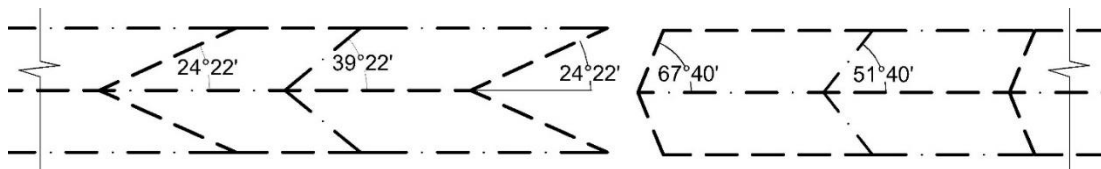
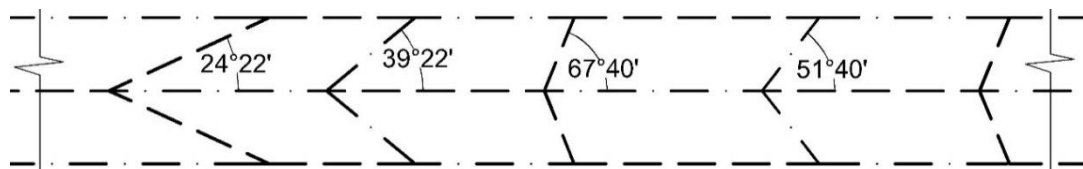


Figure 67. Line₂ Pattern.

The parts are connected together in order to get whole pattern. To combine parts, β of previous parts is attached with α of next part. During this combination, different angles generate a problem. As a solution of the problem, last vertex angle of the previous part is accepted as α of next part. The change of α is only take up first plate. For the next plate current vertex angles continue (Figure 68).



a) Parts before combination.



b) Parts after combination.

Figure 68. Combination of Different Parts.

Whole pattern is composed of 64 plates (Figure 69).

Connected parts are multiplied in order to design its shelter. The full shelter is composed from 544 plates (Figure 70).

6. Determining of the excessive links and joints

$$\sum plates = a \times b \quad (4.4)$$

$$\sum j = a (b-1) + b (a-1) \quad (4.5)$$

In there,

$$\sum plates = 32 \times 17 = 544$$

$$\sum j = 17 \times 31 + 32 \times 16 = 1039$$

7. Identify excessive rigid plates

$$M = 3 (n-1) - 2 j_1 + q_{max} = 1 \quad (4.6)$$

$$1629 - 2078 + q_{max} = 1$$

$$q_{max} = 450$$

The system has 450 excessive plates.

8. Layout maximum excessive plates and joints

$$q_1 = q_{max} \quad (4.7)$$

$$j_{q1} = 2 \times q_{max} \quad (4.8)$$

In there, first and maximum excessive plate is 450, first excessive joint is 840 (Figure 71). So, revise mobility calculation of the pattern,

$$q_1 = 450$$

$$j_1 = 2 \times 450 = 900$$

$$450L900j$$

$$M = 3((544-450)-1) - 2 \times (1039-900) = 279 - 278 = 1$$

9. Layout 236th excessive plates and joints

$$q_n = q_1 - 2(n-1) \quad (4.14)$$

$$j_n = j_1 - 3(n-1) \quad (4.16)$$

Thus,

$$q_{236} = q_1 - 2(n-1) = 544 - 2(236-1) = 74$$

$$j_{236} = j_1 - 3(n-1) = 1039 - 3(236-1) = 334$$

236th excessive plates and joints can be expressed as 74L334j.

10. Pickup the excessives

First excessive plates and joints (450L900j) are indicated maximum excessive plates and joints. The excessives are removed from the pattern and the resulted simple pattern also has single DoF (Figure 71).

236th excessive plates and joints (74L334j) are removed from the pattern and the resulted pattern still has single DoF (Figure 72). To choose 74L334j, 74 plates and 296 joints (four joints for each plates) are reduced firstly. However, 38 joints out of the 334 are reduced without plates.



Figure 69. Example of the Unfolded Whole Pattern.

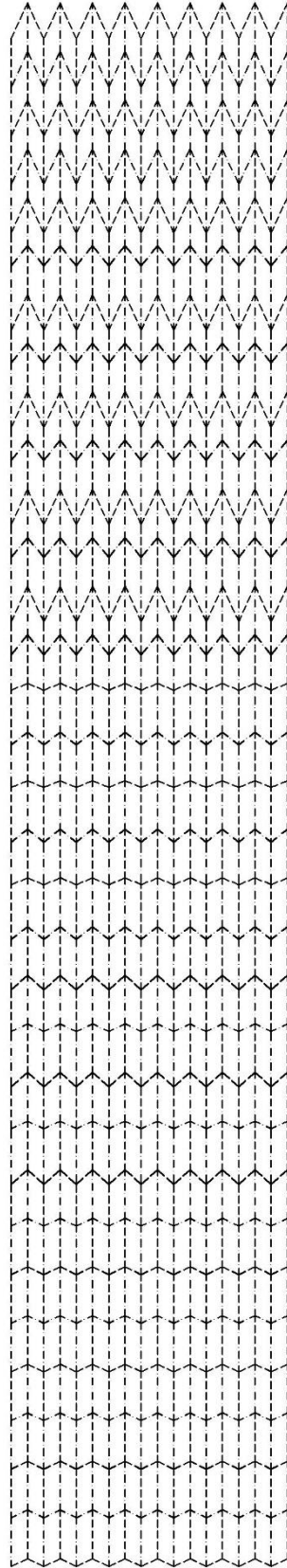


Figure 70. Pattern of the Shelter.

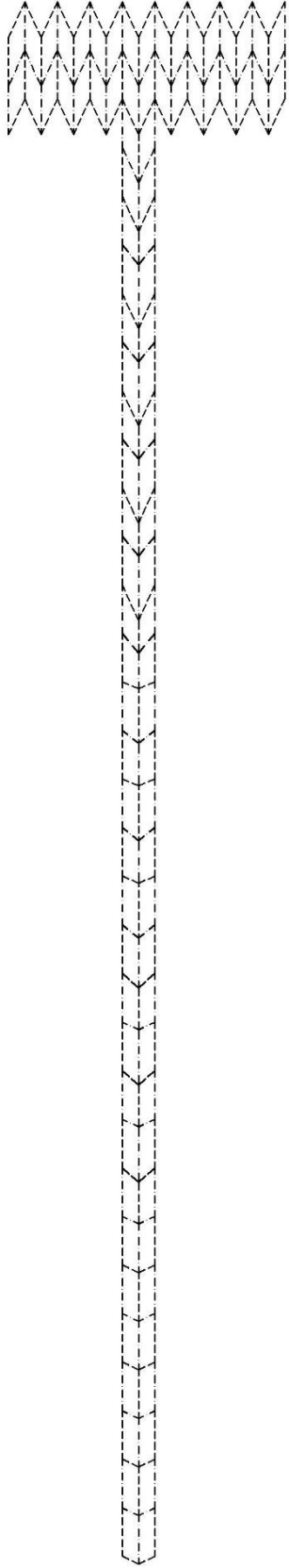


Figure 71. Minimum number of plates without changing the mobility.

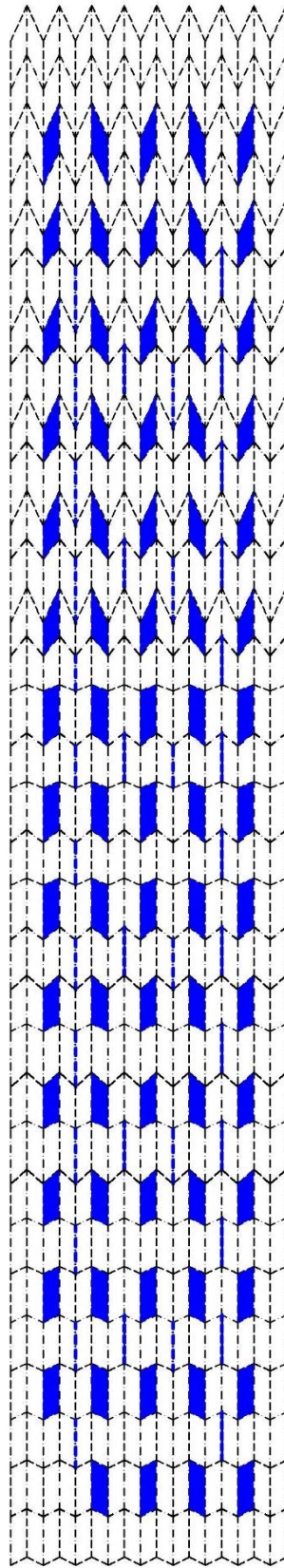


Figure 72. Samples of Removing 236th Excessives (the excessives are in blue color, blue lines are excessive joints.).

11. Fold the pattern

According to the calculation, all given parameters of the problem are established (Figure 73).

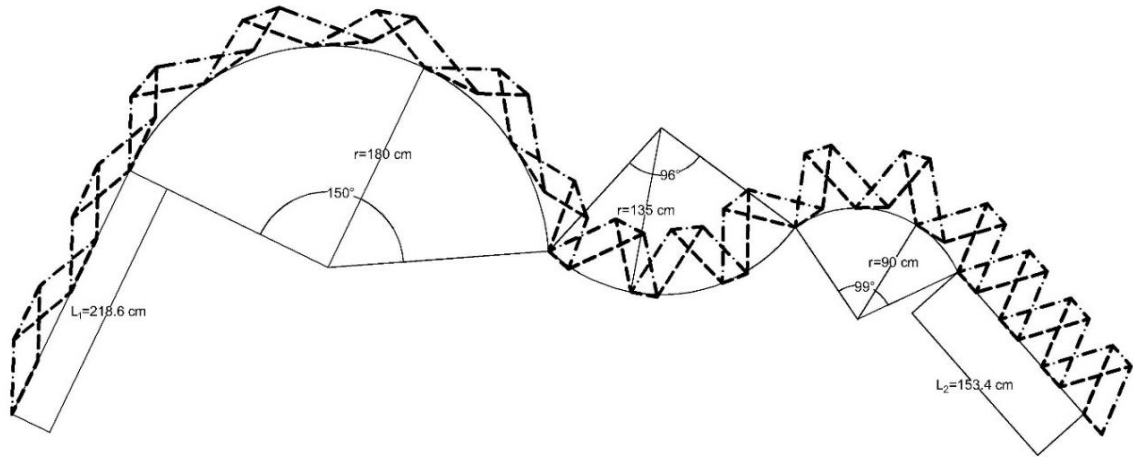


Figure 73. Folded Shelter.

12. Vizualize the architectural origami shelter

Designed n is proposed as a deployable roof. It is vizualized in the architectural softwares of the 3d MAX and Lumion (Figure 74).



Figure 74. Shelter Visualizations.

(cont. on next page)

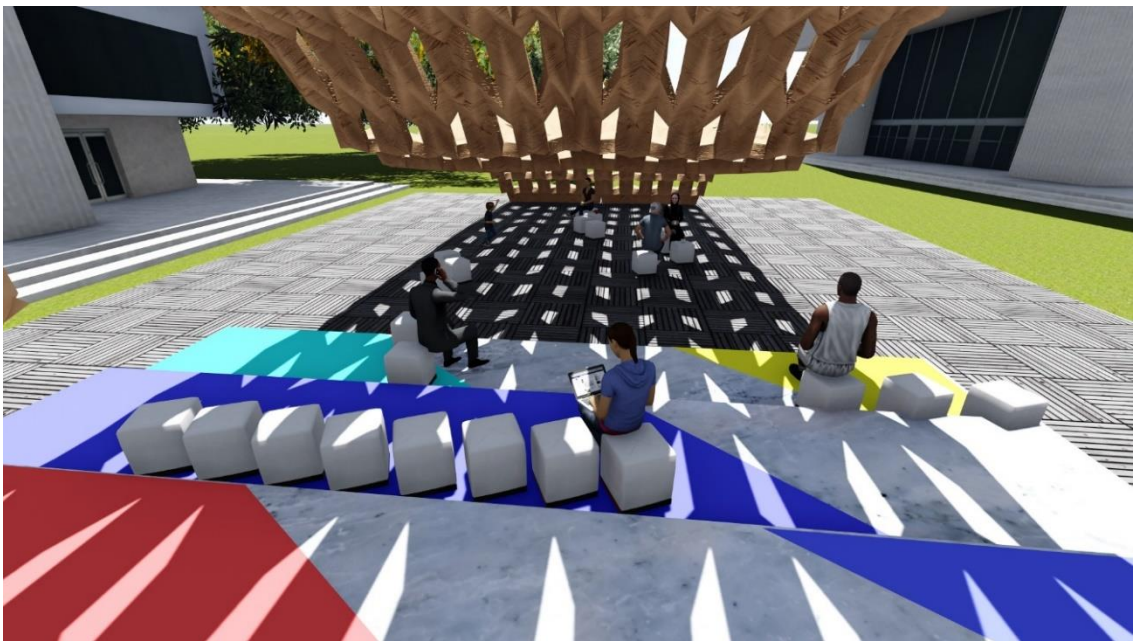
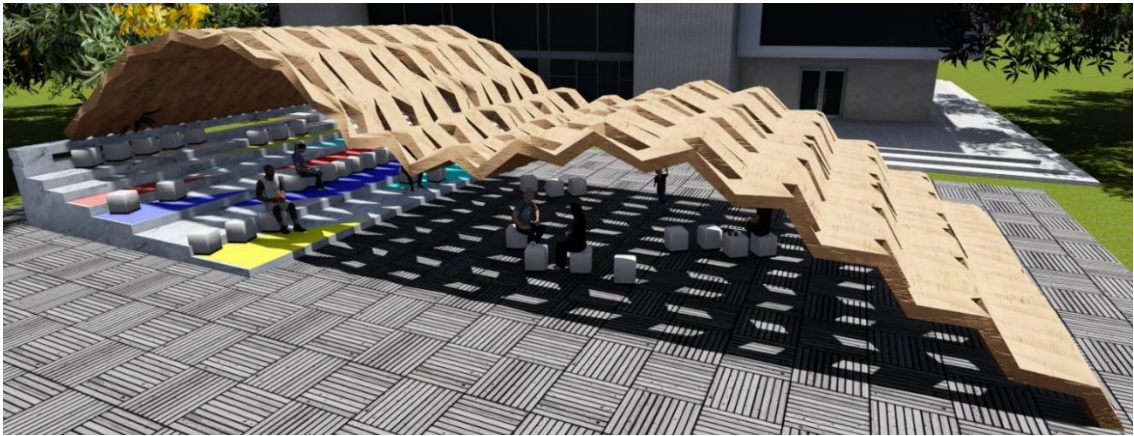
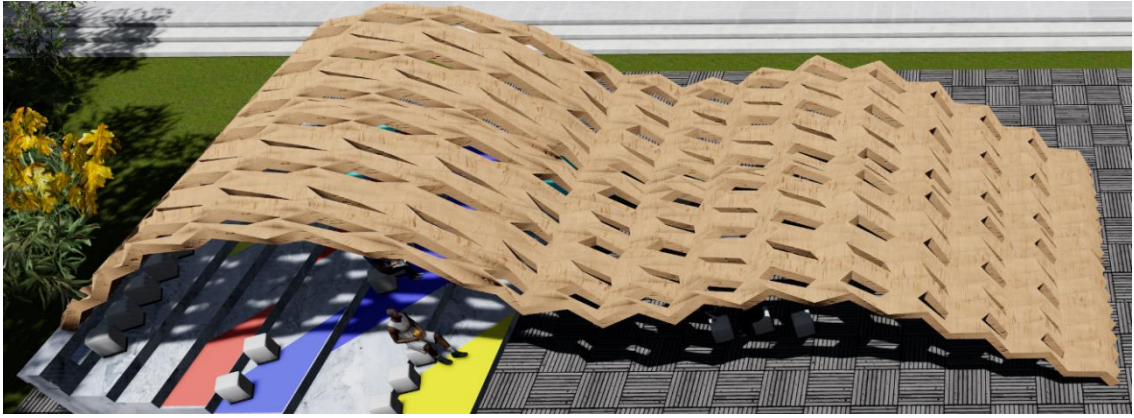


Figure 74. (cont.)

CHAPTER 6

CONCLUSION

In this thesis, Miura-Ori pattern and its derivations have been analyzed in geometric and mobility aspects.

Studied derivations are Arc-Miura, Tapered-Miura and Tapered Arc-Miura patterns. The main differences between these patterns are around the vertex angles (α , β), span lengths (a , b) and tapered line (which creates taper angle ω).

Behind the input parameters (α , β , a , b), several depended parameters are identified. By the changing input parameters, different geometries of the Miura-Ori pattern and its derivations are investigated. At the end of the geometric analysis, the patterns are drawn with Autocad and calculated with Excel in order to validate the study.

Besides, twelve different Miura-Ori patterns' mobility are analyzed with Grubler Kutzbach formula. Although the pattern is single DoF mechanism, studied six patterns give negative mobility results. Negative mobility results mean that there are excessive plates. Then fourteen different excessive placements are found in the six patterns. After all the research on the number and placement of excessive plates, two steps are developed to determine excessive plates and joints. First step is determining the first and n^{th} term of a plates and joints for the patterns with Modified Grubler Kutzbach formula, and second step is using the Method of Double Arrangement (MoDA).

In the last chapter, in order to utilize geometrical and mobility analysis, example problem is proposed as an architectural origami shelter. The shelter is composed of five different Miura derivations. The geometry of the derivations are developed with given parameters. Later, number of excessive plates and joints of the shelter application were calculated and reduced according to the MoDA. 174th excessive alternative is found that there are 74 plates and 321 excessive joints. Introduced folded origami shelter is modelled in 3Ds Max and Lumion.

We suggest further research for the geometric analysis of partly deployed of Miura-Ori and its derivations. Also the research can be expanded with various rigid origami patterns.

REFERENCES

- AlGeddawy, T., Abbas, M., & ElMaraghy, H. (2014). Design for Mobility—A Customer Value Creation Approach. *Procedia CIRP*, 16, 128-133.
- Beltman, G., & Spit, T. E. (1962). *Vouwschaal voor douaneloods te Glanerbrug*. Cement.
- Bern, M. H., Barry (1996). *Chapter 1. The Complexity of Flat Origami*. Paper presented at the Proceedings of the seventh annual ACM-SIAM symposium on Discrete algorithms.
- Boake, T. M., Bes, B., & Arch, M. (2014). Hot climate Double Facades: Avoiding Solar Gain: University of Waterloo.[pdf] available at: https://www.academia.edu/4812685/Hot_Climate_Double_Facades_Avoiding_Solar_Gain in [accessed on 6/1/2014].
- Bowen, L. A., Baxter, W., Magleby, S. P., & Howell, L. L. (2014). A position analysis of coupled spherical mechanisms found in action origami. *Mechanism and Machine Theory*, 77, 13-24.
- Boyer, C. B., & Merzbach, U. C. (2011). *A history of mathematics*: John Wiley & Sons.
- Buri, H. U. (2010). Origami-folded plate structures.
- Burry, M. (2006). In M. G. s. Hyposurface (Ed.), <http://hyposurface.org/> SIAL, RMIT, Melbourne.
- Cai, J., Deng, X., Xu, Y., & Feng, J. (2015). Geometry and Motion Analysis of Origami-Based Deployable Shelter Structures. *Journal of Structural Engineering*, 141(10), 06015001.
- Carrek. (2014). Kirigami scheme. Retrieved from <http://paper-life.ru/en/kirigami-scheme>
- Cheng, Q., Song, Z., Ma, T., Smith, B. B., Tang, R., Yu, H., . . . Chan, C. K. (2013). Folding paper-based lithium-ion batteries for higher areal energy densities. *Nano letters*, 13(10), 4969-4974.
- Demaine, E. (2010). Geometric Folding Algorithms: Linkages, Origami, Polyhedra. *Lecture 1: Overview*. Massachusetts Institute of Technology: MITOPENCOURSEWARE.
- Demaine, E. O. E., Joseph (2007). *Geometric Folding Algorithms*: Cambridge University Press.
- Dias, M. A., Dudte, L. H., Mahadevan, L., & Santangelo, C. D. (2012). Geometric mechanics of curved crease origami. *Physical review letters*, 109(11), 114301.

- Douglas, S. M., Bachelet, I., & Church, G. M. (2012). A logic-gated nanorobot for targeted transport of molecular payloads. *Science*, 335(6070), 831-834.
- Dureisseix, D. (2011). An Overview of Mechanisms and Patterns with Origami. *International Journal of Space Structures*.
- Engel, P. (2011). *ORIGAMI ODYSSEY: A Journey to the Edge of Paperfolding*. Tokyo/Rutland, Vermont/ Singapore: TUTTLE.
- Fei, L. J. S., D. . (2013). Origami Theory and its Applications:A Literature Review. *World Academy of Science, Engineering and Technology International Journal of Social, Management, Economics and Business Engineering Vol:7 No:1*.
- Fuse, T. (1990). *Mutlidimensional Transformation UNIT ORIGAMI*. Japan Publications, Inc.
- Gattas, J. M., Wu, W., & You, Z. (2013). Miura-base rigid origami: Parameterizations of first-level derivative and piecewise geometries. *Journal of Mechanical Design*, 135(11), 111011.
- Gjerde, E. (2007). *Tesellation a primer for OUSA 2007*.
- Gordon, M. (1954). US Air Force Academy Cadet Chapel.
- Greenberg, H. C. G., M. L.; Magleby, S. P.; Howell, L. L. . (2011). Identifying links between origami and compliant mechanisms. *Mechanical Sciences*.
- Hart, G. (2007). *Modular Kirigami*. San Sebastian Spain.
- Hoover, A. (2006-2014). "Who Invented Origami?". Retrieved from <http://origami.lovetoknow.com/>
- Hull, T. (2011). *Combinatorial Geometry*.
- Ishii, T. (2013). *One Thousand Paper Cranes: The Story of Sadako and the Children's Peace Statue*: Laurel Leaf Library.
- Jackson, P. (1990). *Classic Origami*. 6 Blundell Street London N7 9BH: The Apple Press.
- Jackson, P. (2011). *FOLDING TECHNIQUES FOR DESIGNERS FROM SHEET TO FORM*. Laurence King Publishing Ltd.
- James, A. (2008). Deployable architecture.
- Karaveli, A. S. (2014). *Andrée Sonad Karaveli*.

- Lang J., R. B. A., Landen; Grames L., Clayton; Magleby P., Spenger; Howell L., Larry. (2013). A Classification of Action Origami as Systems of Spherical Mechanisms. *Journal of Mechanical Design*.
- Lang, L. S. d. (2015). Glass Pavillon. In notes (Ed.). BRUNO IN BERLIN.
- Lang, R. J. (2004-2014a). Huzita-Justin Axioms. Retrieved from www.langorigami.com/science/math/hja/hja.php
- Lang, R. J. (2004-2014b). Origami Design Secrets. Retrieved from www.langorigami.com
- Lang, R. J. (2004-2014c). Treemaker.
- Lang, R. J. (2004-2014d). Wet-folding Paper. Retrieved from http://www.langorigami.com/paper/wetfolding_papers.php
- Lim, S. H. (2007). Origami : Flat Foldability. Retrieved from <http://stellar.pe.kr>
- Lum, M. J. H., Rosen, J., Sinanan, M. N., & Hannaford, B. (2006). Optimization of a spherical mechanism for a minimally invasive surgical robot: theoretical and experimental approaches. *IEEE Transactions On Bio-Medical Engineering*, 53(7), 1440-1445.
- Mariano, R. (2012). Standing at the edge of the possible: The Folding Architecture of Jørn Utzon.
- Mooth, N. (2014). Origami Spherical Mechanism. Brigham Young University: CompliantMechanisms Research Group (CMR).
- Origami, A. (2014). Wet folding basics / List for paper shops. In W. Folding (Ed.), *Youtube help video*.
- Phillips, J. (2006). Freedom in Machinery. *Cambridge University Press*.
- Piano, R. (1966). Early Works 1964-1974. In M. S. f. S. Extraction (Ed.), (pp. Constructed in Pomezia (Rome), Italy). <http://www.rpbw.com/project/72/early-works/>: RPBW.
- Schenk, M. (2012). *Origami in Engineering and Architecture (An art spanning Mathematics, Engineering and Architecture)*. Retrieved from Research Homepage for Mark Schenk:
- Schneider, J. (2004). Flat-Foldability of Origami Crease Patterns. Retrieved from www.sccs.swarthmore.edu
- Smith, J. S. (2005). *Notes on the history of origami (3rd edition)*. First edition published as Booklet 1 in a series by the British Origami Society, 1972. Retrieved from <http://www.bitsofsmith.co.uk/history.htm>

- Sorguç, A. G., Hagiwara, I., & Selçuk, S. A. (2009). Origamics in architecture: a medium of inquiry for design in architecture. *Metu Jfa*, 2, 26.
- Spooky. (2012). Mind-Blowing Modular Origami Models of Famous Cathedrals. *Art, Pics*. Retrieved from <http://www.odditycentral.com/pics/russian-teacher-creates-mind-blowing-modular-origami-models-of-famous-cathedrals.html>
- Tachi, T. (2010). Freeform Rigid-Foldable Structure using Bidirectionally Flat-Foldable Planar Quadrilateral Mesh *Advances in Architectural Geometry 2010*. The University of Tokyo.
- Tachi, T. (2013). *Freeform Origami Tessellations by Generalizing Resch's Patterns*. Paper presented at the ASME 2013 International Design Engineering Technical Conferences and Computers and Information in Engineering Conference.
- Trautz, M., & HERKRATH, R. (2009). *The application of folded plate principles on spatial structures with regular, irregular and free-form geometries*. Paper presented at the Symposium of the International Association for Shell and Spatial Structures (50th. 2009. Valencia). Evolution and Trends in Design, Analysis and Construction of Shell and Spatial Structures: Proceedings.
- Vyzoviti, S., & de Souza, P. (2012). *Origami Tessellations in a Continuum / Integrating design and fabrication in architectural education*. Paper presented at the Scaleless - Seamless | Performing a less fragmented architectural education and practice, European Network of Heads of Schools of Architecture, European Association for Architectural Education, Münster School of Architecture.
- WikiBooks. (2014). Origami/Techniques/Model bases. Retrieved from http://en.wikibooks.org/wiki/Origami/Techniques/Model_bases
- Wu, W., & You, Z. (2011). *A solution for folding rigid tall shopping bags*. Paper presented at the Proceedings of the Royal Society of London A: Mathematical, Physical and Engineering Sciences.
- You, L. J., Hao, L. J., Yong, G.Hui, L., L. G., A., L. S., K., & W., L. Sun and Architecture. *National University of Singapore*.
- Zirbel, S. A., Lang, R. J., Thomson, M. W., Sigel, D. A., Walkemeyer, P. E., Trease, B. P., . . . Howell, L. L. (2013). Accommodating thickness in origami-based deployable arrays. *Journal of Mechanical Design*, 135(11), 111005.